Process Design and Simulation of Producing Liquid Transportation Fuels from Biomass

by

Pengcheng Li

A thesis submitted to the Graduate Faculty of
Auburn University
in partial fulfillment of the
requirements for the Degree of
Master of Science

Auburn, Alabama
May 06, 2017

Keywords: Process Design, Process Simulation, Aspen Plus, Economic Analysis, Biomass, Renewable Energy

Approved by

Mario R. Eden, Chair, Joe T. & Billie Carole McMillan Professor of Chemical Engineering
Xinyu Zhang, Associate Professor of Chemical Engineering
James G. Radich, Assistant Professor of Chemical Engineering

Abstract

Although the global energy sector is driven by fossil fuels, renewable and more environmental friendly energy sources need to be explored due to the insecurity of crude oil availability in the future and the environmental problems associated with fossil fuel consumption. The conversion of biomass to liquid transportation fuels is one such environmentally friendly process. This is the case since biomass acts as a renewable carbon-based source, having absorbed atmospheric CO_2 via photosynthesis. There is also an abundance of biomass on earth. In this work, a process has been designed and analyzed in Aspen Plus. The conversion of biomass to gasoline, diesel, and kerosene at varying design/operating conditions has been simulated. In this process, biomass is dried and gasified to generate synthesis gas, which is converted to a mixture of hydrocarbons via Fischer-Tropsch synthesis (FTS). Given the same biomass feedstock, three FTS technologies including conventional FTS, once-through FTS, and supercritical FTS have been comparatively studied. Hydrocarbons after FTS undergo upgradation to liquid transportation fuels through several technologies (hydrocracking, hydrotreating, isomerization, catalytic reforming, and alkylation) meeting all necessary physical property standards. This study first investigates the product distribution of biomass conversion process associated with the three FTS technologies. Then heat integration is performed to optimize the heat exchanger network. Lastly, a detailed economic analysis is performed using Aspen Process Economic Analyzer and unit cost functions obtained from literature.

Acknowledgments

I would like to express my most sincere gratitude to my advisor and mentor, Dr. Mario R. Eden. Without Dr. Eden, I would not be where I am today. I was in a very tough situation 3 years ago when my previous advisor left Auburn University. Dr. Eden provided me with a very welcoming and stimulating environment where I could continue my graduate studies and research. I will be forever grateful to him for his guidance, support, encouragement and generosity.

My gratitude also goes to my committee members, Dr. Xinyu Zhang and Dr. James Radich, for their valuable input and their constant support and encouragement. I would also like to thank the previous and current graduate students and postdoctoral fellows in our research group. This includes Dr. Robert Herring, Dr. Zhihong Yuan, Mr. Vikrant Dev, Dr. Narendra Sadhwani, Mr. Shounak Datta and Mr. Bernardo Lousada. They were fun to work with and they guided me with their depth of understanding of their respective research topics. I am also indebted to the faculty and staff in the Department of Chemical Engineering at Auburn University who set me on the right path, towards success.

I would also like to show my gratitude to the friends I have made in Auburn for their unflinching support. They made living in a foreign country easier and interesting. I want to thank Xinquan Cheng and Xiu Wang who took care of me, when I fell sick, without me

even asking them. I will forever cherish the friendship and the memories. I also give my gratitude to Marcel Fidelak for his encouragement, support and patience.

Lastly, I want to thank my lovely family for their support. My mother and father, Yanrong Wang and Xiaojun Li, have always stood by me and have reposed their trust in me. They encouraged me to make the most out of available opportunities and were confident that I would make the right decisions. When I was stressed, they guided me with love and patience. I will forever cherish all the support bestowed by them in my life.

Table of Contents

List of Tables

List of Figures

List of Abbreviations

AEA	Aspen Energy Analyzer
APEA	Aspen Process Economic Analyzer
ASF	Anderson-Schulz-Flory
ASU	Air Separation Unit
BEOP	Break-Even Oil Price
COP	Crude Oil Price
DPI	Direct Permanent Investment
EIA	Energy Information Administration
FT	Fischer-Tropsch
FTS	Fischer-Tropsch Synthesis
HP	High Pressure
L&M	Labor and Maintenance
LP	Low Pressure
NPV	Net Present Value
NREL	National Renewable Energy Laboratory
RM	Refinery Margin
SGP	Saturated Gas Plant
SOC	Subtotal Operating Costs
SSD	Superheated Steam Dryers

TIC	Total Installed Cost
TPI	Total Permanent Investment

Chapter 1

Introduction

1.1 Motivation

The Energy Information Administration (EIA) projects that the total energy consumption worldwide will shoot up by 48% between 2012 and 2040, from 549 quadrillion Btu to 815 quadrillion Btu (EIA, 2016b). On the other hand, world population is expected to reach 9.7 billion by 2050, which is one third more population than in 2015 (DESA, 2015). The rise in energy consumption and world population urges us to explore more sources of energy to meet the upcoming energy demand. Among all available fuel sources, fossil fuels will continue to supply nearly 80% of world energy through 2040. Among fossil fuels, petroleum-based liquid fuels remain the largest source of energy consumption worldwide (EIA, 2016b). EIA show that crude oil reserves as of 2015 are 1,661.8 billion barrels, which will last only 48.7 more years. This is according to the 2014 petroleum consumption rate (EIA, 2015).

Concerns about using fossil fuels with regards to energy security, effects of fossil fuel emissions on the environment, and sustained, long-term high oil prices worldwide support expanded use of non-fossil renewable energy sources. Renewables are the world's fastest growing energy source according to the EIA. Renewable energy consumption is projected to increase by an average of 2.6% per year between 2012 and 2040 (EIA, 2016b). However, major technological developments need to occur for alternative energy sources such as solar, wind and nuclear energy to play a significant role in the world energy market and to

help control the emission of CO_2 to the environment. Biomass conversion to liquid transportation fuels can help alleviate rising environmental concerns of fossil fuel usage.

Biomass conversion to liquid transportation fuels has been a topic of significant research world-wide in recent years (Saxena et al., 2009). There are several reasons for this enhanced interest:

- technological developments relating to the conversion promise the application of biomass at lower cost and with higher conversion efficiency than was previously possible
- the use of biomass as energy source can alleviate global warming because the emitted CO_2 can be used for growing new biomass through photosynthesis (McKendry, 2002)
- biomass is available in most countries and its application may diversify the fuel-supply in many situations, which in turn may lead to a more secure energy supply (McKendry, 2002)

Therefore, biomass could be a promising energy source to solve the energy crisis in the world. It is necessary to study the efficiency of biomass to liquid transportation fuels before the process is employed in industries.

1.2 Biomass Conversion Overview

Diverse technologies can be used to convert biomass into useful forms of energy. The choice of technology depends on the type, property and quantity of biomass feedstock, the desired form of energy, environmental standards, economic conditions and project-specific

factors (Saxena et al., 2009). Nowadays the most common technologies for biomass conversion process are chemical, biochemical, and thermochemical conversion processes.

Chemical conversion processes use chemical agents to convert biomass to other forms of usable energy, typically in the form of liquid fuels (EPA, 2007). The principal chemical conversion reaction is the transesterification reaction. Transesterification is the chemical-based conversion through which fatty acids from oils, fats and greases are reacted with alcohol. This process reduces the viscosity of the fatty acids and makes them combustible. Transesterification systems can accept any oil, fat, or grease, including used cooking oils, animal fat, and plant oils. Typically, feedstocks with fatty acid content exceeding 4% must be pretreated in an esterification process; a chemical process that reduces the fatty acids in the feedstock to an acceptable concentration for the transesterification reaction (EPA, 2007).

Biochemical conversion processes use biocatalysts, such as enzymes, bacteria, or other microorganisms, in addition to heat and other chemicals, to break down biomass to make the carbohydrates available for processing into intermediate sugars (DOE, 2013). These sugars are intermediate building blocks that can then be fermented or chemically catalyzed into a range of advanced biofuels and value-added chemicals. Biomass biochemical conversion process involves five major steps: feedstock preparation, pretreatment, hydrolysis, biological conversion/chemical conversion and product recovery (DOE, 2013). Pretreatment is essential for enzyme catalyzed cellulose conversion. Without pretreatment, enzymatic hydrolysis of cellulose is ineffective as native cellulose is well protected by hemicellulose and lignin (Soudham, 2015). Biomass biochemical conversion process is challenging due to the considerable cost and difficulty involved in breaking down the

tough, complex structures of the cell walls in cellulosic biomass. It is necessary to explore more efficient and cost-effective ways to gain access to the useful sugars for conversion processing (DOE, 2013).

Thermochemical conversion processes are the application of heat and chemical processes in the production of products from biomass. There are two basic approaches for thermochemical conversion process. The first is the gasification of biomass and its conversion to hydrocarbons. The second approach is to liquefy biomass directly by high-temperature pyrolysis, high-pressure liquefaction, ultra-pyrolysis, or supercritical extraction (Goyal et al., 2008). Combustion of biomass in an oxygen rich environment is the oldest process and most well known for producing heat. It should be noted that the thermochemical conversion routes differ in the products generated and the relative proportions of these products (Tian et al., 2014). The primary product of gasification is syngas, which can be converted to hydrocarbons via Fischer-Tropsch synthesis. Gasification has inherent advantages over combustion for emission control. Emission control is simpler in gasification because the produced syngas in gasification is at a higher temperature and pressure than the exhaust gases produced in combustion. Gasification also has the advantage of feedstock flexibility. Several gasifier designs have been developed to accommodate various grades of coal and various biomass types. Gasifiers can also handle pet coke and other refinery products. Based on all these advantages, the focus in this study has been placed on gasification of biomass.

1.3 Scope and Objectives

This research focuses on designing a cost-effective biomass conversion process that leads to production of liquid transportation fuels to ease the energy shortage in the world. The overall goal of this research is to compare three biomass conversion processes with respect to their product yield and economic effectiveness. In this research, conceptual processes have been developed for liquid transportation fuels production. The methodology consists of several steps to achieve the stated research objective. The first step is to gather process data including the possible process routes and operating conditions. In this step, the general process technologies and process operating conditions are determined. After the processes and operating conditions are determined, Aspen Plus is used to simulate the process to carry out the energy and mass balances. The simulation results provide an overview of which process can produce the most liquid transportation fuels. Most process units can be modeled by Aspen Plus built-in blocks. However, some user-defined blocks have been developed to employ models found in literature. Heat integration has been performed for all three biomass conversion processes based on the simulation results to optimize the heat exchanger network in Aspen Energy Analyzer (AEA). The optimal heat exchanger networks have been obtained using the pinch analysis approach. This key step ensures the minimum usage of heating and cooling duties in the designed process. Optimized models have been utilized to perform the economic analysis for the proposed biomass conversion processes. Economic analysis shows the cost effectiveness and competitiveness of the proposed processes.

1.4 Organization

The format of this thesis is such that the proposed processes are first described in chapter two. The first section in chapter two introduces the process design basis through an overall block flow diagram. It shows the main units in the proposed biomass conversion process. The main units are feed handling and drying, biomass gasification, syngas cleanup process, Fischer-Tropsch synthesis, hydrocarbon upgrading process, and air separation unit. The second to the seventh section in chapter two describe the main process units used in this research in detail. In the eighth section, the power generation process is described.

The process modeling of each process units has been described in chapter three. The first section in chapter three introduces simulation in Aspen plus. The following sections show the detailed process models used in this research. The modeling information has all been gathered from literature.

Chapter four shows the steady-state process simulation results. The first section shows the effect of feedstocks on the product yield. For studying the effect of feedstocks, the same once-through FTS biomass conversion process has been used. Five different feedstocks, which are pine bark, hybrid poplar, corn stover, switchgrass, and hardwood, have been compared. Three FTS simulation results have been provided in the second section. The third section compares the liquid transportation fuels product yield for all the three biomass conversion processes. Based on the simulation results, heat integration is performed and the results shown in the fourth section.

Chapter five gives the economic analysis results for the three proposed biomass conversion processes. The first two sections give the capital costs and operating costs assumptions used for the economic analysis. The discounted cash flows over the entire

economic life of the plant have been calculated based on the capital costs and operating costs. Break-even oil price has been calculated for the three biomass conversion processes to compare their economic competitiveness.

Chapter 2

Process Design

2.1 Process Design Basis

A biomass conversion process has been designed to produce liquid transportation fuels via syngas intermediate. Figure 2.1 shows a simplified generic process block diagram. The detailed process flowsheet diagrams are shown in Appendix A.

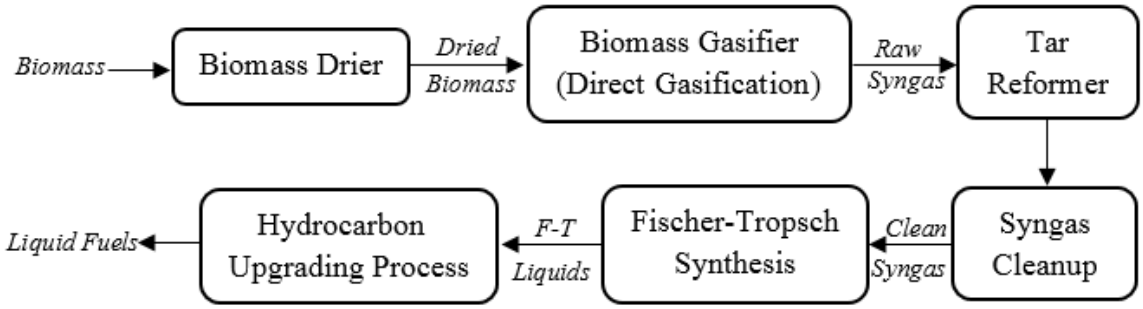

Figure 2.1: Overall biomass conversion process block diagram

The process can be broken down into the following major components:

- Feed handling and drying
- Gasification
- Syngas cleanup
- Fischer-Tropsch synthesis
- Hydrocarbon upgrading
- Air separation unit

2.2 Feed Handling and Drying

2.2.1 Biomass Drying Technology

There are three main choices for drying biomass (Amos, 1998). These utilize rotary dryers, flash dryers, and superheated steam dryers respectively.

Rotary dryers are the most common type used for drying biomass. The most widely-used rotary dryer is the directly heated single-pass rotary dryer (see Figure 2.2). Biomass comes in contact with hot gases inside a rotating drum. The biomass and hot gases normally flow co-currently through the dryer, while in cases where temperature is not a concern, the hot gas and biomass flow counter-currently. This way, the driest biomass is exposed to the hottest gases with the lowest humidity. Counter-current flow of biomass and hot gases generates the lowest moisture (Amos, 1998).

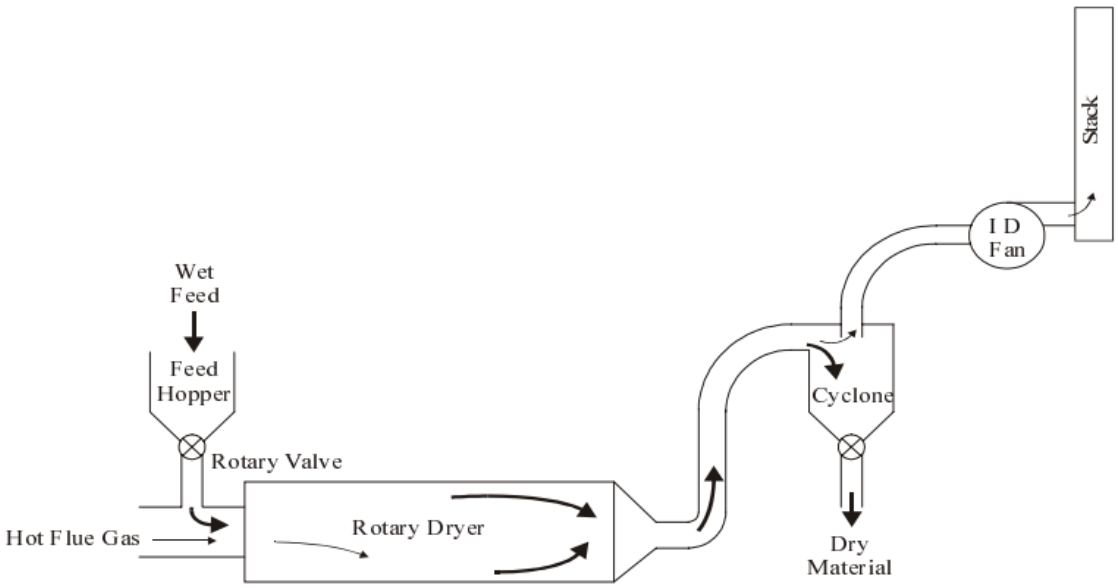

Figure 2.2: Single-pass rotary dryer

For a flash dryer, biomass is mixed with a high-velocity hot air stream (see Figure 2.3). The intimate contact of biomass with the air leads to very rapid drying. After the dryer, biomass and air are separated by a cyclone. The flash dryer equipment is more compact than a rotary dryer due to the short drying time in a flash dryer. However, it

consumes more electricity due to the faster air flow through the dryer. The gas temperatures are lower for flash dryers than for rotary dryers (Amos, 1998).

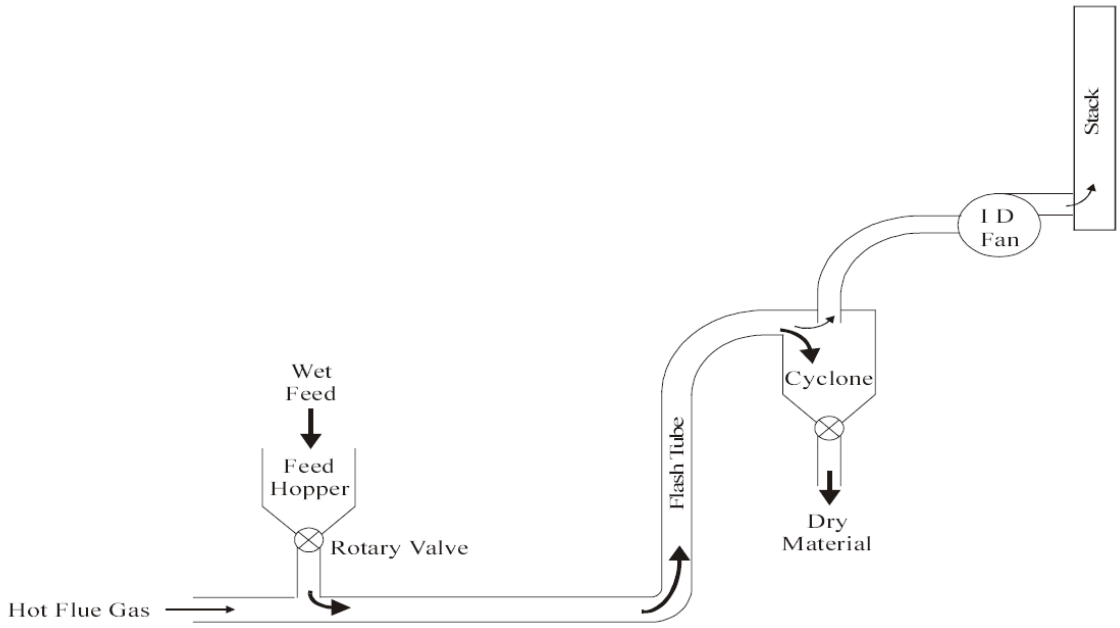

Figure 2.3: Flash dryer

Most superheated steam dryers (SSD) are similar to flash dryers, except that SSD uses steam to provide heat instead of hot air. Typically, 90% of the steam is recirculated back to the dryer, while 10% of the steam, representing the amount of water evaporated from the biomass, is removed (Amos, 1998).

2.2.2 Feed Handling and Drying Description

The design of this section is based on a National Renewable Energy Laboratory (NREL) report (Dutta & Phillips, 2009). The purpose of this section is to accommodate the delivery of biomass feedstock, short term on-site storage, and the preparation of the feedstock for processing in the gasifier. The design for this section is the same for all cases of liquid transportation fuels production from different kinds of biomass sources. Biomass is

delivered to the plant primarily by trucks. Then biomass is dumped into a storage pile. Biomass is then granulated to particles which are conveyed through a magnetic separator and screened. Particles larger than 2 inches are sent through a hammer mill for further size reduction.

Figure 2.4 shows the biomass drying flowsheet. Biomass is dried through contact with hot gas directly. The wet biomass enters each rotary biomass dryer through a dryer feed screw conveyor. The dried biomass is pressurized in a lock hopper and conveyed to the gasifier through a feed hopper and a screw conveyor.

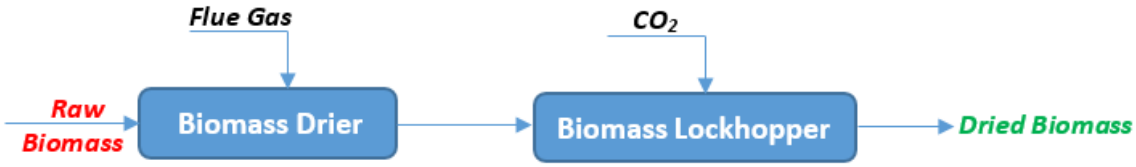

Figure 2.4: Biomass drying flowsheet

2.3 Gasification

2.3.1 Biomass Gasification Background

Biomass gasification is a thermochemical partial oxidation process in which biomass is converted into syngas (mainly H_2 and CO) in the presence of a gasifying agent (air, steam, oxygen, CO_2 or a mixture of these) (Ruiz et al., 2013). Thermal gasification of biomass represents a convenient route to produce syngas from intractable materials, particularly materials derived from waste which are not cost effective to process for use in biocatalytic or other milder catalytic processes (Jahangiri et al., 2014). The main operating parameters of biomass gasification include type and design of gasifier, gasification temperature, flow rates of biomass and oxidizing agents, type and amount of catalysts, and biomass type and properties (Kumar et al., 2009).

Gasifiers can be categorized by the type of gasifier, which are fixed-bed gasifiers and fluidized-bed gasifiers. Fixed-bed gasifiers can be classified further as updraft (countercurrent) or downdraft (concurrent). For updraft gasifiers, the combustion takes place at the bottom of the bed and product gas exits from the top of the gasifier at low temperature (around 500^{o}C), which makes the gases contain a lot of tar. For downdraft gasifiers, the product gases leave the gasifier from the bottom at a high temperature (around 800^{o}C), which helps remove most of the tars. In fluidized-bed gasifiers, the fluidization improves the heat transfer to the biomass which leads to the increase in reaction rates and conversion efficiencies. Gasifiers can be also categorized by the method of heat source provided for the gasification reactions, which are direct gasification and indirect gasification. For direct gasification, biomass is combusted in the gasifier to provide the heat required for the gasification reactions. For indirect gasification, part of the biomass is combusted in another reactor and the heat is then transferred to the gasifier.

Table 2.1: Main gasification reactions at 25^{o}C

Char or gasification reactions	$C+CO_2 \leftrightarrow 2CO$ +172 kJ/mol
	$C+H_2O \leftrightarrow CO+H_2$ +131 kJ/mol
	$C+2H_2 \leftrightarrow CH_4$ -74.8 kJ/mol
	$C+0.5O_2 \leftrightarrow CO$ -111kJ/mol
Oxidation reactions	$C+O_2 \rightarrow CO_2$ -394 kJ/mol
	$CO+0.5O_2 \rightarrow CO_2$ -284 kJ/mol
	$CH_4+2O_2 \leftrightarrow CO_2+2H_2O$ -803 kJ/mol
	$H_2+0.5O_2 \rightarrow H_2O$ -242 kJ/mol
Shift reaction	$CO+H_2O \leftrightarrow CO_2+H_2$ -41.2 kJ/mol
Methanation reactions	$2CO+2H_2 \rightarrow CH_4+CO_2$ -247 kJ/mol
	$CO+3H_2 \leftrightarrow CH_4+H_2O$ -206 kJ/mol
	$CO_2+4H_2 \rightarrow CH_4+2H_2O$ -165 kJ/mol
Steam reactions	$CH_4+H_2O \leftrightarrow CO+3H_2$ +206 kJ/mol
	$CH_4+0.5O_2 \rightarrow CO+2H_2$ -36 kJ/mol

Gasification takes place at high temperatures (between 500 and 1400^{o}C) and pressures ranging from atmospheric pressure to 33 bar (Morrin et al., 2012). There are different stages during gasification reactions but there are no clear boundaries between these stages. Thermogravimetric analysis shows that there are generally three stages in gasification, which are the dehydration stage (below 125^{o}C), the active pyrolysis stage (125 – 500^{o}C), and the passive pyrolysis stage (above 500^{o}C). The dehydration reflects loss of water, the active pyrolysis reflects the loss of hemicellulose, cellulose and part of lignin, and the passive pyrolysis reflects the slow and continuous loss of residual lignin. Biomass gasification involves several reactions, which are shown in Table 2.1 (Ruiz et al., 2013).

2.3.2 Gasification Process Description

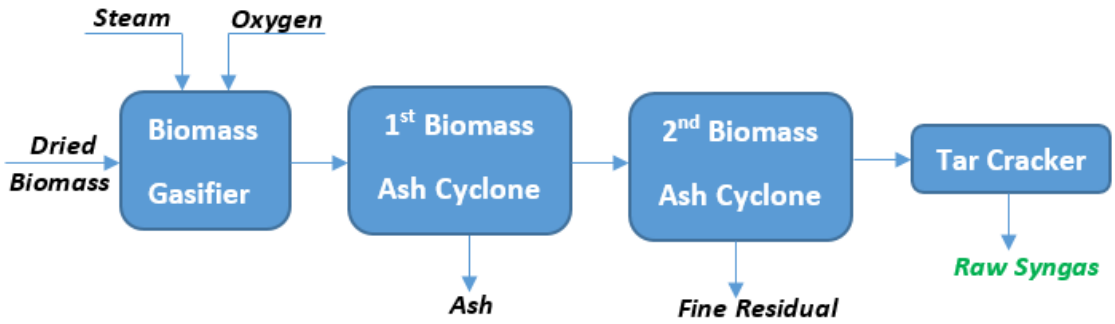

Figure 2.5: Gasification flowsheet

Figure 2.5 shows the biomass gasification flowsheet. The dried biomass from the feed handling and drying section enters a high-pressure oxygen blown bubbling fluidized-bed gasifier. In this work, direct gasification is used to convert biomass to syngas, which means the required heat is provided by partial combustion of biomass with oxygen and steam. A typical gasifier for direct gasification is shown in Figure 2.6. The gasifier fluidization

medium is steam. The steam-to-feed ratio is 0.2 lb of steam per lb of dried biomass. The temperature of the gasifier is set at 1600^{o}F. Oxygen input is controlled to maintain the temperature of the gasifier. Oxygen feed is about 0.23 lb per lb of bone dry feed.

Particulate removal after the biomass gasifier is performed using two-stage cyclone separators. Nearly all the ash and char is separated in the primary cyclone. A secondary cyclone removes the residual fines. The solids are depressurized and cooled. Before the landfill of ash and char, the solids are cooled and water is added to the ash stream for conditioning to prevent the mixture from being too dusty to handle. After the cyclones, a tar cracker is used to convert the tar species and C_1-C_2 hydrocarbons to CO and H_2, while NH_3 is converted to N_2 and H_2.

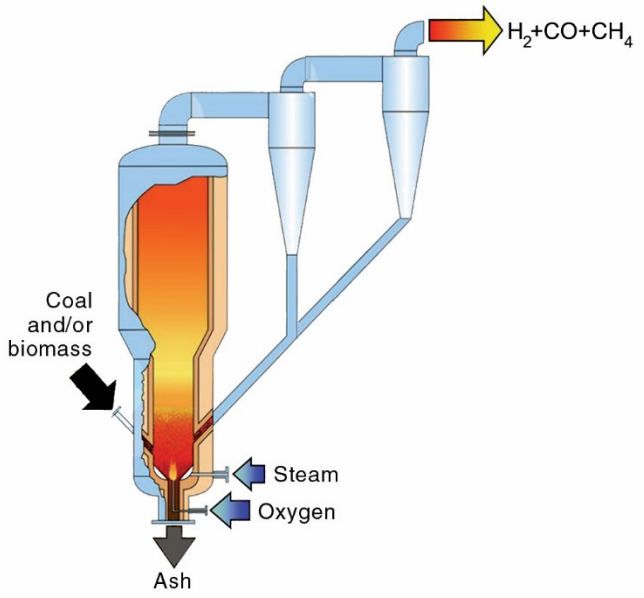

Figure 2.6: Typical direct gasifier (Lalou, 2014)

2.4 Syngas Cleanup Description

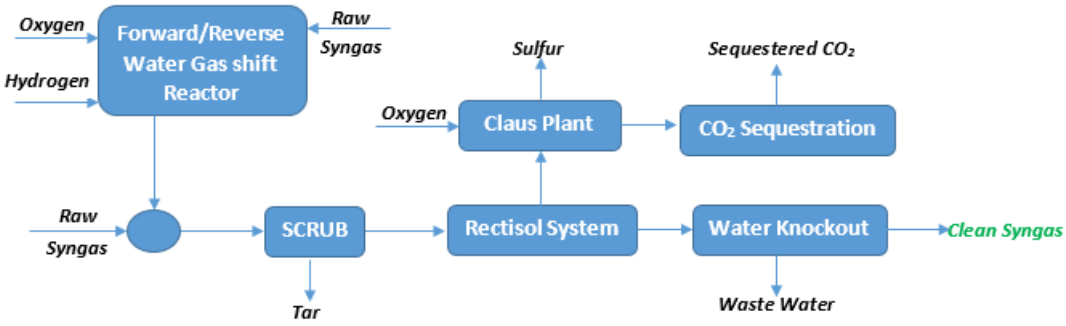

Figure 2.7: Syngas cleanup flowsheet

The raw syngas exiting the tar cracker is directed to a syngas cleanup section where the raw syngas is cleaned so that the gas can be synthesized into fuels. Figure 2.7 shows the syngas cleanup flowsheet.

The raw syngas is cooled to 185°C and sent to a scrubbing system (SCRUB) to remove any residual tar, particulates, and NH_3 from the gas phase. The wastewater generated from the scrubbing system is sent to a biological digester for treatment of the organic contaminants, and the scrubbed syngas is directed to a dual-capture Rectisol system (Baliban et al., 2013). Before the raw syngas enters the scrubbing system, it may be partially passed through a water-gas shift reactor which can operate in the presence of sulfur species. The water-gas shift reactor is operated at 28 bar and at temperatures between 400 and 600°C. The water-gas shift reactor serves either of the following two purposes:

- increase the H_2/CO ratio of the syngas through the forward water-gas shift reaction
- decrease the CO_2 concentration of the syngas through the reverse water-gas shift reaction

The decision to incorporate the dedicated water-gas shift unit into the biomass conversion process depends on the H_2/CO ratio for syngas conversion in Fischer-Tropsch synthesis unit.

The Rectisol unit is used to remove acid gases, such as CO_2 and H_2S, from the syngas. This provides a clean gas system which is ready for Fischer-Tropsch synthesis. The Rectisol unit is necessary to remove sulfur species to prevent poisoning of the catalysts used in the Fischer-Tropsch reactor. The Claus plant recovers sulfur and CO_2 and is put into a CO_2 sequestration unit to get sequestered CO_2. After the Rectisol system, syngas passes over a water knockout unit to knock out the waste water.

2.5 Fischer-Tropsch Synthesis

2.5.1 Background

Fischer-Tropsch (FT) synthesis which converts syngas to high-molecular-weight hydrocarbons is a very important route for the production of fuels and chemicals due to the depletion of fossil fuels. In 1923, Franz Fischer (1877-1947) and Hans Tropsch (1889-1935) made an important contribution by discovering high hydrocarbon productivity and selectivity in the conversion of coal-derived syngas (Fischer & Tropsch, 1923). Fischer and Tropsch published their hydrocarbon synthesis work in 1926, and the process has since been called Fischer-Tropsch synthesis (FTS) (Keim, 1983; Khodakov et al., 2007). In 1934, the first commercial FT process was licensed by Ruhrchemie, Germany, and in two years the first large-scale FT plant was operational in Braunkohle-Benzin, Germany (Khodakov et al., 2007). The main reactions for FTS are summarized in Table 2.2 (Van Der Laan & Beenackers, 1999).

Table 2.2: Main reactions in Fischer-Tropsch synthesis

Main reactions	
1. Paraffins	$(2n+1)H_2 + nCO \rightarrow C_nH_{2n+2} + nH_2O$
2. Olefins	$2nH_2 + nCO \rightarrow C_nH_{2n} + nH_2O$
3. WGSR	$CO + H_2O \leftrightarrow CO_2 + H_2$
Side reactions	
4. Alcohols	$2nH_2 + nCO \rightarrow C_nH_{2n+2}O + (n-1)H_2O$
5. Catalyst oxidation/reduction	(a) $M_xO_y + yH_2 \leftrightarrow yH_2O + xM$
	(b) $M_xO_y + yCO \leftrightarrow yCO_2 + xM$
6. Bulk carbide formation	$yC + xM \leftrightarrow M_xC_y$
7. Boudouard reaction	$2CO \rightarrow C + CO_2$

The FT reaction is a polymerization process, involving adsorption, chain initiation and chain growth termination. Figure 2.8 shows a classic FTS mechanism pathway. CO is absorbed on metal atoms to form the carbide species. The absorbed dissociated hydrogen inserts into the carbide species to produce the active CH_2 intermediate which leads to the propagation step. The resulting alkyl chain desorbs from the metal after hydrogenation and β-scission, which forms olefins or paraffin.

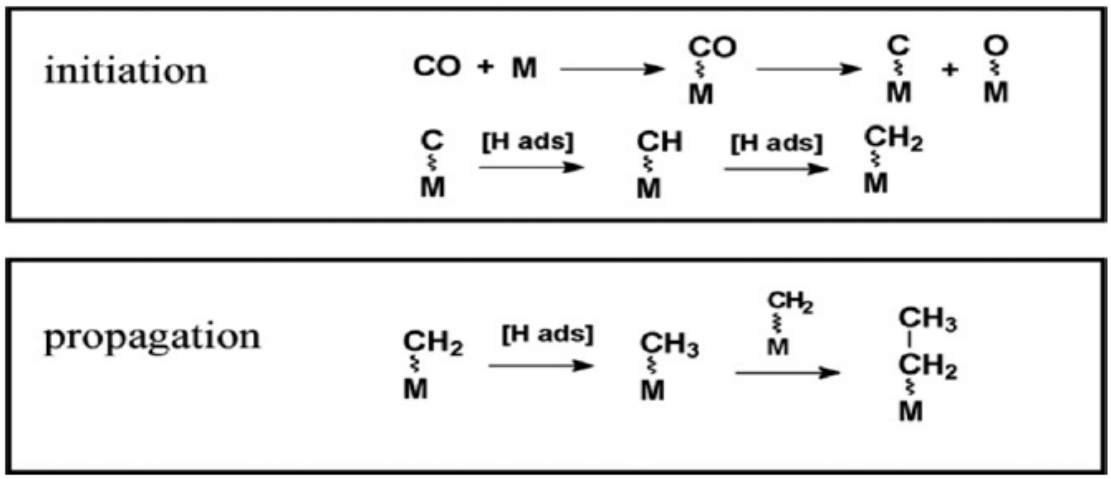

Figure 2.8: Classic FTS mechanism pathway (Perego et al., 2009)

The FTS product spectrum consists of a complex multicomponent mixture of linear and branched hydrocarbons and oxygenated products. Main products are linear paraffins and α-olefins. The distribution of FTS hydrocarbons follows the Anderson-Schulz-Flory (ASF) distribution, which can be modeled by Eq. 2.1-2.2.

$$W_n/n = (1- \alpha)^2 \alpha^{(n-1)} \quad \text{(Eq. 2.1)}$$

$$\alpha = r_p/(r_p + r_t) \quad \text{(Eq. 2.2)}$$

where W_n/n is the weight fraction of product with n^{th} carbon; r_p is the propagation rate constant; r_t is the termination rate constant (Pegego, 2007).

Figure 2.9 gives the ASF distribution. It shows that the maximum amount of gasoline that can be theoretically obtained is around 45% for the value of α at 0.75, while the maximum amount of diesel is only 23% with α at 0.9 (Pegego, 2007). As the α-parameter is closely related to the catalyst characteristics, a good catalyst design strategy is of paramount importance for a successful industrial program. Iron, cobalt, nickel, ruthenium and osmium are the best catalytic metals for FTS. Long chain hydrocarbons can be obtained by using ruthenium as catalyst without any promoters in FTS at low reaction temperature. However, the high cost and limited availability of ruthenium makes it an unsustainable option for industrial uses. The high production of methane due to the high hydrogenation activity of nickel during FTS makes it an unsuitable candidate. Therefore, iron and cobalt are deemed to be the best metals for catalyzing industrial scale FTS processes (Schulz, 1999).

Fuels produced via FTS are of a high quality due to very low aromaticity and zero sulfur content. The middle distillate fraction has a high cetane number, which gives superior combustion properties and reduced emissions. New and stringent regulations may promote

replacement or blending of conventional fuels by sulfur and aromatic-free FT products (Fox, 1993; Gregor, 1990).

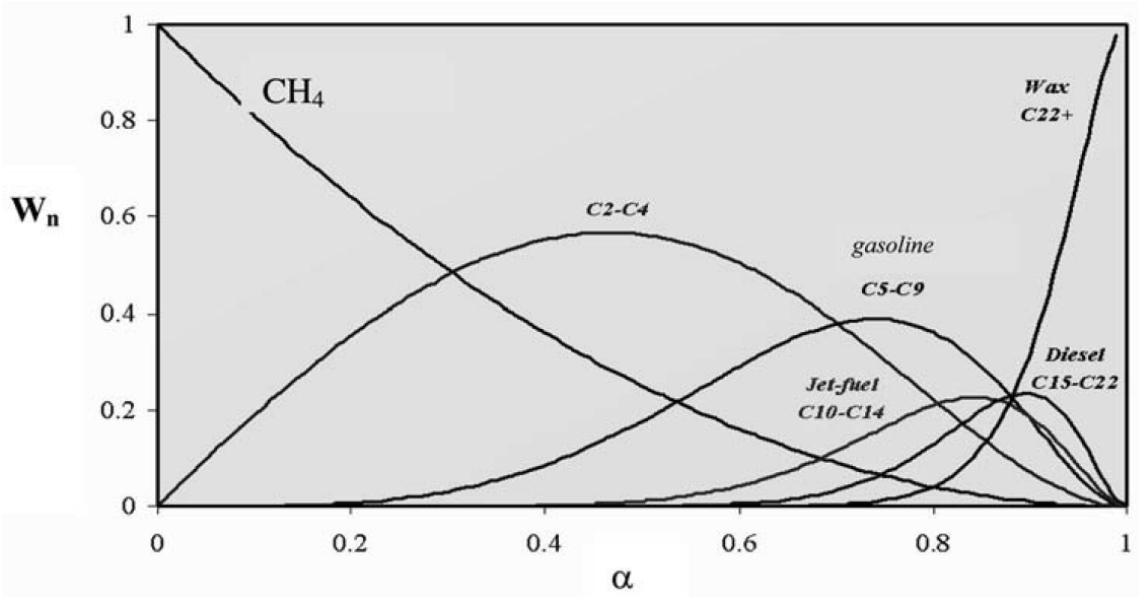

Figure 2.9: ASF distribution

2.5.2 Supercritical Fischer-Tropsch Synthesis

Traditional gas phase FT reaction suffers from a series of problems, such as localized overheating which leads to undesired selectivity and loss of catalyst activity (Fan & Fujimoto, 1999). A slurry phase process was used to improve the characteristics of heat transfer and to extract the wax from the catalyst surface by Kölbel and Ralek (1980). However, in slurry phase reaction, the diffusion of syngas in the micropores is so slow that the overall reaction rate is lower than that in the gas phase reaction (Fujimoto and Kajioka, 1987). Supercritical FT was developed to mitigate the weaknesses of the gas phase reaction by using supercritical fluid as media.

A supercritical fluid refers to a substance that is heated beyond its critical temperature and compressed beyond its critical pressure. At the critical point, the properties of the liquid

and gas phase become identical. Supercritical fluids have properties somewhere between that of gases and liquids, i.e. the density is sufficient to cause substantial dissolution. Also, the solvation capability is close to that of liquids, and the diffusivity and viscosity are comparable to that of gases (Elbashir, 2004). Supercritical fluids have been increasingly used as solvents in chemical reactions in oil, food, pharmaceutical and biochemical industries. Their main advantages are (Lang et al., 1995; Abbaslou et al., 2009):

- gases are completely miscible with supercritical fluids resulting in high concentrations compared to that in liquid solvents
- the ability to dissolve non-volatile substances is very similar to conventional liquid solvents due to the liquid-like densities of supercritical fluids
- supercritical fluids have superior mass transfer characteristics considering that they have low viscosity and high diffusivity
- high compressibility of supercritical fluids near the critical point induces large changes in density with very small changes in pressure and/or temperature enabling easy separation of the dissolved material from the supercritical fluids
- the surface tension of the supercritical fluids is low enabling easy access into the pores of the catalyst for extraction of non-volatile materials in the pores

The effect of supercritical media on FTS has been studied considerably in recent years (Bukur et al., 1997; Elbashir et al., 2005; Fan & Fujimoto, 1999; Huang et al., 2004; Huang & Roberts, 2003; Linghu et al., 2006; Yokota & Fujimoto, 1991). Yokota et al. studied FTS in supercritical n-hexane for the first time, which showed that the removal of reaction heat and waxy products from the catalyst surface in supercritical FTS was much more

effective than in the gas phase reaction (Yokota et al., 1990). Therefore, supercritical FTS can be used to improve the performance of FT reactions, which leads to more liquid fuels.

2.5.3 Process Description of Fischer-Tropsch Synthesis

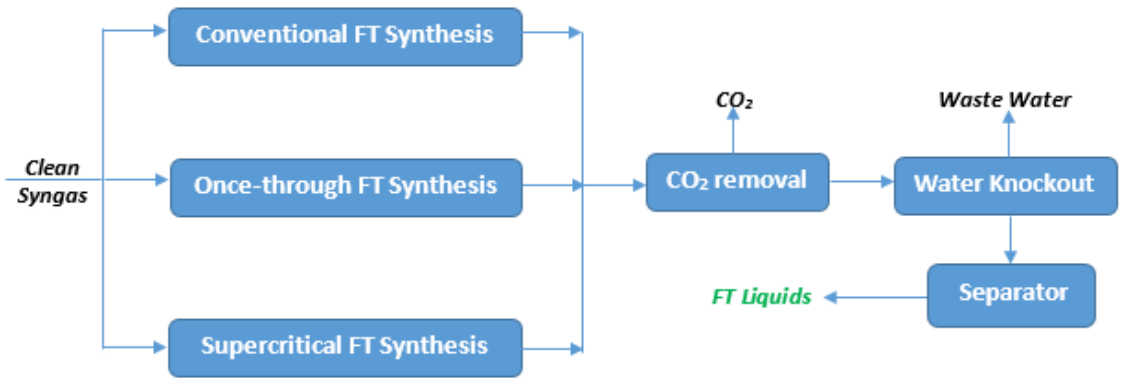

Figure 2.10: FTS process flowsheet

Figure 2.10 illustrates the FTS process flowsheet. The principal function of this plant is to convert syngas to hydrocarbon products. The clean syngas after the syngas cleanup unit enters the FT reactor through a gas distributor. In the FT reactor, the syngas bubbles upward through the catalyst and is converted into hydrocarbon products at the catalyst interface. The catalyst/hydrocarbons mixture is withdrawn from the FT reactor and passed through a hydroclone. The catalyst is recovered and sent back to the FT reactor. The overflow from the top of the hydroclone is sent to the Kerr McGee's ROSE-SR unit for catalyst-hydrocarbon separation. The hydrocarbons from the separation unit are cooled and then sent to a separator where the liquid hydrocarbons and the vapor stream are separated. The vapor stream is sent to a CO_2 recovery plant to remove the CO_2. A water knockout unit is used to remove the waste water which is sent to the waste water treatment facility.

In this study, three FTS technologies have been investigated for the biomass conversion process. These are conventional FTS, once-through FTS, and supercritical FTS. In the conventional FTS biomass conversion process, the produced $C_1/C_2/C_3$ light gas in the hydrocarbon upgrading process is reformed to produce additional syngas and then recycled back to the FTS reactor along with the unconverted syngas from the FT reactor to improve the overall carbon conversion rate. For once-through FTS, the $C_1/C_2/C_3$ light gas from hydrocarbon upgrading process and the unreacted syngas from the FTS reactor are directed to a gas turbine for co-production of electrical power. In supercritical FTS, supercritical hexane is used as the reaction medium to improve/tailor the performance of the FTS reactions. After the FT reactor, the supercritical hexane is separated from the liquid hydrocarbons and recycled back to the FT reactor. The unconverted syngas and the reformed syngas from the auto-thermal reforming reactor are recycled back to the FT reactor to improve the carbon conversion rate.

2.6 Hydrocarbon Upgrading Process

Fischer-Tropsch synthesis produces a wide spectrum of hydrocarbon products, which cannot be used directly as fuels in their raw state. It is crucial to upgrade the hydrocarbons to high-quality transportation fuels for resale to the transportation sector. The hydrocarbon upgrading process uses conventional technologies to upgrade and refine the FT products to high-quality fuels. The process layout follows a Bechtel design (DOE, 1994) and includes a hydrocarbon recovery system, a wax hydrocracker, a distillate hydrotreater, a kerosene hydrotreater, a naphtha hydrotreater, a catalytic reformer, a C_4 isomerizer, a C_5/C_6

isomerizer, and a $C_3/C_4/C_5$ alkylizer. Figure 2.11 gives the hydrocarbon upgrading process flowsheet.

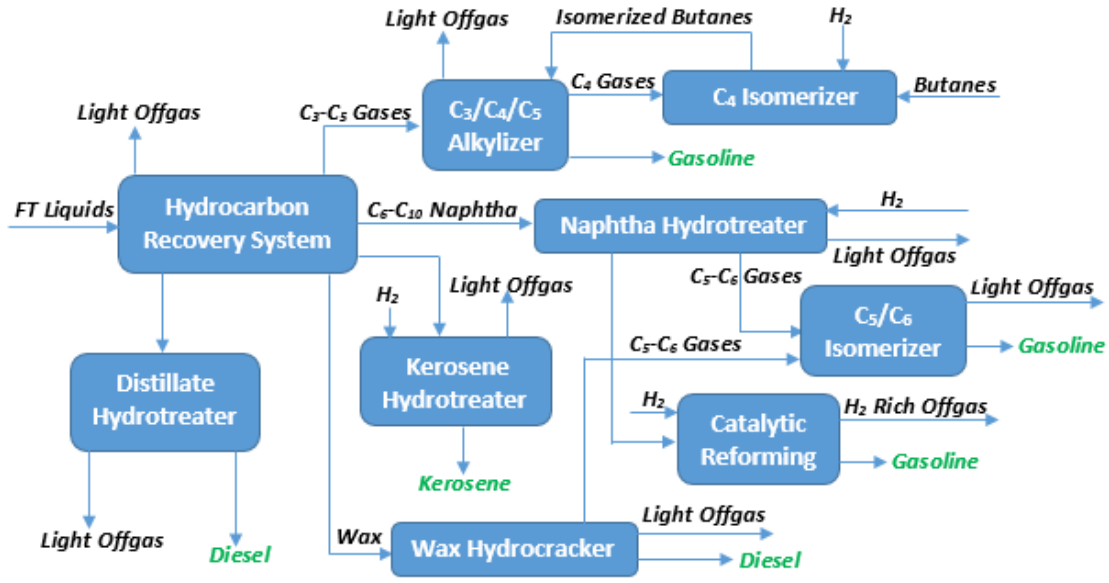

Figure 2.11: Hydrocarbon upgrading process flowsheet

2.6.1 Hydrocarbon Recovery System

The water-lean FT hydrocarbons are sent to a hydrocarbon recovery column after the FTS process. The hydrocarbons are split into light offgas, C_3-C_5 gases, naphtha, kerosene, distillate, and wax. The naphtha contains C_6-C_{10} hydrocarbons which are sent into the naphtha hydrotreater. The kerosene contains C_{11}-C_{13} hydrocarbons which are sent to the kerosene hydrotreater. The distillate contains C_{14}-C_{20} hydrocarbons which are sent into the distillate hydroteater. The wax contains C_{21}-C_{30+} hydrocarbons which are sent to the wax hydrocracker.

2.6.2 Wax Hydrocracking

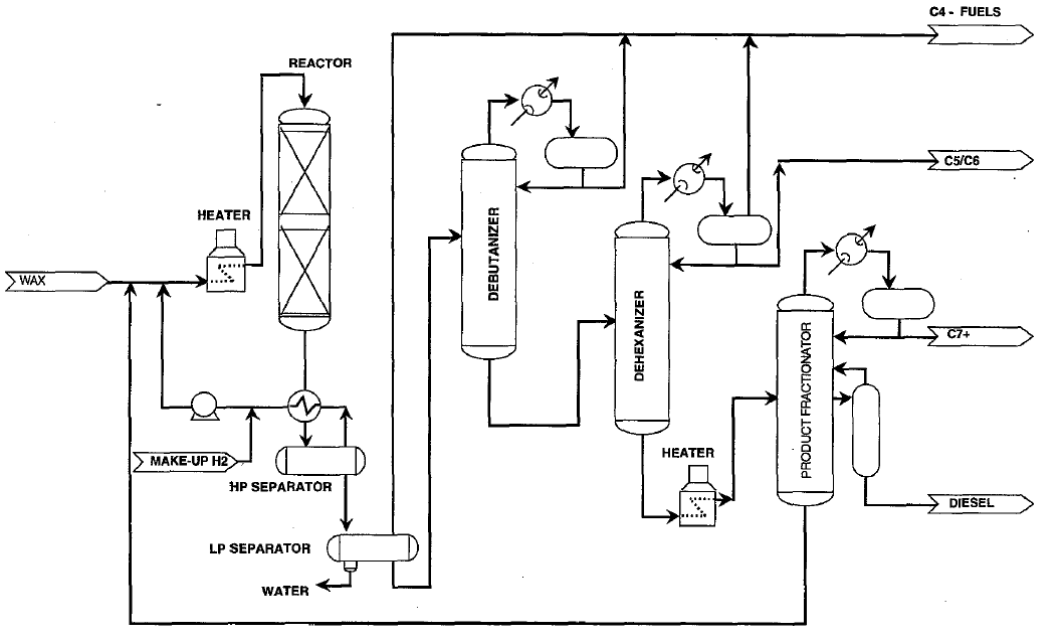

Figure 2.12: Typical wax hydrocracking process flowsheet (DOE, 1994)

The objective of wax hydrocracking is to catalytically crack the FT wax under a hydrogen environment to yield more desirable gasoline and diesel products. Figure 2.12 shows a typical process flow diagram. Wax is first mixed with hydrogen. Then the mixture of wax and hydrogen is preheated in a furnace, which is fed into the hydrocracker. The effluent after the hydrocracker is cooled and sent to a high-pressure separator. The gas after the separator is compressed and recycled back to the hydrocracker. The liquid after the separator is routed to a series of separation towers for product fractionation, where the separation gas is directed to the Saturated Gas Plant (SGP). The products from the wax hydrocracking process are C_1-C_4 offgases, C_5/C_6, gasoline, and diesel.

2.6.3 Distillate Hydrotreating

In the distillate hydrotreater, olefins are saturated to produce a high-cetane diesel product. A typical distillate hydrotreating flow diagram is shown in Figure 2.13. C_{14}-C_{20}

hydrocarbons are mixed with hydrogen, which are sent into a heat exchanger to raise the temperature. The hot mixture is sent to the hydrotreating reactor. The effluent from the reactor is cooled and sent to a high-pressure separator. The gas from the separator is sent to the SGP, while the liquid is collected as the liquid fuel product. The products in this plant are C_1-C_4 off-gases and diesel product.

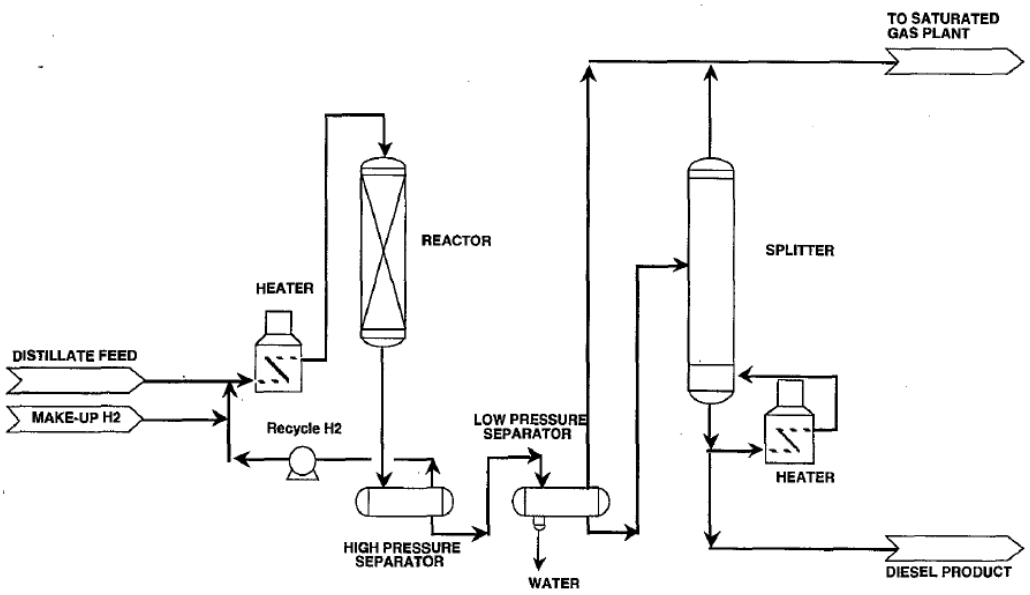

Figure 2.13: Typical distillate hydrotreating process flowsheet (DOE, 1994)

2.6.4 Kerosene Hydrotreating

Kerosene hydrotreating process involves saturating olefins to produce kerosene product. A typical kerosene hydrotreating process flowsheet is shown in Figure 2.14. C_{11}-C_{13} hydrocarbons are mixed with hydrogen, which are sent into a heat exchanger. The hot mixture is sent to the hydrotreating reactor. The effluent from the reactor is cooled and sent to a high pressure separator. The off-gases from the separator are sent to the SGP, while the liquid is collected as the liquid fuel product. The products in this plant are C_1-C_4 off-gases and kerosene product.

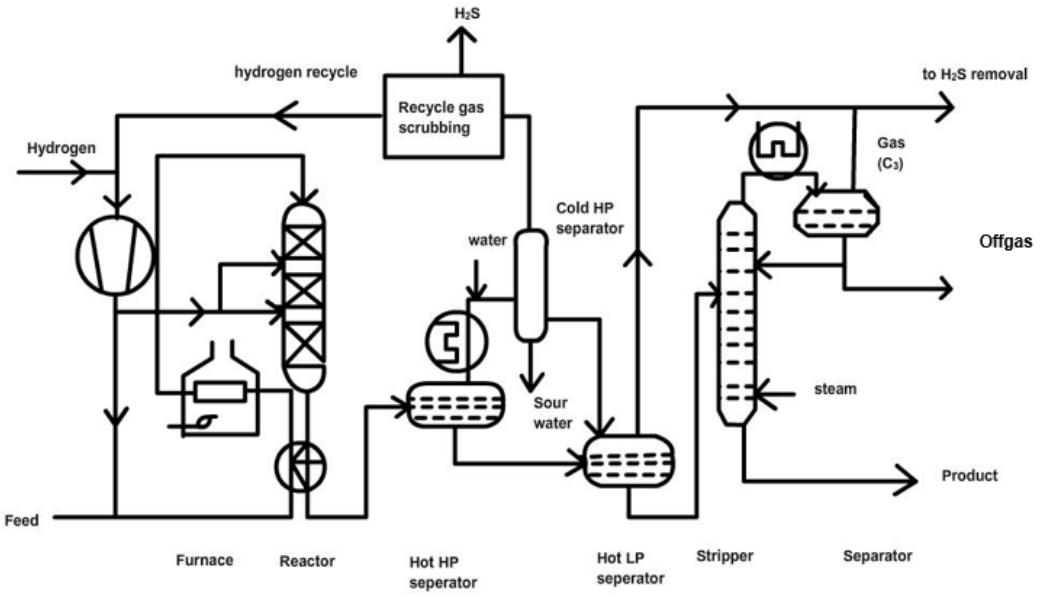

Figure 2.14: Typical kerosene hydrotreating process flowsheet

2.6.5 Naphtha Hydrotreating

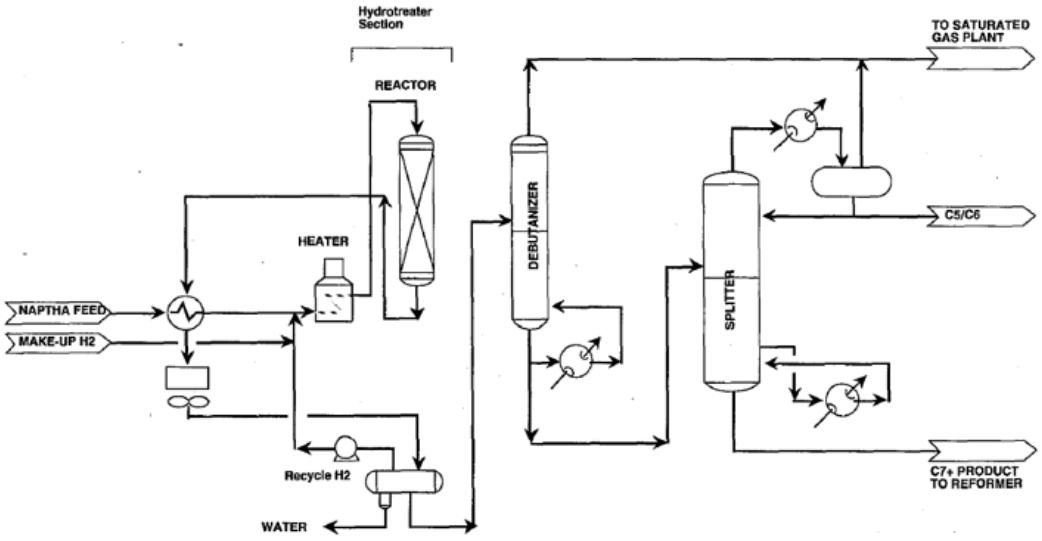

Figure 2.15: Typical naphtha hydrotreating process flowsheet (DOE, 1994)

Naphtha hydrotreating is used to convert olefins from the FTS process to get the feed for the C_5/C_6 isomerization and catalytic reforming process. Figure 2.15 shows a typical naphtha hydrotreating process flow diagram. C_6-C_{10} hydrocarbons are mixed with

hydrogen, which are sent into a heat exchanger. The hot mixture is sent to the hydrotreating reactor. The effluent from the reactor is cooled and sent to a high pressure separator. The C_1-C_4 off-gases from the separator are sent to the SGP. The C_5/C_6 gases are sent to the C_5/C_6 isomerizer. The liquid is collected and sent to a catalytic reformer to get high octane number gasoline. The products in this plant are C_1-C_4 off-gases, C_5/C_6, and treated naphtha.

2.6.6 Naphtha Catalytic Reforming

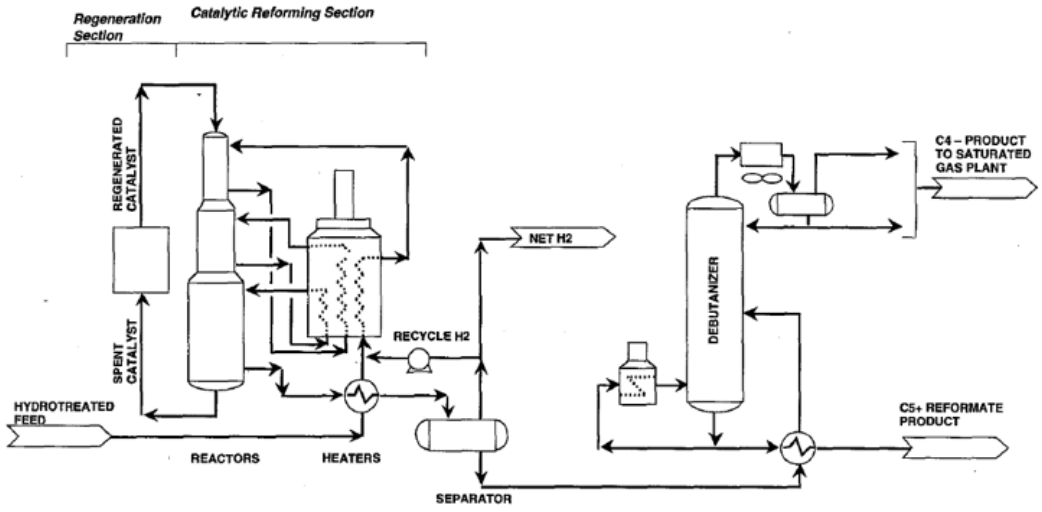

Figure 2.16: Typical catalytic reforming process flowsheet

Naphtha catalytic reforming is used to increase the octane number of gasoline. Figure 2.16 shows a typical catalytic reforming process flow diagram. Hydrotreated naphtha from both the naphtha hydrotreating process and wax hydrocracking process is mixed with hydrogen. The mixture of naphtha and hydrogen is heated by in heat exchanger and sent to the catalytic reformer. The effluent of the catalytic reformer is cooled and sent to a separator. The C_1-C_4 off-gases from the separator are sent to SGP, while the liquids are collected as the gasoline product.

2.6.7 C_4 Isomerization

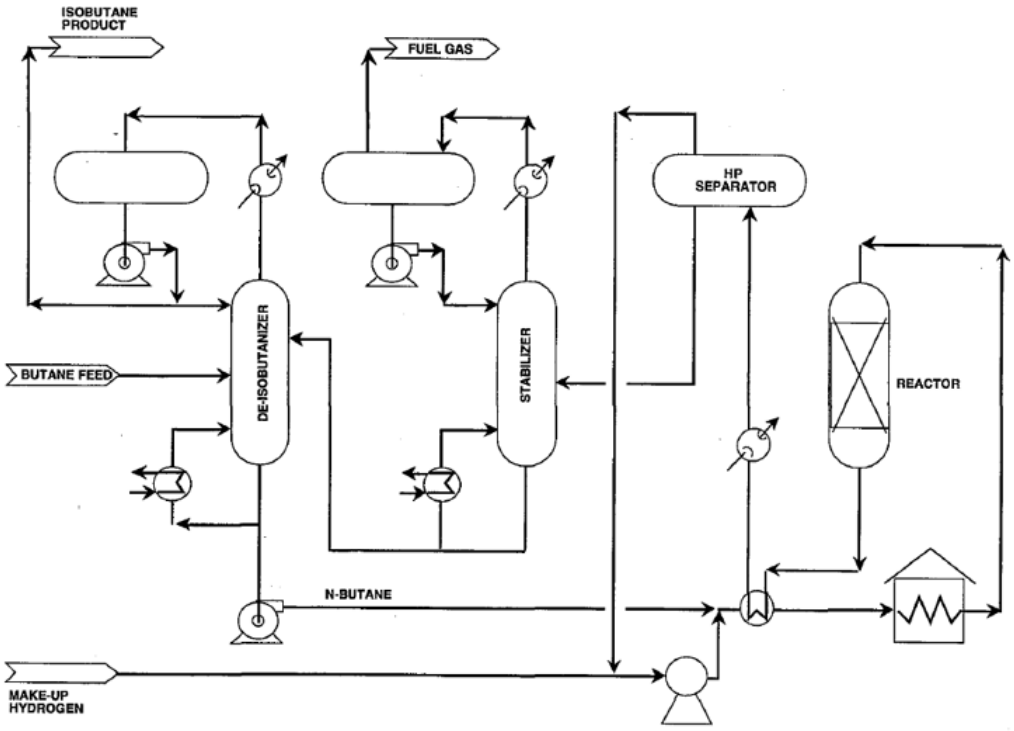

Figure 2.17: Typical C_4 isomerization process flowsheet

In the C_4 isomerization process, n-butane purchased and generated from SGP is converted to isobutene for the alkylation process. A typical C_4 isomerization process flow diagram is shown in Figure 2.17. The n-butane purchased and generated from SGP is mixed with hydrogen. The mixture is heated to the reaction temperature in a heat exchanger, and then sent into the C_4 isomerizer. The n-butane is isomerized to a near-equilibrium concentration of isobutane. The isomerization products are sent into a separator to get C_1-C_3 offgases, n-butane, and isobutane. The C_1-C_3 off-gases and n-butane are recycled back to SGP, while isobutane is sent to the alkylation process.

2.6.8 C_5/C_6 Isomerization

C_5/C_6 isomerization is used to convert low-octane straight chained C_5 and C_6 paraffins to higher-octane branched iso-paraffins. Figure 2.18 shows a typical C_5/C_6 isomerization flow diagram. The C_5/C_6 hydrocarbons from the wax hydrocracker and naphtha hydrotreater are mixed with hydrogen. This mixture is heated by a heat exchanger to the reaction temperature and then sent to the isomerization reactor. The isomerization products are sent into a separator to get C_1-C_4 off-gases, C_5/C_6 iso-paraffins. The C_1-C_4 off-gases are sent to SGP, while the C_5/C_6 isoparaffins are collected as the gasoline product.

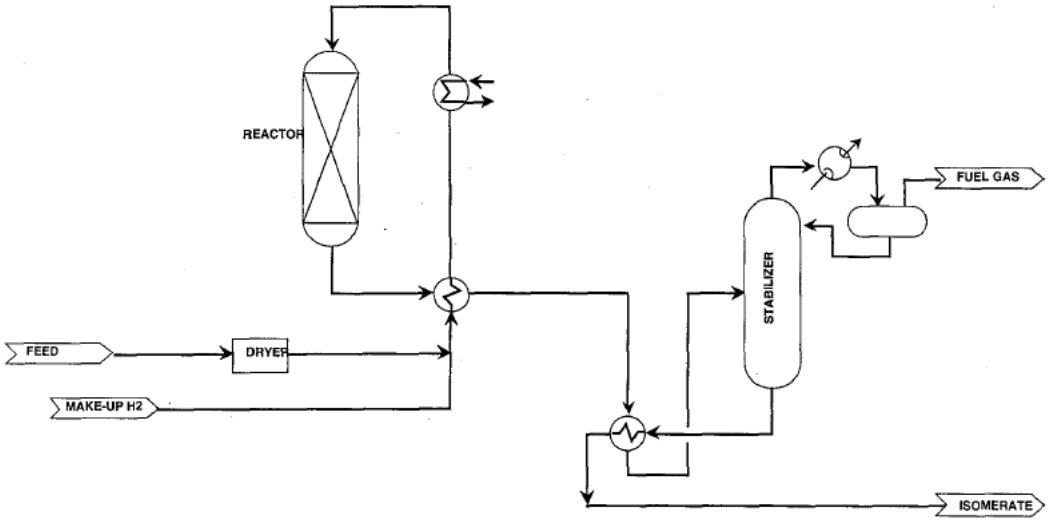

Figure 2.18: Typical C_5/C_6 isomerization process flowsheet

2.6.9 $C_3/C_4/C_5$ Alkylation

A $C_3/C_4/C_5$ alkylation process is used to convert C_3, C_4 and C_5 olefins to a high-octane gasoline blending stock. Figure 2.19 gives a typical $C_3/C_4/C_5$ alkylation process diagram. The $C_3/C_4/C_5$ hydrocarbons from the FTS process is mixed with the isobutane from the C_4

isomerization process. The mixture is heated to the reaction temperature and then sent to the alkylation reactor. The alkylation products are C_3 off-gas, n-butane, and alkylate. C_3 off-gas is sent to SGP. n-butane is sent to C_4 isomerization process. Alkylate is collected as the gasoline product.

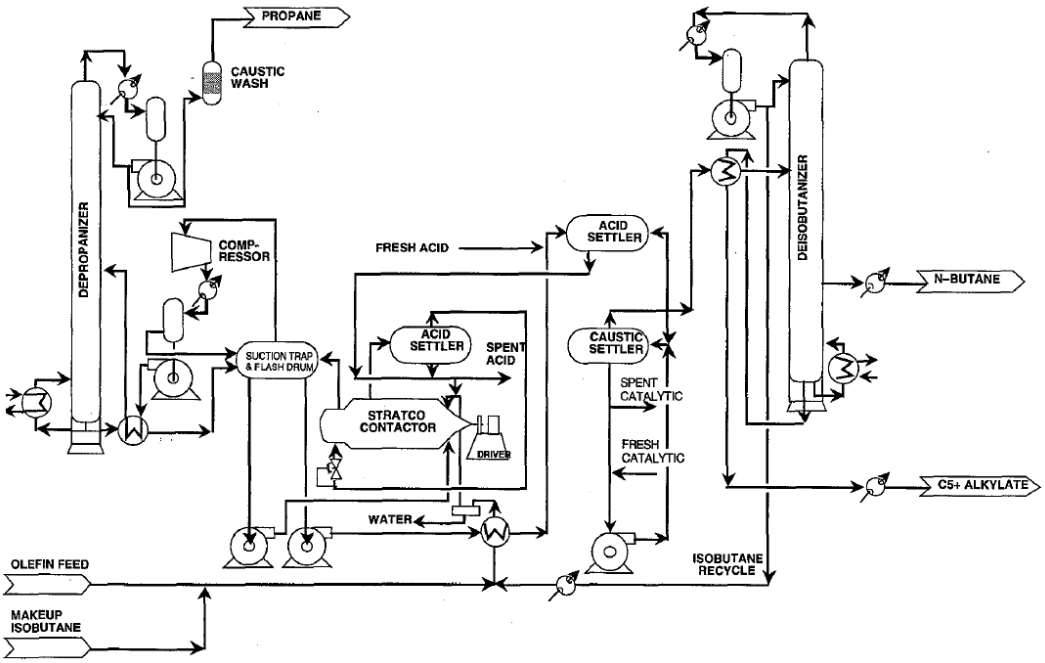

Figure 2.19: Typical $C_3/C_4/C_5$ alkylation process flowsheet

2.7 Air Separation Unit

Nitrogen, oxygen, and argon, which are the main composition of air, are used in several industries, such as the steel, chemical, semiconductor, aeronautical, refining, food processing, and medical industries. An air separation unit (ASU) separates atmospheric air into its primary components, typically nitrogen and oxygen. Because of the different demands for the gas purity, gas amount, and gas usage, there are two different types of air separation processes, i.e. cryogenic process and non-cryogenic process (Li et al., 2014). Non-cryogenic processes are used to generate lower volume, gaseous oxygen or nitrogen

products. Cryogenic processes are used to produce liquid products, larger volume gaseous products, high purity products, or the recovery of argon.

2.7.1 Non-cryogenic Air Separation Process

Non-cryogenic processes are cost effective choices when demand of gases is relatively small and when very high purity of the gases is not required. Non-cryogenic processes use physical property differences such as molecular structure, size and mass to produce nitrogen and oxygen. Non-cryogenic processes are based on either selective adsorption or permeation through membranes (Satyendra, 2013).

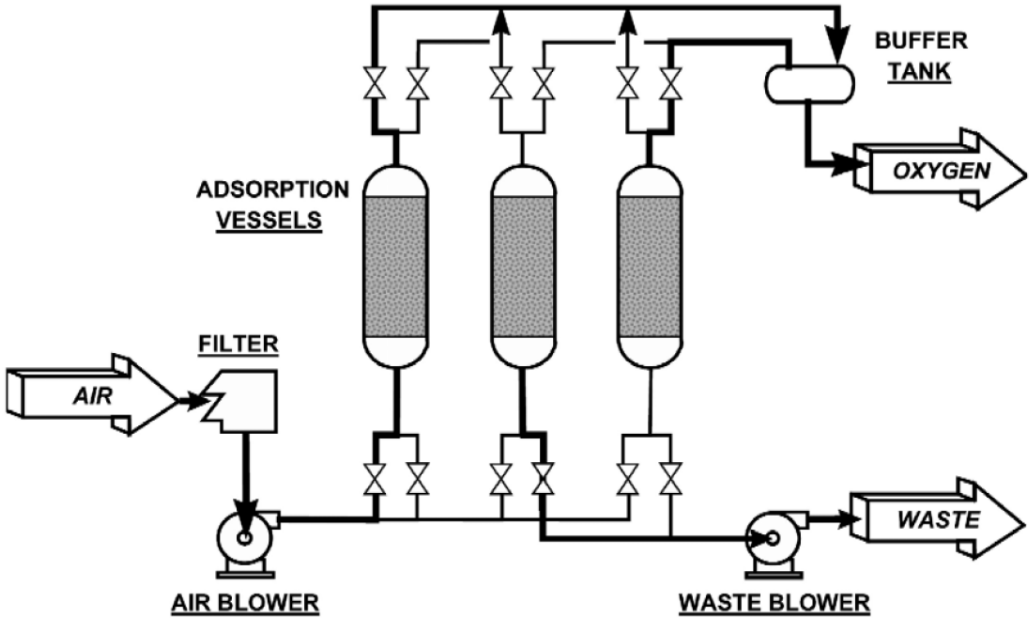

Figure 2.20: Typical flowsheet of adsorption-based air separation process

Adsorption processes are based on the ability of some natural and synthetic materials to preferentially adsorb nitrogen. For air separation process, nitrogen molecules are more strongly adsorbed than oxygen or argon molecules. When air passes through a bed of adsorption material, nitrogen is adsorbed in the pores of the adsorption material, while an

oxygen-rich stream exits the bed. Zeolites are typically used as adsorption material for oxygen production. Figure 2.20 shows a typical flowsheet of using zeolites to get oxygen from air. Pressurized air enters a vessel containing the adsorbent. Nitrogen is adsorbed by the adsorption material and the exit is oxygen-rich product. The operating efficiency of adsorption-based air separation process is affected by the separate pretreatment of air, multiple beds to permit pressure energy recovery during bed switching, and vacuum operation during depressurization. Oxygen purity from this process is typically 93-95 vol.% (Smith & Klosek, 2001).

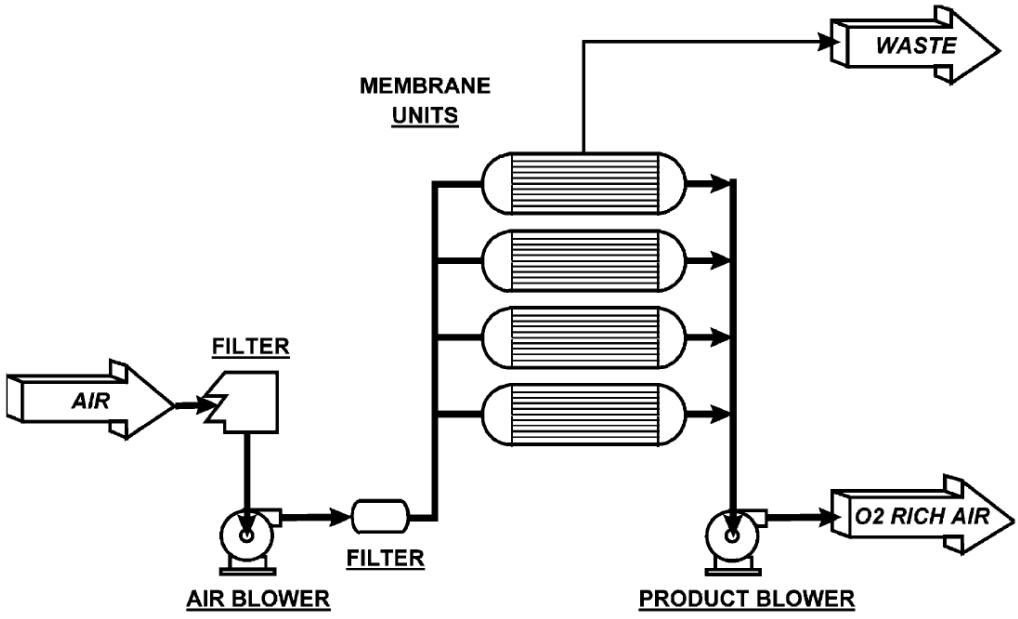

Figure 2.21: Typical flowsheet of membrane air separation process

Membrane processes for air separation are based on the difference in rates of diffusion of oxygen and nitrogen through a membrane which separates high-pressure and low-pressure process streams. The smaller size of oxygen molecules makes the membrane materials more permeable to oxygen than to nitrogen. Membrane systems are usually limited to the production of oxygen enriched air (25-50% oxygen). Figure 2.21 shows a typical membrane process for air separation. To overcome the pressure drop for air passing

through the filters, membrane tubes and piping, an air blower is used to supply sufficient head pressure. Oxygen is produced by permeating through a fiber (hollow fiber type) or through sheets (spiral wound type). A major benefit of membrane air separation is the simple, continuous nature of the process and operation at near ambient conditions (Smith & Klosek, 2001).

2.7.2 Cryogenic Air Separation Process

Cryogenic air separation is the most efficient and widely used technology for producing large quantities of oxygen, nitrogen, and argon as gaseous or liquid products. An ASU uses a conventional, multi-column cryogenic distillation process to produce oxygen at high recoveries and purities. The five major unit operations of a cryogenic air separation process is shown in Figure 2.22. The air pretreatment section removes process contaminants after air is compressed. After the pretreatment section, the air is then cooled to cryogenic temperatures and distilled into oxygen, nitrogen, and, optionally, argon streams. Numerous configurations of heat exchange and distillation equipment can separate air into the required products.

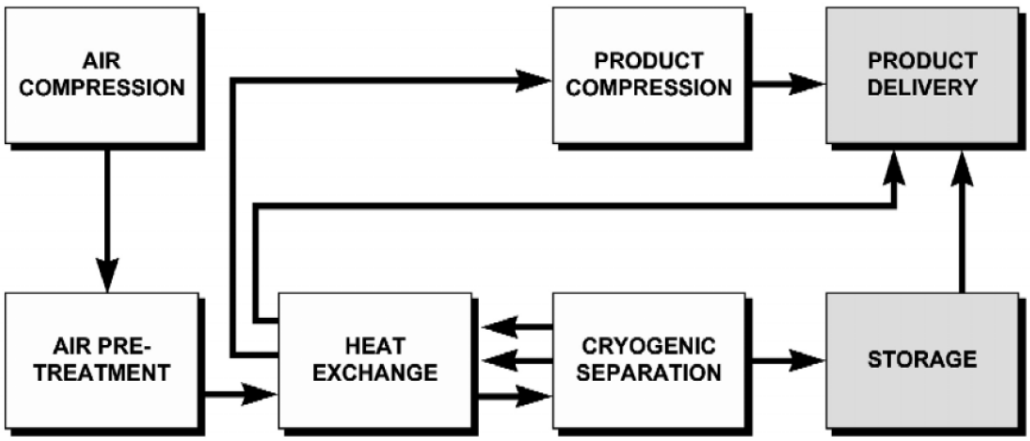

Figure 2.22: Major unit operations of a cryogenic air separation process

2.7.3 Process Description of ASU

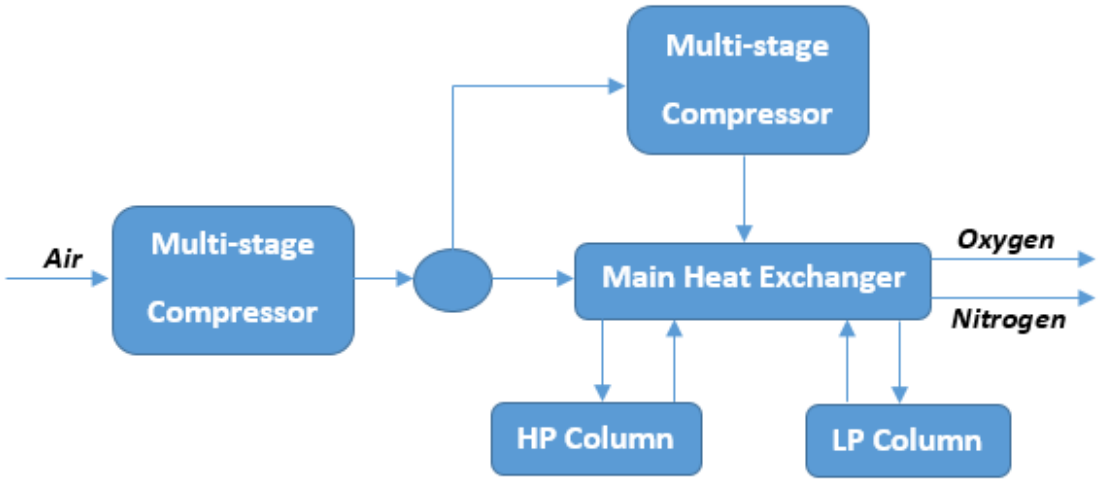

Figure 2.23: ASU flowsheet

Cryogenic air separation process has been used in this study. Figure 2.23 shows the ASU flowsheet. Ambient air is filtered and compressed in a three-stage axial centrifugal compressor with inter-stage cooling. The air from the final compression stage enters a direct contact aftercooler where it contacts cooling water (DOE, 1994). The compressed air then enters a main heat exchanger and is further cooled and partially liquefied by a countercurrent heat exchanger with cold nitrogen and oxygen streams from the distillation columns (Raibhole & Sapali, 2012). Partially liquefied air enters the high-pressure distillation column. The separated N_2 gas condenses to provide reflux to the high pressure (HP) distillation column and enters the low pressure (LP) distillation column after sub cooling in the sub-cooler. The oxygen-rich liquid stream after the main heat exchanger is discharged to a certain pressure and then fed into a low-pressure distillation column. This column separates a N_2 gas stream from the top of the low pressure distillation column and

a liquid oxygen stream from bottom of the low pressure distillation column, which are fed to the main heat exchanger and heated to ambient temperature.

2.8 Power Generation

A gas turbine power cycle is integrated into once-though FTS biomass conversion process. Figure 2.23 shows the power generation plant flowsheet. Air is compressed in a compressor and preheated in the heat exchangers. Then the light gases from the SGP are mixed with the compressed air, which are sent into the combustion chamber to get combusted. Hot gases from combustion are expanded in the gas turbine to generate electricity (Løver, 2007). Expanded exhaust gas is then cooled down in the heat exchangers and sent to a water knockout unit to remove the water.

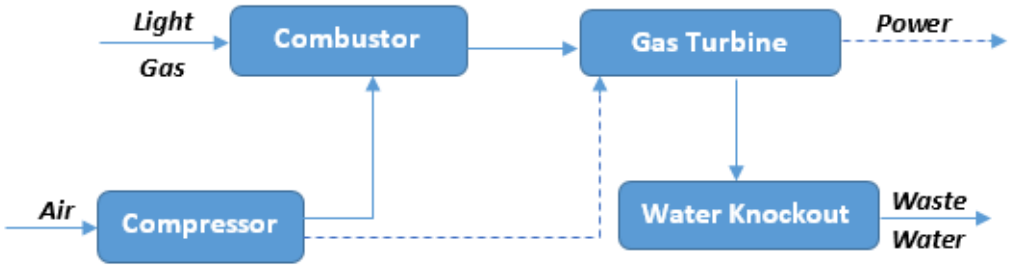

Figure 2.24: Power generation plant flowsheet

Chapter 3

Process Modeling

Chapter 2 provided the main process sections used in the biomass conversion process designed in this study to obtain transportation fuels. However, it remains unclear how exactly transportation fuels from the raw biomass will be obtained. In this chapter, process models for the main parts are developed to establish the mass and energy balances of the process. Aspen Plus™ is used as the simulation tool.

3.1 Simulation in Aspen Plus

The Aspen Plus™ simulation environment provides a flexible input language for describing biomass conversion process components, connectivity, and computational sequences. Use of Aspen Plus™ leads to an easier way of model creation, maintenance and updating since small sections of complex and integrated systems can be created and tested as separate modules before they are integrated. It has an extensive physical property database which can be used for modeling biomass conversion process (Ong'iro et al., 1995). Aspen Plus™ has many built-in model blocks, such as heat exchangers, mixers, reactors, compressors etc., which represent processes taking place in an actual chemical plant and can be used directly for biomass conversion process simulation. By specifying configurations of model blocks and the flow of material, heat and work streams, a process can be simulated in Aspen Plus™. It has mathematical routines (convergence algorithms) to solve different equations of material and energy balances as well as equilibrium

equations (Magnusson, 2005). When more sophisticated block ability is required, Fortran subroutines can be used, or user-defined blocks can be used to simulate the process. In this study, the FT reactor for the conventional FTS biomass conversion process and all the hydrocarbon upgrading units are modeled as user-defined blocks.

3.2 Biomass Handling and Drying Modeling

As mentioned in chapter 2.2, biomass is delivered to the plant and treated to reduce the particle size prior to drying in order to enhance the heat and material transfer rate. Screw conveyors are also used to move the reduced biomass particles. However, these specific pieces of hardware are not available for modeling in Aspen Plus™.

The biomass drying process is modeled based on the Aspen Plus™ guide for solids (ASPEN, 2013). In Aspen Plus™, biomass is defined as a nonconventional component. The wet biomass is fed to the dryer at 77°F and 14.7 psia. The Aspen Plus™ stoichiometric reactor model RStoic and Flash2 are used to simulate a single piece of plant equipment for drying biomass. Nitrogen provides the heat for biomass drying. Both the RStoic and Flash2 models are isobaric and adiabatic. The pressure is set as 14.7 psia and the duty is set as 0 Btu/hr in both reactors. Although biomass drying is not normally considered as a chemical reaction, an RStoic block is used to convert a portion of the biomass to form water. Eq. 3.1 is assumed as the chemical reaction for biomass drying:

$$\text{biomass (wet)} \rightarrow 0.0555084\ H_2O \qquad \text{(Eq. 3.1)}$$

Aspen Plus™ treats all nonconventional components as if they have a molecular weight of 1.0. The above reaction indicates that 1 mole of biomass reacts to form 0.0555084 mole of water.

A calculator block is used to control biomass drying. The material balance equations for biomass drying process define relations between the following quantities:

- water content of the biomass feed
- fractional conversion of biomass to water
- water content of the dried biomass

Eq. 3.2 is derived to calculate the conversion specification in RStoic.

$$CONV=\frac{M^{i}-M^{o}}{100-M^{o}} \qquad \text{(Eq. 3.2)}$$

Where *CONV* indicates the drying efficiency; M^{i} and M^{o} denote the moisture contents of biomass before and after being dried, respectively. The final moisture in this study is set as 5.0 wt. %.

3.3 Biomass Gasification Modeling

Since biomass is classified as nonconventional component in Aspen Plus™, certain thermodynamic parameters cannot be directly calculated by the software. Therefore, a yield reactor, RYIELD, is used to simulate the decomposition of biomass to actual chemical components. In the yield reactor, biomass is converted to its constituent parts including carbon, hydrogen, oxygen, sulfur, nitrogen, and ash. The yield is specified according to the biomass ultimate analysis.

After the decomposition process, biomass is sent to a gasifier combined with oxygen and steam. The gasifier used in this study is a high-pressure oxygen blown bubbling fluidized bed gasifier. The gasifier is modeled using correlations based on data from the Gas Technology Institute (GTI) 12 tonne/day test facility (Evans et al., 1988). The correlations are presented in Appendix B. Oxygen from ASU and steam are mixed and

heated to the gasifier temperature. Oxygen feed is about 0.23 lb per lb of bone dry biomass. Adding more steam or increasing the target temperature increases the amount of combustion, which depletes the amount of syngas that can be used for FTS. The composition of the outlet gas from the gasifier is shown in Table 3.1.

Table 3.1: Gasifier operating parameters and gas compositions

Gasifier Variable	**Value**	
Temperature	1600°F	
Pressure	438 psia	
Gasifier outlet gas composition	mol % (wet)	mol % (dry)
H_2	18.59	21.52
CO	17.51	20.27
CO_2	29.43	34.07
CH_4	17.54	20.30
C_2H_6	1.04	1.20
C_6H_6	1.40	1.63
tar ($C_{10}H_8$)	0.52	0.60
NH_3	0.30	0.34
H_2S	0.05	0.06
H_2O	13.62	--
H_2 : CO molar ratio	1.06	

3.4 Tar Reformer Modeling

The raw syngas after the gasifier cyclone is sent to the catalytic tar reformer. In this bubbling fluidized bed reactor the C_1-C_2 hydrocarbons and tar species are reformed to CO and H_2, while NH_3 is reformed to N_2 and H_2. A stoichiometric reactor, RStoic, is used to model the tar reformer. The temperature and pressure are set as 1517°F and 431 psia, respectively. The pressure of 431 psia is chosen because it is slightly lower than the gasifier exit pressure of 438 psia. Additional steam input is used to increase the carbon conversion in tar reformer. The reactions are modeled as Eq. 3.3 – Eq. 3.7.

$$CH_4 + H_2O \rightarrow CO + 3H_2 \quad \text{(Eq. 3.3)}$$

$$C_2H_6 + 2H_2O \rightarrow 2CO + 5H_2 \quad \text{(Eq. 3.4)}$$

$$C_{10}H_8 + 10H_2O \rightarrow 10CO + 14H_2 \quad \text{(Eq. 3.5)}$$

$$C_6H_6 + 6H_2O \rightarrow 6CO + 9H_2 \quad \text{(Eq. 3.6)}$$

$$2NH_3 \rightarrow N_2 + 3H_2 \quad \text{(Eq. 3.7)}$$

The conversion of each compound is based on the current bench-scale performance of a tar reformer from NREL (Dutta & Phillips, 2009; Phillips et al., 2011). The target design performance of tar reformer is shown in Table 3.2.

Table 3.2: Target design performance of tar reformer

Compound	Target Conversion to CO & H_2
Methane (CH_4)	80%
Ethane (C_2H_6)	99%
Benzene (C_6H_6)	99.60%
Tar ($C_{10}H_8$)	99.60%
Ammonia (NH_3)	90%

3.5 Fischer-Tropsch Synthesis Modeling

3.5.1 Supercritical FTS Modeling

After the syngas scrubbing system, the H_2/CO ratio is very low, which is not suitable for supercritical FTS. To adjust the H_2/CO ratio, a water gas shift reactor is used. In Aspen Plus™, an RGibbs reactor is used to model the water gas shift reactor. The temperature and pressure are set as 560°C and 28 bar.

Elbashir and Roberts (2005) studied the effect of reaction temperature and pressure on CO conversion in supercritical FTS. The results indicated that the optimal operating

conditions to maximize FT fuel production are 250°C and 65 bar with a CO conversion of 0.85.

Table 3.3: Reactions in supercritical FTS reactor

Reaction	CO conversion
$CO + 3H_2 \rightarrow CH_4 + H_2O$	0.14718332
$2CO + 5H_2 \rightarrow C_2H_6 + 2H_2O$	0.00504988
$3CO + 7H_2 \rightarrow C_3H_8 + 3H_2O$	0.01066858
$4CO + 9H_2 \rightarrow C_4H_{10} + 4H_2O$	0.01238410
$5CO + 11H_2 \rightarrow C_5H_{12} + 5H_2O$	0.01757500
$6CO + 13H_2 \rightarrow C_6H_{14} + 6H_2O$	0.01805530
$7CO + 15H_2 \rightarrow C_7H_{16} + 7H_2O$	0.03314586
$8CO + 17H_2 \rightarrow C_8H_{18} + 8H_2O$	0.02893211
$9CO + 19H_2 \rightarrow C_9H_{20} + 9H_2O$	0.04958491
$10CO + 21H_2 \rightarrow C_{10}H_{22} + 10H_2O$	0.05129589
$11CO + 23H_2 \rightarrow C_{11}H_{24} + 11H_2O$	0.04196833
$12CO + 25H_2 \rightarrow C_{12}H_{26} + 12H_2O$	0.04456514
$13CO + 27H_2 \rightarrow C_{13}H_{28} + 13H_2O$	0.05179173
$14CO + 29H_2 \rightarrow C_{14}H_{30} + 14H_2O$	0.05111690
$15CO + 31H_2 \rightarrow C_{15}H_{32} + 15H_2O$	0.04268219
$16CO + 33H_2 \rightarrow C_{16}H_{34} + 16H_2O$	0.04247476
$17CO + 35H_2 \rightarrow C_{17}H_{36} + 17H_2O$	0.04252344
$18CO + 37H_2 \rightarrow C_{18}H_{38} + 18H_2O$	0.04200030
$19CO + 39H_2 \rightarrow C_{19}H_{40} + 19H_2O$	0.03033064
$20CO + 41H_2 \rightarrow C_{20}H_{42} + 20H_2O$	0.02319241
$21CO + 43H_2 \rightarrow C_{21}H_{44} + 21H_2O$	0.01897179
$22CO + 45H_2 \rightarrow C_{22}H_{46} + 22H_2O$	0.01502597
$23CO + 47H_2 \rightarrow C_{23}H_{48} + 23H_2O$	0.01146745
$24CO + 49H_2 \rightarrow C_{24}H_{50} + 24H_2O$	0.01056270
$25CO + 51H_2 \rightarrow C_{25}H_{52} + 25H_2O$	0.00745130

Therefore, the supercritical FT reactions operates at the optimal conditions of 250°C and 65 bar in the supercritical hexane solvent with a CO conversion of 0.85. Supercritical

hexane/syngas molar ratio is set as 3. Prior to being fed to the FTS reactor, syngas and supercritical hexane are heated to the reactor temperature and compressed to the reactor pressure, which is 250^{o}C and 65 bar, respectively. The main products are paraffins, olefins and oxygenated products. In this study, only paraffins are considered as the products. A stoichiometric reactor, RStoic, is used to model the supercritical FTS reactor. Table 3.3 gives the detailed reactions in the supercritical FTS reactor.

In the RStoic specification, the CO conversion for each reaction is specified. The total CO conversion of all the reactions is 0.85 (Yuan, 2011). In Aspen Plus^{TM}, two SEP separators are used to model the separation of FT hydrocarbons. The first separator is used to separate light gases, C_3-C_5 gases, supercritical hexane, and heavy hydrocarbons. The second separator is used to separate C_6-C_{10} naphtha, C_{11}-C_{13} kerosene, C_{14}-C_{20} distillate, and C_{21}-C_{25} wax.

3.5.2 Once-through and Conventional FTS Modeling

The FT reactor is modeled using the USER2 block in Aspen Plus^{TM} for once-through and conventional FTS modeling. The USER2 block allows the Aspen Plus^{TM} engine to dynamically link to a Microsoft Excel^{TM} spreadsheet, where user-input calculations can provide the necessary effluent concentrations. The outlet stream conditions of the USER2 block can be set to a given temperature and pressure. The USER2 block serves as a means of implementing a probabilistic FT model based on the chain growth factor α (Baliban et al., 2010). According to Song et al. (2004), the chain growth factor depends on the molar fraction of H_2 and CO, temperature of the reactor, and the type of catalyst. Each type of

catalyst has different values of α ranging from 0.6 to 0.9. In this study, the chain growth factor α is modeled as Eq. 3.8 (Wang et al., 2013).

$$\alpha = \left[0.2332\left(\frac{mf_{CO}}{mf_{H_2}+mf_{CO}}\right)+0.633\right][1-0.0039(T^{fts}-533)]$$

(Eq. 3.8)

where T^{fts} is the FTS reactor temperature in K; mf_{CO} and mf_{H_2} are the mole fraction of CO and H_2 in feed streams to FTS reactor. In this study, the FTS reactor temperature is set as 250°C.

Although the FT product distribution follows the theoretical ASF alpha distribution, the observed yields of the lighter hydrocarbons are higher than what the ASF distribution predicts (Oukaci, 2002; Zwart & Boerrigter, 2005). A slightly modified ASF distribution is used to model the FT unit to incorporate the deviation in Eq. 3.9-3.12 (Baliban et al., 2010).

$$W_1 = \frac{1}{2}\left(1-\sum_{n=5}^{\infty} W_n\right) \quad \text{(Eq. 3.9)}$$

$$W_j = \frac{1}{6}\left(1-\sum_{n=5}^{\infty} W_n\right) \quad j = 2,3,4 \quad \text{(Eq. 3.10)}$$

$$W_n = n(1-\alpha)^2\alpha^{n-1} \qquad \forall 5 \le n \le 29 \quad \text{(Eq. 3.11)}$$

$$W_{wax} = \sum_{n=30}^{\infty} n(1-\alpha)^2\alpha^{n-1} \quad \text{(Eq. 3.12)}$$

where W_n is the weight fraction of C_n compounds and α is the chain growth factor.

Based on the weight fractions, the carbon present at each hydrocarbon length, cr_n, is defined in Eq. 3.13.

$$cr_n = \frac{nW_n}{\sum_{n=1}^{29} + n_{Wax}W_{wax}} \quad \text{(Eq. 3.13)}$$

where cr_n represents the fraction of carbon that is present at chain length n for all desired n.

The input-output relationships between incoming and outgoing species in the FTS reactor are given in Eq. 3.14-3.16.

$$F_s^{CS} = F_s^{FT} \qquad \forall s \in S_{FT}^{Inert} \tag{Eq. 3.14}$$

$$(1 - fc_{CO}^{FT})F_{CO}^{CS} = F_{CO}^{FT} \tag{Eq. 3.15}$$

$$cr_s^{FT} fc_{CO}^{FT} F_{CO}^{CS} = F_s^{FT} \qquad \forall s \in S_{FT}^{HC} \tag{Eq. 3.16}$$

where S_{FT}^{Inert} is the set of all inert species that do not participate in the FT reactions; S_{FT}^{HC} is the set of all hydrocarbon species in the FT reactor; F_s^{CS} is the flow rate of component *s* in the clean syngas stream; F_s^{FT} is the total flow rate of component s exiting the FT reactor; fc_{CO}^{FT} is the fractional conversion of CO in the FT reactor, which is assumed to be 0.8; cr_s is calculated for each species *s* based on the chain length of the species. Eq. 3.14 sets the inlet and outlet flow rates of the components, which do not participate in the FT reactions equal to each other. Eq. 3.15 gives the flow rate of unconverted CO exiting the FT reactor. Eq. 3.16 gives the exiting composition of the hydrocarbon products from FT reactor. Additionally, the amounts of H_2 consumed and H_2O produced are calculated according to the stoichiometric reactions for each hydrocarbon species, and their output flow rates can be obtained (Baliban et al., 2010).

The hydrocarbon products from once-through FTS and conventional FTS are represented by paraffins, olefins, oxygenated products. In this study, hydrocarbon products up to C_{20} are represented by paraffins and olefins (one double bond). The fraction of paraffins is 20% for C_2-C_4, 25% for C_5-C_6, and 30% for C_7-C_{20} (Bechtel, 1998). C_4-C_6 hydrocarbons are present in both linear and branched form with a branched carbon fraction

of 5% for C_4 and 10% for C_5-C_6 (Bechtel, 1998). C_{21}-C_{29} hydrocarbons are represented by pseudo-components that have properties consistent with 70 mol % olefin and 30 mol % paraffin. All C_{30+} compounds are represented by a generic wax pseudo-component ($C_{52.524}H_{105.648}O_{0.355}$) (Bechtel, 1998). The chemical composition of the pseudo-components is shown in Table 3.4. The input properties for pseudo-components are shown in Table 3.5 (Baliban et al., 2010), which can be put in Aspen Plus™ for calculation.

Table 3.4: Chemical composition of pseudo-components in FT reactor modeling

Pseudo-component	# C	# H	# O
C21OP	21	42.6	0
C22OP	22	44.6	0
C23OP	23	46.6	0
C24OP	24	48.6	0
C25OP	25	50.6	0
C26OP	26	52.6	0
C27OP	27	54.6	0
C28OP	28	56.6	0
C29OP	29	58.6	0
C30WAX	52.524	105.648	0.335

Table 3.5: Input properties for pseudo-components in FT reactor modeling

Pseudo-component	Average Boiling Point (F)	API gravity	Molecular weight
C21OP	672.2	45.24	295.169
C22OP	694.2	44.68	309.196
C23OP	715.3	44.23	323.223
C24OP	735.4	43.83	337.25
C25OP	754.6	43.45	351.277
C26OP	773.4	43.07	365.304
C27OP	791.2	42.69	379.331
C28OP	808.4	42.42	393.357
C29OP	825	41.87	407.384
C30WAX	1274.3	36.42	742.712

The separation of hydrocarbons from conventional FTS and once-through FTS is modeled by using two SEP separators in Aspen Plus™. The output of first separator is light gases, C_3-C_5 gases, C_6-C_{10} naphtha, and heavy hydrocarbons. The output of the second separator is C_{11}-C_{13} kerosene, C_{14}-C_{20} distillate, and C_{21}-C_{30+} wax.

3.6 Hydrocarbon Upgrading Process Modeling

The modeling of the hydrocarbon upgrading process follows the Bechtel design (DOE, 1994). Since the kerosene hydrotreater is not included in the Bechtel design, it is assumed that the distribution of the input carbon to kerosene and light gases is exactly the same as the distillate hydrotreater (Baliban et al., 2010). The appropriate mass balances for the baseline Illinois No. 6 coal case study (DOE, 1993) were used to determine the output of the hydrocarbon upgrading units. Based on that, the distribution of the input carbon for each upgrading unit is determined either exactly matching or closely approximating the distribution reported by Bechtel. The carbon fraction of hydrocarbon upgrading process is summarized in Table 3.6

All hydrocarbon upgrading units are modeled using USER2 block in Aspen Plus™. The output of hydrocarbon upgrading units can be calculated by linking a Microsoft Excel™ spreadsheet. The wax hydrocracker, distillate hydrotreater, kerosene hydrotreater, naphtha hydrotreater, C_5/C_6 isomerizer, and C_4 isomerizer all require an input of hydrogen. After distributing all input oxygen as the wastewater stream, the effluent of each upgrading unit can be set exactly match the Bechtel output by adjusting the flow of hydrogen. Eq. 3.17-3.21 model the upgrading units.

Table 3.6: Carbon fraction that will be output as particular species.

Component	Carbon Fraction							
	W-Crack*	D-HT*	K-HT*	N-HT*	N-RF*	$C_{56}I$*	C_4I*	$C_{345}A$*
CH_4	0.00039	0.00093	0.00093	0.00393	0.00835	0.00077	0.00170	--
C_2H_6	0.00042	0.00132	0.00132	0.01537	0.02419	--	0.00407	--
C3H8	0.01411	0.00304	0.00304	0.02001	0.03122	0.00407	0.01129	0.02492
iC_4H_{10}	0.01893	0.00137	0.00137	0.00289	0.01914	0.00511	0.94367	--
nC_4H_{10}	0.01536	0.00240	0.00240	0.01350	0.02381	--	0.03927	0.05791
iC_5H_{12}	0.02004	--	--	0.01408	--	0.29387	--	0.00502
nC_5H_{12}	0.02375	--	--	0.00049	--	--	--	0.01635
iC_6H_{14}	0.02320	--	--	0.07412	--	0.68845	--	--
nC_6H_{14}	0.03786	--	--	0.00829	--	--	--	--
iC_7H_{16}	--	--	--	--	--	--	--	0.32323
nC_7H_{16}	--	--	--	0.50574	--	--	--	--
iC_8H_{18}	--		--	--	--	--	--	0.31168
nC_8H_{18}	--	--	--	0.34158	--	--	--	--
iC_9H_{20}	--		--	--	--	--	--	0.26089
Gasoline	0.18840	--	--	--	0.89328	--	--	--
Kerosene	--	--	0.99094	--	--	--	--	--
Diesel	0.65754	0.99094	--	--	--	--	--	--

*W-Crack is wax hydrocracker. D-HT is distillate hydrotreater. K-HT is kerosene hydrotreater. NHT is naphtha hydrotreater. N-RF is naphtha catalytic reformer. $C_{56}I$ is C_5/C_6 isomerizer. C_4I is C_4 isomerizer. $C_{345}A$ is $C_3/C_4/C_5$ alkylation unit.

$$\sum AN_{C,s}F_s^{in} = F_C^{out} \quad \text{(Eq. 3.17)}$$

$$cf_pF_C^{out} = AN_{C,p}F_p \quad \text{(Eq. 3.18)}$$

$$\sum AN_{H,s}F_s^{in} = F_H^{in} \quad \text{(Eq. 3.19)}$$

$$\sum AN_{H,p}F_p = F_H^{out} \quad \text{(Eq. 3.20)}$$

$$\frac{\left(F_H^{out} - F_H^{in}\right)}{2} = F_H^{add} \quad \text{(Eq. 3.21)}$$

where $AN_{C,s}$, $AN_{H,s}$, $AN_{H,p}$, $AN_{C,p}$ are the atomic number of carbon and hydrogen in compound *s* and compound *p*, respectively, while *s* is the hydrocarbon that enters in the upgrading unit and *p* is the product of the upgrading unit; F_s^{in} and F_p is the molar flow rate

of compound *s* that goes into the upgrading unit and the molar flow rate of products from the upgrading unit; F_C^{out} and F_H^{in} are the total atomic input flow rates for carbon and hydrogen to the upgrading unit; cf_p is the carbon fraction in compound *p* of the output streams obtained from the Bethtel case study; F_H^{out} is the atomic flow rates of hydrogen from the products;F_H^{add} is the additional hydrogen that must be put into the upgrading unit to satisfy the atomic balance.

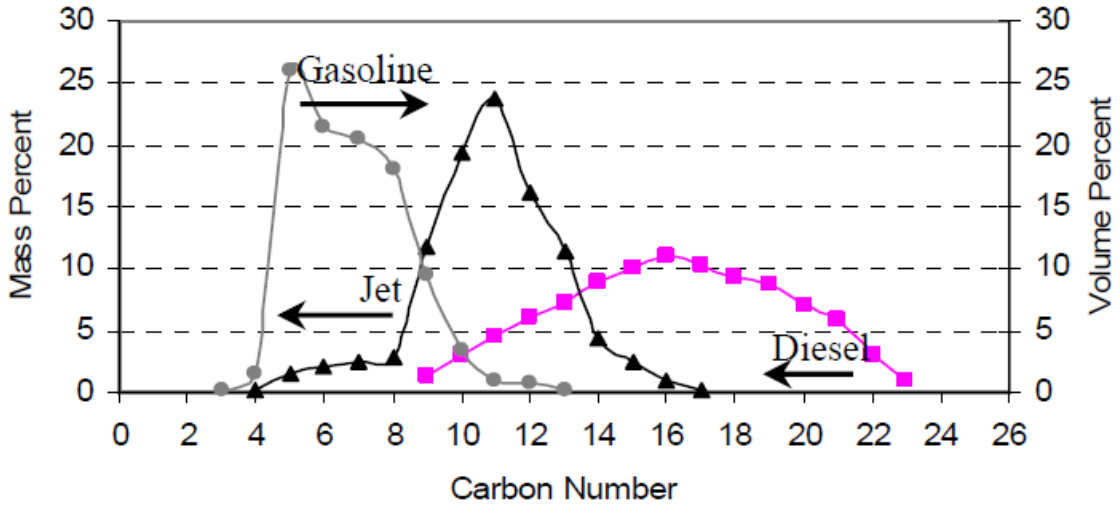

Figure 3.1: Carbon number distribution of typical petroleum fuels

Liquid transportation fuels, i.e. gasoline, kerosene, and diesel, contain a complex mixture of hundreds of hydrocarbons. The hydrocarbons vary by class - paraffins, olefins, and aromatics, depending on the nature of chemical bonding between the carbon atoms in hydrocarbon molecules. The molecular composition of liquid transportation fuels determines their physical properties, engine performance, and thermal stability characteristics. In general, fuels are produced to meet the property limits dictated by the industrial specifications and regulations, not to achieve a specific distribution of hydrocarbons by class, or size (Altin & Eser, 2004). The molecular composition of

gasoline, diesel, and kerosene is modeled in this study. Carbon number distribution of typical gasoline, jet fuel, and diesel is shown in Figure 3.1 (Altin & Eser, 2004).

Based on Figure 3.1, the carbon number distribution of gasoline, kerosene, and diesel in this study is summarized in Figure 3.2.

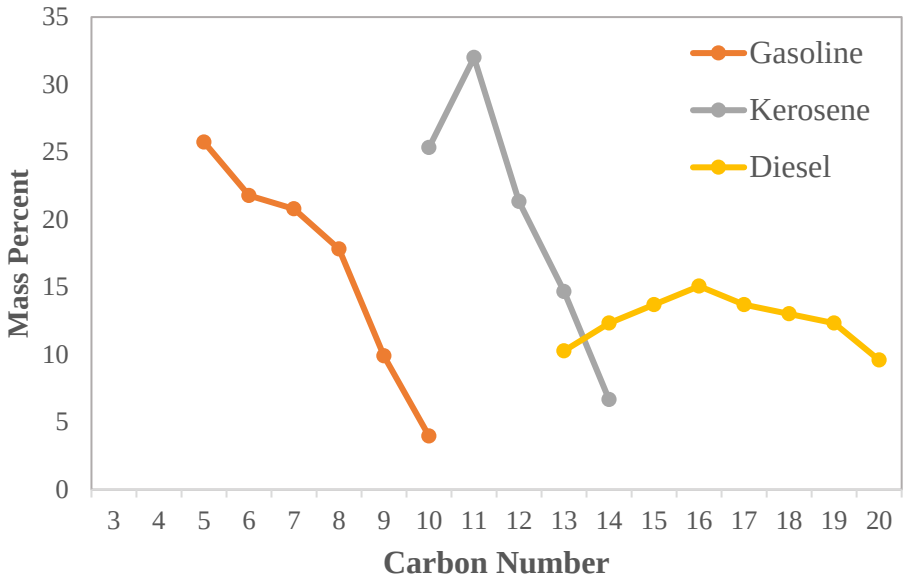

Figure 3.2: Carbon number distribution of gasoline, kerosene, and diesel in this study

Gasoline is modeled as C_5-C_{10} hydrocarbons. Kerosene product is modeled as C_{10}-C_{14} hydrocarbons. Diesel is modeled as C_{13}-C_{20} hydrocarbons. The molecular composition of gasoline, kerosene, and diesel is shown in Table 3.7 (Shafer et al., 2006; Thomas et al.).

Table 3.7: Molecular composition of liquid transportation fuels

Hydrocarbon group type	**Percentage**		
	Gasoline	Kerosene	Diesel
Lineal Paraffin	15%	15%	52%
Branched Paraffin	30%	45%	17%
Cyclo Paraffins	15%	23%	2%
Olefins	5%	--	--
Aromatics	35%	17%	9%
Alkyl Naphthalene	--	--	20%

3.7 Cryogenic Air Separation Modeling

Air is modeled as a mixture of oxygen, nitrogen, and argon. To simulate the ASU, the Peng-Robinson EOS is used. In Aspen Plus™, a multistage compressor/turbine, MCompr, is used to model the three-stage axial centrifugal compressor. The discharge pressure from last stage is set as 4.2 bar. A FSplit is used to model the split of cooled air. 30% of the cooled air is compressed to a pressure of 50 bars in a multistage compressor, MCompr, which gives a positive temperature difference. A multistream heat exchanger, MHeatX, is used to model the main heat exchanger in ASU. Two RadFrac columns are used to model the distillation process. A 2-stream countercurrent heat exchanger, HeatX, is used to model the heat exchanger between the N_2 gas stream from the top of the LP distillation column and the separated N_2 gas from the top of the HP distillation column. The simulation specifications for the ASU are summarized in Table 3.8.

Table 3.8: Simulation specification in ASU

Configurations	Parameters	Value
3-stage MCompr	Discharge pressure	4.2 bar
Fsplit	Split fraction	0.3
2-stage Mcompr	Discharge pressure	50 bar
	Pressure	1.2 bar
LP column	No. of stages	56
	Reflux ratio	0.72
	Pressure	4.2 bar
HP column	No. of stages	40
	Reflux ratio	0.95

3.8 Power Plant Modeling

The model for the power plant includes realistic representation of the various units used in commercial power plants reflecting pressure drops and characteristic temperature differences in heat transfer components. Both air compressor and gas turbine are modeled

in Aspen Plus™ by a block called Compr. In this study, Compr models isentropic air compressor and gas turbine. Compr calculates the power required or produced using the pressure ratio, isentropic and mechanical efficiencies. The operating parameters for air compressor and gas turbine in Aspen Plus™ are given in Table 3.9 (Jana & De, 2014; Ong'iro et al., 1995). The Combustor converts the chemical energy to heat energy, which is transferred to the working fluid. The Combustor in the power plant is modeled as RGibbs reactor in Aspen Plus, which calculates equilibrium by Gibbs free energy minimization. The operation conditions for combustor is also summarized in Table 3.9 (Carroni et al., 2002).

Table 3.9: Operating parameters for power plant in Aspen Plus

Configurations	Parameters	Value
Air Compressor	isentropic efficiency	0.9
	mechanical efficiency	0.99
	pressure ratio	14
Gas Turbine	isentropic efficiency	0.9
	discharge pressure	1 atm
	pressure ratio	14
Combustor	Temperature	1200^{o}C
	pressure	30 bar

Chapter 4

Steady-State Process Simulation

Based on the process design and models presented in chapter 2 and chapter 3, this chapter will discuss the steady-state process simulations of the proposed biomass conversion process. The effect of feedstocks is studied to compare the different feedstocks. The amount of liquid transportation fuels from all the three FTS biomass conversion process is compared. Heat integration is also studied which can be used in the economic analysis. The simulation results are summarized in this chapter. The detailed simulation results are shown in Appendix A.

4.1 Effect of Feedstocks

Table 4.1: Proximate and ultimate analyses of feedstocks

Component wt %	Hybrid Poplar	Switchgrass	Corn Stover	Pine Bark	Hardwood
C	50.88	46.90	46.80	47.80	50.19
H	6.04	5.85	5.74	5.46	5.90
N	0.17	0.58	0.66	0.72	0.32
S	0.09	0.11	0.11	0.00	0.03
O	41.90	41.50	41.59	35.40	41.42
Ash	0.92	5.06	5.10	10.62	2.14
Moisture	50.00	8.20	6.10	16.20	45.00
Higher Heating Value, HHV (MJ/kg)	20.10	18.64	18.10	19.54	19.13

Biomass is composed of cellulose, hemicellulose and three types of lignin monomers, and the distribution of each monomer in the biomass species is determined by the proximate and ultimate analysis and atomic balances. Five feedstocks, i.e. hybrid poplar,

switchgrass, corn stover, pine bark, and hardwood, are used to study the effect of feedstocks on the distribution of liquid transportation fuels. The proximate and ultimate analyses of the feedstocks are shown in Table 4.1.

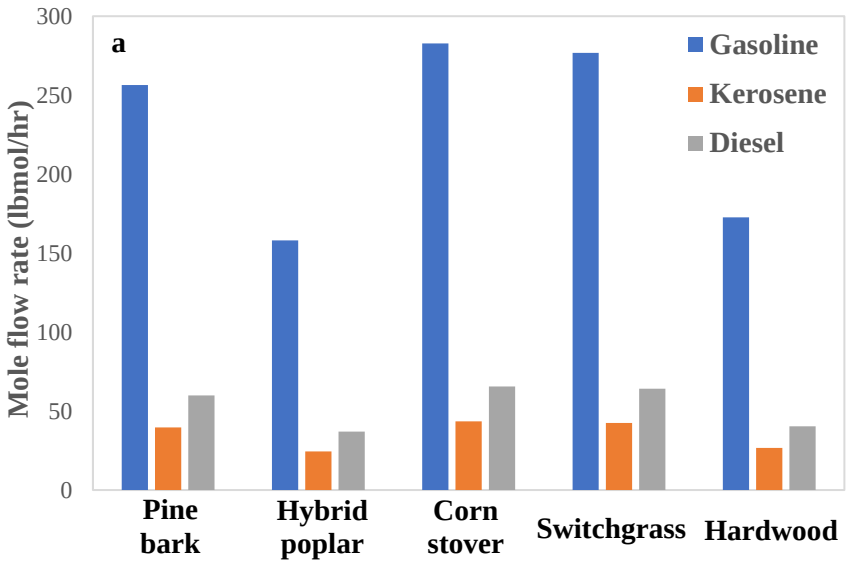

Figure 4.1: Comparison of product outputs for different feedstocks conversion through once-through FTS technology

To compare the product outputs and CO_2 emission of different feedstocks, biomass conversion process with once-through FTS technology is used. The comparison of product outputs from different feedstocks is shown in Figure 4.1. The amount of CO_2 emission from different feedstocks is shown in Figure 4.2. The results show that corn stover generates the most liquid transportation fuels, while hybrid poplar produces the least liquid transportation fuels. At the same time, corn stover to liquid transportation fuels conversion process generates the most CO_2. This means that corn stover as feedstock to the liquid transportation fuels process has the highest carbon conversion rate. This may be caused by the low moisture of corn stover feedstock. In this study, the same amount of feedstock is used to compare the effect of feedstocks on the production of liquid transportation fuels.

Since corn stover has the lowest moisture, it means that it has the highest carbon amount to get converted to the product.

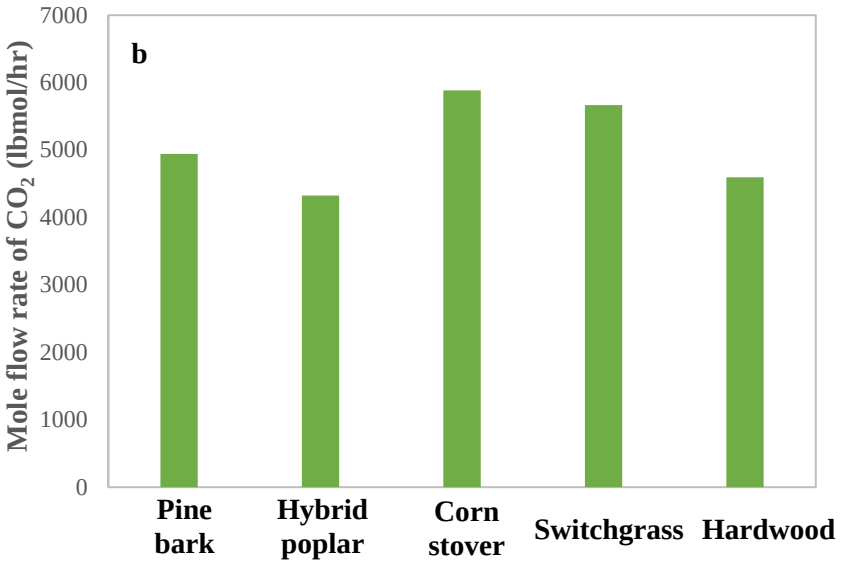

Figure 4.2: Comparison of CO_2 emission for different feedstocks conversion through once-through FTS technology

4.2 Fischer-Tropsch Simulation Results

The output of FTS is summarized in Table 4.2. It shows that supercritical FTS and conventional FTS produces more light gases than once-through FTS. This results from the auto-thermal reforming in the supercritical FTS and conventional FTS biomass conversion process. The recycle of syngas contributes to more light gases at the output of the FTS process. For the once-through process, the light gases are sent to the power generation plant, which causes less light gases from FTS process. The light gases from supercritical FTS process is more than that from conventional FTS process, which is caused by the higher CO conversion to methane in supercritical FTS process. The supercritical fluid is

supposed to help decrease the production of methane in FT reactor (Elbashir & Roberts, 2005). However, the model used in this study gives higher CO conversion to methane.

Table 4.2 also shows that supercritical FTS process produces more heavy hydrocarbons, i.e. raw kerosene, distillate, and wax, than once-through FTS and conventional FTS process. Due to the high compressibility, very small changes in pressure and/or temperature can lead to large changes in density-dependent properties with the presence of supercritical fluid in FTS process, which improves the generation of long-chain olefins (Elbashir & Roberts, 2005). More long-chain olefins means more heavy hydrocarbons, which explains more raw kerosene, distillate, and wax in supercritical FTS process. Conventional FTS process generates more heavy hydrocarbons than once-through FTS process, which results from the recycle of syngas in conventional FTS process. The recycle of syngas means more syngas in FTS, which improves carbon conversion rate to generate more hydrocarbons.

Table 4.2: FTS simulation results

Output (lbmol/hr)	Supercritical FTS	Once-through FTS	Conventional FTS
light gases	4645.954	2148.421	3491.140
C_3-C_5 gases	58.267	114.318	158.035
Naphtha	143.830	168.099	227.298
Raw kerosene	65.980	46.251	61.092
Distillate	95.946	37.987	49.005
Wax	16.179	8.202	10.105

4.3 Liquid Transportation Fuels

The comparison of liquid transportation fuels outputs for the three FTS biomass conversion processes is shown in Figure 4.3. It shows that biomass conversion process with conventional FTS technology produces the most gasoline product, while biomass conversion process with supercritical FTS generates the largest amounts of heavy liquid

transportation fuels, i.e. kerosene and diesel. This result is attributed to the use of supercritical hexane in supercritical FTS biomass conversion process. In supercritical FTS, small changes in pressure and/or temperature can lead to large changes in the density-dependent properties of the supercritical media due to the high compressibility (Elbashir & Roberts, 2005). This causes increased generation of long-chain olefins, which results in more heavy products in the hydrocarbon upgrading process. Therefore, the supercritical FTS biomass conversion process can produce more kerosene and diesel, but less gasoline than the once-through FTS and conventional FTS processes. In conventional FTS, the syngas produced from light gas reforming along with the unreacted syngas are recycled back to FTS reactor, which results in more hydrocarbons being generated in the FTS reactor, thus yielding more product compared to the once-through FTS process.

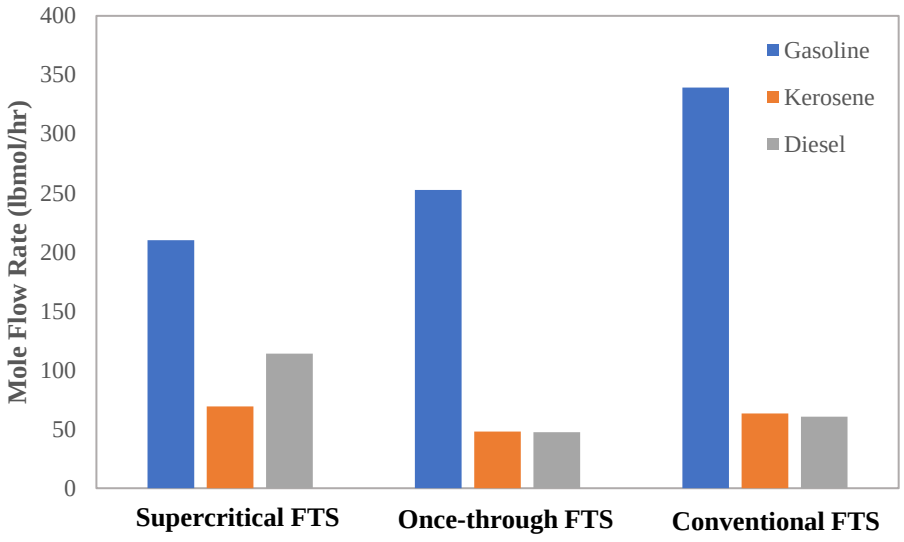

Figure 4.3: Comparison of liquid transportation fuels outputs for the three FTS biomass conversion processes

Figure 4.4 gives the comparison of CO_2 emission for the three biomass conversion processes. It shows that biomass conversion process with once-through FTS process

generates the most CO_2, while the process with supercritical FTS process generates the lowest amounts of CO_2. Supercritical fluids have high thermal conductivity and consequently the heat transfer is enhanced in the supercritical FTS reactor. This improved heat transfer prevents carbon (coke) formation on the surface of the catalyst, which results in longer catalyst lifetime as well as suppression of undesired side reactions such as the water-gas shift reaction (Huang & Roberts, 2003). This explains why the supercritical FTS process generates the least CO_2. The increased CO_2 emissions in once-through FTS process compared to conventional FTS process is attributed to the combustion of light hydrocarbons in the power generation plant which leads to more carbon conversion to CO_2.

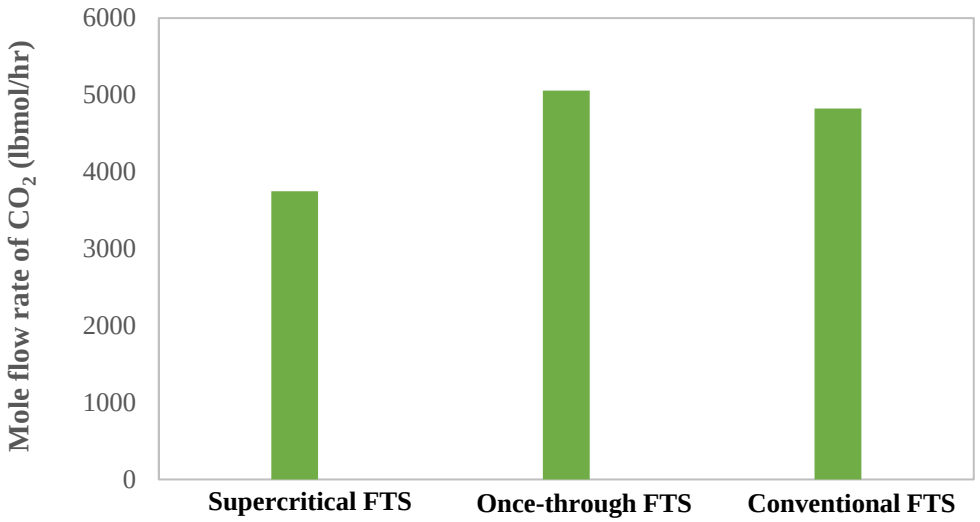

Figure 4.4: Comparison of CO_2 emission for the three FTS biomass conversion processes

4.4 Heat Integration Results

Heat integration is performed in Aspen Energy Analyzer™ (AEA) to calculate the minimum energy requirement based on the process simulation results. The minimum approach temperature is set at 10°C for all the three processes. The composite curves are

used to indicate the minimum energy target for the process. Figure 4.5 shows the composite curves for supercritical FTS biomass conversion process. It shows the heating target is 3.196×10^{5} kJ/h, while the cooling target is 1.773×10^{8} kJ/h for supercritical FTS biomass conversion process. Figure 4.6 shows the composite curves for once-through FTS biomass conversion process. It shows that the heating target is 1.481×10^{7} kJ/h, while the cooling target is 3.136×10^{8} kJ/h. Figure 4.7 shows the composite curves for conventional FTS biomass conversion process. It shows that the heating target is 3.196×10^{5} kJ/h, while the cooling target is 1.687×10^{8} kJ/h.

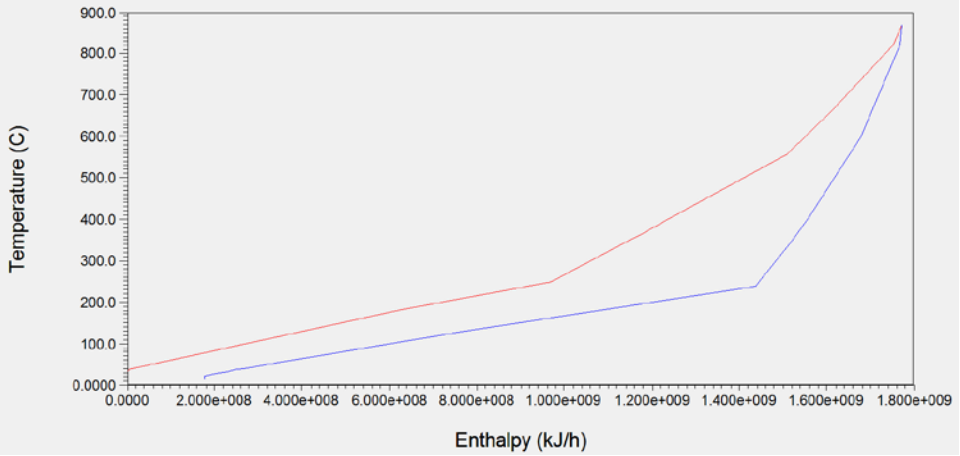

Figure 4.5: Composite curves for supercritical FTS biomass conversion process

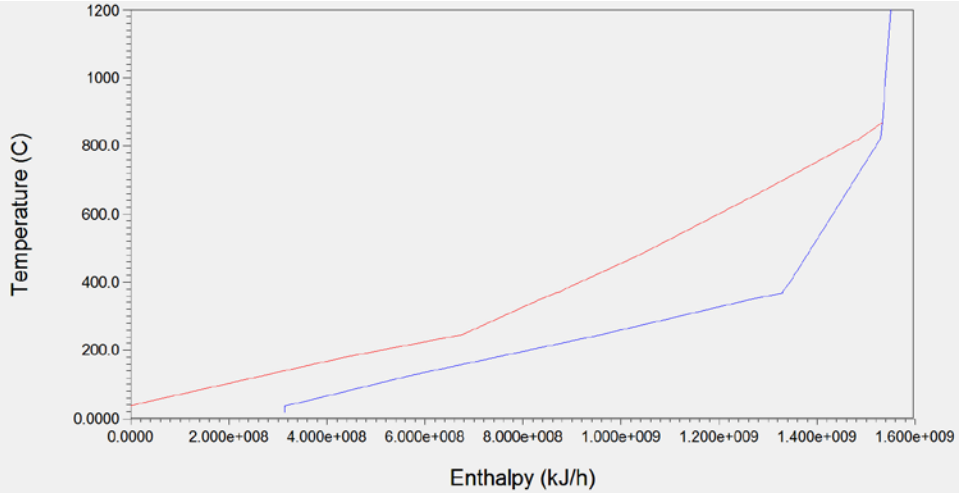

Figure 4.6: Composite curves for once-through FTS biomass conversion process

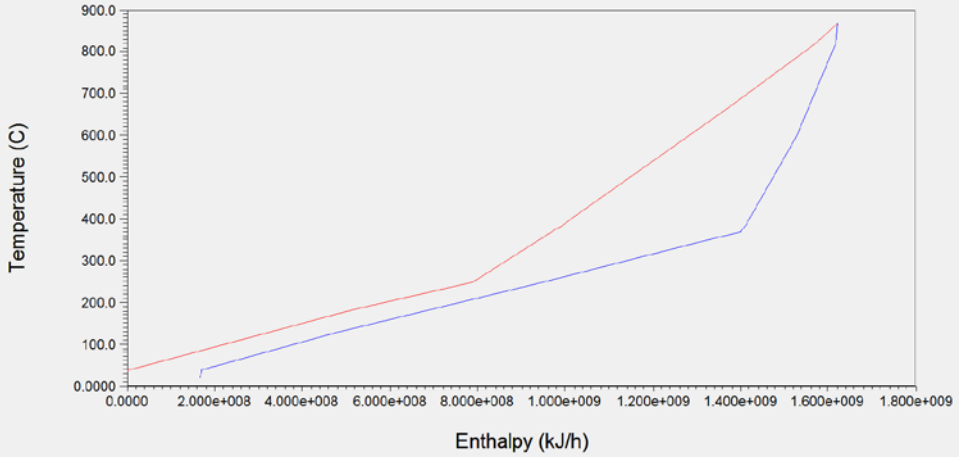

Figure 4.7: Composite curves for conventional FTS biomass conversion process

The optimal heat exchanger network design is obtained through AEA. The capital cost for heat exchangers and the heat exchanger network performance are summarized in Table 4.3. It shows that the performance from the heat exchanger network design for both supercritical FTS biomass conversion process and conventional FTS biomass conversion process surpasses the heating target significantly. The capital cost of heat exchanger network for once-through FTS biomass conversion process is the lowest. The heat exchangers needed in the biomass conversion process are shown in Appendix C.

Table 4.3: Heat integration results

Network performance	**Supercritical FTS**	**Once-through FTS**	**Conventional FTS**
Capital cost	2.059×10^{7}	1.206×10^{7}	2.239×10^{7}
Heating (kJ/h)	9.807×10^{6}	2.738×10^{7}	1.027×10^{7}
Cooling (kJ/h)	1.868×10^{8}	3.216×10^{8}	1.786×10^{8}

Chapter 5

Economic Analysis

Economic analysis is performed in this chapter to compare the cost of the three proposed biomass conversion processes. The capital costs (based on the total equipment cost), as well as operating costs, are determined first. The discounted cash flow is then calculated over the entire economic life of the plant. The net present value is calculated by summing the discounted cash flows. The break-even oil price that makes the net present value of the process equal to zero is then calculated.

5.1 Aspen Process Economic Analyzer

Aspen Process Economic Analyzer™ (APEA) is used to estimate the equipment cost in this research. APEA is designed to automate the preparation of detailed designs, estimates, investment analysis and schedules from minimum scope definition, whether from process simulation results or sized equipment lists. A project overflow in APEA is shown in Figure 5.1 Output results from Aspen Plus™ is first linked to APEA, then the mapping of simulator models to process equipment types is done in APEA. Mapping relates each process simulator model to one or more of APEA's list of several hundred types of process equipment. After the process equipment is chosen for the process simulator models, the equipment size is specified in APEA based on the process simulation results. After additional necessary project component information is specified, the equipment cost can be obtained through running the project evaluation (ASPEN, 2014).

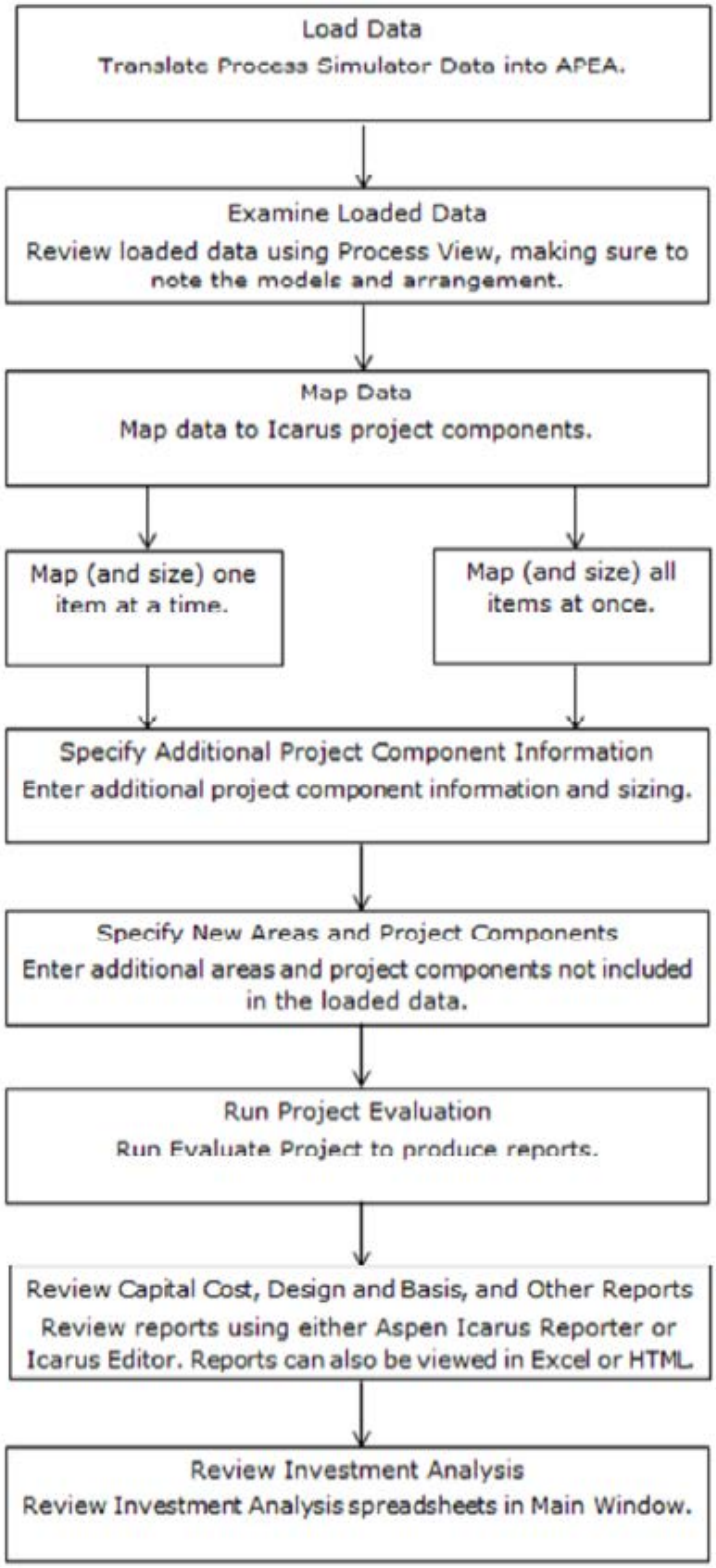

Figure 5.1: Project overflow in APEA

5.2 Capital Cost Assumptions

This section discusses the methods and sources for determining the capital cost of each piece of equipment within the biomass conversion process. A summary of the individual equipment costs is provided in Appendix D.

Biomass handling and gasification area capital cost estimates are from NREL report (Dutta & Phillips, 2009). The direct permanent investment (DPI) estimates of other areas are primarily from APEA based on the simulation results. The capital costs of heat exchangers from pinch analysis are obtained from Aspen Energy Analyzer™. Since the models used for evaluating the equipment cost are same in all three biomass conversion processes in APEA, it puts the processes on a similar cost basis for comparison purposes. Using the estimated equipment costs, the purchased cost of the equipment for the specific size of the processes and the cost year was calculated. Cost factors are then used to determine the installed equipment cost. The factors used in determining the total installed cost (TIC) of each piece of equipment are based on the NREL report mentioned above and are shown in Table 5.1.

Table 5.1: Cost factors to determine total installed equipment costs

	% of TPEC
Total Purchased Equipment Cost (TPEC)	100
Purchased equipment installation	39
Instrumentation and controls	26
Piping	31
Electrical systems	10
Buildings (including services)	29
Yard Improvements	12
Total Installed Cost (TIC)	247

The non-manufacturing fixed-capital investment costs are set as indirect costs, which are estimated using the cost factors in the NREL report. The factors are shown in Table 5.2

and have been put as percentages in terms of TIC. The costs of reactors, compressors, separators, and heat exchangers are estimated in APEA and AEA using material and energy balance results from the Aspen Plus™ simulation. For the various pieces of equipment, the design temperature is determined to be the operating temperature plus 50°F. The design pressure is the higher of the operating pressure plus 25 psi or the operating pressure times 1.1 (Dutta & Phillips, 2009). The capital cost for the ASU is obtained from literature (Tijmensen et al., 2002). Installed cost provided was converted to equipment cost using a factor of 2.47, which is the average installation factor for this study. The total permanent investment (TPI) is the sum of the installed cost and the indirect cost.

The main purpose of this work is to compare the three biomass conversion processes rather than develop a rigorous economic evaluation. Only the main equipment for each area is considered in the economic analysis. To maintain the consistency of the comparison, the sizing approach is the same for all the three processes.

Table 5.2: Indirect Cost Factors

Indirect costs	**% of TIC**
Engineering	13
Construction	14
Legal and contractors fees	9
Project contingency	3
Total Indirect Costs	39

5.3 Operating Costs Assumptions

Operating costs, such as utilities, personnel, chemicals, and feedstock costs, have been taken into account. This section discusses the operating costs, including the assumptions and values for these costs. The operating costs assumptions are shown in Table 5.3 (Swanson et al., 2010). Hexane cost is applied to biomass conversion process with

supercritical FTS. The labor costs are calculated based on the NREL report where it shows the annual expense for labors is $2MM. The maintenance and insurance costs are calculated as 2% of total installed equipment cost (Aden et al., 2002). The sum of labor costs and maintenance costs is termed the operating labor and maintenance (L&M) costs. The subtotal operating cost (SOC) is defined as the sum of the raw materials, utilities, and L&M costs (Baliban et al., 2010). The operating expenses are estimated to be 8% of the SOC. The plant overhead is assumed to be 50% of the L&M.

Table 5.3: Operating costs assumptions

Parameter	Value
Feedstock	$75/dry short ton ($82.67/dry Mg) *
Hexane	$1.00/ton *
Butane	$355.83/Metric ton
Electricity	$0.054/kW h *
Labor costs	$2MM/year *
Maintenance costs (% of TIC)	2% *
Insurance (% of TIC)	2% *
Operating expenses (% of SOC)	8% *
Plant overhead (% of L&M)	50% *

*Assumed

5.4 Break-Even Oil Price

This section discusses the break-even oil price (BEOP) based on the biomass conversion process designed in this research. The calculation of BEOP is based on the study from Baliban et al. (Baliban et al., 2010). The economic assumptions for calculating BEOP are summarized in Table 5.4.

BEOP is defined as the crude oil price (COP) for which the net present value (NPV) of the biomass conversion process is equal to zero. NPV of the plant can be calculated by Eq.

5.1 by summing the discounted cash flows over the entire economic life of the plant. A discounted cash flow is shown in Appendix E using the price of $75/dry ton of biomass.

$$NPV = \sum_{y \leq y_{End}} \frac{CF_y}{(1+RR)^y} \quad \text{(Eq. 5.1)}$$

where CF_y is the discounted cash flow at year y, RR is the desired rate of return.

Table 5.4: Economic assumptions for calculating BEOP

Parameter	Value
Economic life of the plant	30 yrs
Yearly operating capacity	8000 h
Propane sale price	$2.05/gallon
Product escalation	1% per year
Tax rate	40%
Depreciation	10 yrs
Working capital (% of TPI)	5%
Construction and startup time	3 yrs
Salvage value (% of TPI)	20%
Desired rate of return	15%
Raw material escalation	1% per year
Utilities escalation	1% per year
Labor and maintenance escalation	1% per year
Insurance escalation	1% per year

The discounted cash flow over the entire economic life of the plant can be calculated by Eq. 5.2. The plant economic life is taken to be 30 years, with a yearly operating capacity of 8000 h.

$$CF_y = (S_y - OP_y)(1 - TR) - (TR)DEP_y - CAP_y \quad \text{(Eq. 5.2)}$$

where S_y is the product sales, OP_y is the yearly operating costs, TR is the tax rate, DEP_y is the depreciation of year y, CAP_y is the capital cost in year y.

The product sales, S_y, can be calculated as the sum of the transportation fuels product sales plus the sale of by-product propane, which is calculated by Eq. 5.3. The transportation

fuel product sale is calculated by Eq. 5.4. The by-product sale is calculated by Eq. 5.5. The propane sale price is the average propane price in 2016 obtained from EIA (EIA, 2016a). The RM is the difference between the sale price of petroleum products and the purchase price of crude oil. The values of RM for transportation fuels are from literature. The RM for gasoline, kerosene, and diesel is \$0.333/gallon, \$0.217/gallon, and \$0.266/gallon, respectively.

$$S_y = PR_y + BY_y \quad \text{(Eq. 5.3)}$$

$$PR_y = (1 + P_{Esc})^y [F_{Gas}(COP + RM_G) + F_{Die}(COP + RM_D) + F_{Ker}(COP + RM_K)] \quad \text{(Eq. 5.4)}$$

$$BY_y = (1 + P_{Esc})^y Cost_{Pro} F_{Pro} \quad \text{(Eq. 5.5)}$$

where PR_y is the transportation fuel product sale at year y, BY_y is the by-product sale at year y, P_{Esc} is the product escalation, F is the flow rate of products, COP is the crude oil price, RM is refinery margin, $Cost_{Pro}$ is the propane sale price.

The yearly operating cost, OP_y, can be calculated using the raw materials, utilities, labor and maintenance, insurance, operating expenses, and plant overhead. The operating labor and maintenance costs will be escalated using the escalation factor. The raw material costs are calculated by Eq. 5.6. Using a straight-line depreciation method over 10 years and a tax rate of 40%. CAP_y is calculated by Eq. 5.7. The TPI is distributed during the construction time using the distribution factor f_y, where f_1 is 0.25, f_2 is 0.5, and f_3 is 0.25, respectively. The working capital is defined as 5% of the TPI and is only utilized during the startup in year 3. The salvage value of the plant is 20% of TPI considered at the end of the economic life of the plant.

$$RM_y = (1 + R_{Esc})^y (Cost_{Bio} F_{Bio} + Cost_{Hyd} F_{Hyd} + Cost_{But} F_{But}) \quad \text{(Eq. 5.6)}$$

where R_{Esc} is the raw material escalation, $Cost_{Bio}$ is the biomass feedstock price, $Cost_{Hyd}$ is the hydrogen price, $Cost_{But}$ is the butane price, F is the raw material flow rate.

$$CAP_y = (1 + C_{Esc})^y f_y TPI + WC_y - SV_y \quad \text{(Eq. 5.7)}$$

where C_{Esc} is the construction escalation, f_y is the distribution factor of startup period, TPI is the total permanent investment, WC_y is the working capital, SV_y is the salvage value.

5.5 Economic Analysis Results

The economic analysis is based on processing 2000 dry tonne of biomass per day in this study. The TPI for the three biomass conversion processes is presented in Figure 5.2. It shows supercritical FTS biomass conversion process has the highest TPI, while once-through FTS process has the lowest TPI. This is due to the higher equipment cost in supercritical FTS biomass conversion process than other two processes. However, the TPI for all the three processes is very close using the estimate method from NREL.

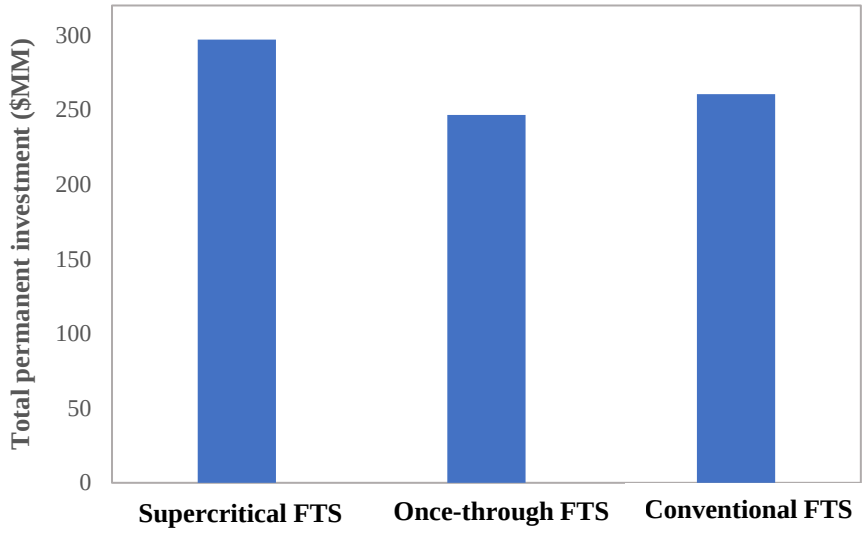

Figure 5.2: Total permanent investment for the three biomass conversions

The price of biomass feedstock influences the competitiveness of the process because of the high requirement of biomass input to the system. The variability in the BEOP, with respect to biomass feedstock price, is presented in Table 5.5 and graphically in Figure 5.3. It shows that no matter what the biomass price is, conventional FTS biomass conversion process is the most competitive process in all the three biomass conversion processes. For biomass price from $35/dry ton to $55/dry ton, once-through FTS process is relatively more competitive than supercritical FTS process. As the biomass price goes higher than $65/dry ton, supercritical FTS process becomes more competitive than once-through FTS process.

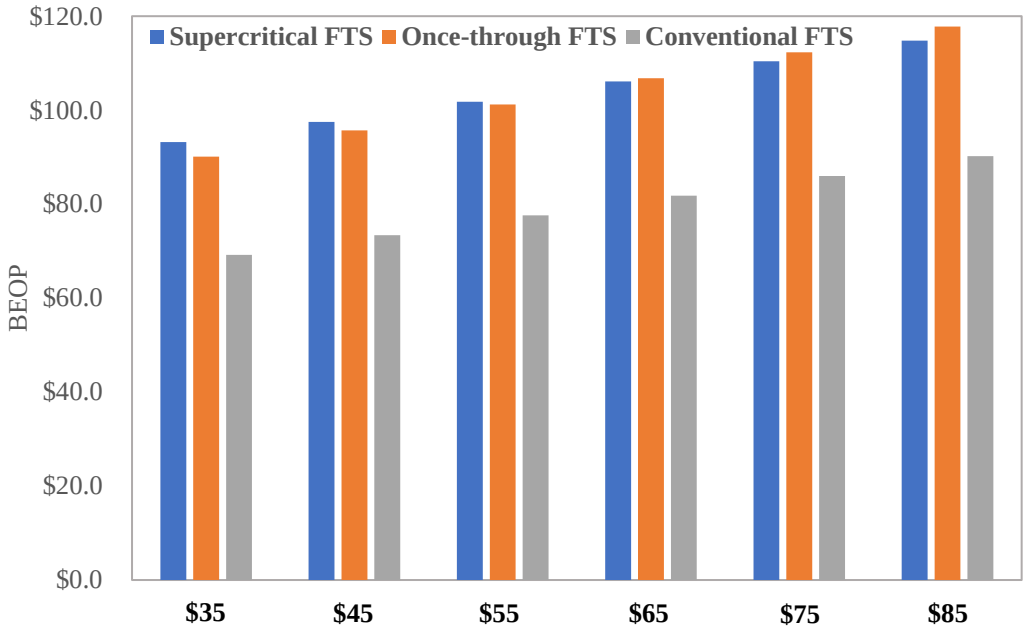

Figure 5.3: Break-even oil price (BEOP) of three biomass conversion processes using distinct biomass feedstock prices

Table 5.5: BEOP of three biomass conversion processes using distinct biomass feedstock prices

biomass price	**BEOP**		
$/dry ton	Supercritical FTS	Once-through FTS	Conventional FTS
$35	$93.2	$90.1	$69.2
$45	$97.5	$95.7	$73.4
$55	$101.8	$101.2	$77.6
$65	$106.1	$106.8	$81.8
$75	$110.4	$112.3	$86.0
$85	$114.8	$117.8	$90.2

Chapter 6

Conclusions

A biomass to liquids process that produces transportation fuels has been introduced in this thesis. A conceptual process has been designed in detail to obtain liquid transportation fuels, i.e. gasoline, kerosene, and diesel, from biomass. Key components of the process include the gasification of biomass feedstock, syngas treatment, Fischer-Tropsch synthesis, and hydrocarbon upgrading process. Direct gasification is used to convert biomass to syngas which is converted to liquids from thermochemical Fischer-Tropsch synthesis technology. Three FTS technologies, which are supercritical FTS, once-through FTS, and conventional FTS, are used to compare the process competitiveness. After a wide range of hydrocarbons are obtained from FTS unit, they are recovered through a hydrocarbon recovery system and then sent into a hydrocarbon upgrading unit to generate the final liquid transportation fuels.

Mathematical models that predict the syngas composition output, hydrocarbon distribution in the FTS unit and product output have been developed and integrated into the process simulation. Steady-state simulation has been performed in Aspen Plus^{TM} to generate the product output. Five feedstocks, which are hybrid poplar, switchgrass, corn stover, pine bark, and hardwood, have been used to compare the effect of feedstocks. The results show that corn stover generates the most liquid transportation fuels, while hybrid poplar produces the least liquid transportation fuels. This means that corn stover as feedstock has the highest carbon conversion rate. The reason for this result is that corn

stover feedstock has the lowest moisture, which means corn stover has the highest carbon amount to be converted to generate products based on the same amount of biomass feedstock. Results from the three biomass conversion processes considered in this research show that conventional FTS biomass conversion process produces the most gasoline product, while biomass conversion process with supercritical FTS generates the largest amounts of kerosene and diesel. This result is attributed to increased generation of long-chain olefins in supercritical FTS process because of the use of supercritical hexane.

Economic analysis has also been performed to compare the process competitiveness among the three proposed biomass conversion processes. The capital costs result shows that supercritical FTS biomass conversion process has the highest capital cost, while once-through FTS process has the lowest cost. The capital costs for all the three processes are very close. The estimation method utilized by NREL has been employed. The economic analysis also provides the break-even oil price with respect to different biomass feedstock prices. Result shows that no matter what the biomass price is, conventional FTS biomass conversion process is the most competitive process in all the three biomass conversion processes, while the competitiveness between supercritical FTS process and once-through FTS process changes with different biomass feedstock prices.

References

Aden, A., Ruth, M., lbsen, K., Jechura, J., Neeves, K., Sheehan, J., & Wallace, B. (2002). *Lignocellulosic biomass to ethanol process design and economics utilizing co-current dilute acid prehydrolysis and enzymatic hydrolysis for corn stover* (NREL/TP-510-32438).

Altin, O., & Eser, S. (2004). Carbon deposit formation from thermal stressing of petroleum fuels. *Prepr. Pap.-Am. Chem. Soc., Div. Fuel Chem., 49*, 764-766.

Amos, W. A. (1998). *Report on Biomass Drying Technology* (NREL/TP-570-25885).

ASPEN. (2013). *Aspen Plus - Getting started modeling processes with solids.* Aspen Technology, Inc.

ASPEN. (2014). *Aspen process economic analyzer - user's guide*. Aspen Technology, Inc.

Baliban, R. C., Elia, J. A., & Floudas, C. A. (2010). Toward novel hybrid biomass, coal, and natural gas processes for satisfying current transportation fuel demands, 1. Process alternatives, gasification modeling, process simulation, and economic analysis. *Ind. Eng. Chem. Res., 49*, 7343-7370.

Baliban, R. C., Elia, J. A., Floudas, C. A., Gurau, B., Weingarten, M. B., & Klotz, S. D. (2013). Hardwood Biomass to Gasoline, Diesel, and Jet Fuel: 1. Process Synthesis and Global Optimization of a Thermochemical Refinery. *Energy & Fuels, 27*(8), 4302-4324.

Bechtel. (1998). *Aspen process flowsheet simulation model of a Battelle biomass-based gasification, Fischer-Tropsch liquefaction and combined-cycle power plant* (DE-AC22-93PC91029).

Bukur, D. B., Lang, X., Akgerman, A., & Feng, Z. (1997). Effect of process conditions on olefin selectivity during conventional and supercritical Fischer–Tropsch synthesis. *Ind. Eng. Chem. Res., 36*, 2580-2587.

Carroni, R., Schmidt, V., & Griffin, T. (2002). Catalytic combustion for power generation. *Catalysis Today, 75*, 287-295.

DESA. (2015). *World Population Prospects: The 2015 Division, Key Findings and Advance Tables* (ESA/P/WP.241).

DOE. (1993). *Baseline design/economics for advanced Fischer-Tropsch technology. Quarterly report, January-March 1993* (DE-AC22-91PC90027).

DOE. (1994). *Baseline design/economics for advanced Fischer-Tropsch technology* (DE-AC22-91PC90027).

DOE. (2013). *Biochemical Conversion: Using Enzymes, Microbes, and Catalysts to Make Fuels and Chemicals* (DOE/EE-0948). bioenergy.energy.gov

Dutta, A., & Phillips, S. D. (2009). *Thermochemical Ethanol via Direct Gasification and Mixed Alcohol Synthesis of Lignocellulosic Biomass* (NREL/TP-510-45913).

EIA. (2015). EIA official website.

EIA. (2016a). EIA official website.

EIA. (2016b). *International Energy Outlook 2016 with Projections to 2040*

Elbashir, N. O., Dutta, P., Manivannan, A., Seehra, M. S., & Roberts, C. B. (2005). Impact of cobalt based catalyst characteristics on the performance of conventional gas-phase and supercritical-phase Fischer–Tropsch synthesis. *Applied Catalysis A: General, 285*, 169-180.

Elbashir, N. O., & Roberts, C. B. (2005). Enhanced incorporation of α-olefins in the Fischer-Tropsch synthesis chain-growth process over an alumina-supported cobalt catalyst in near-critical and supercritical hexane media. *Ind. Eng. Chem. Res., 44*, 505-521.

Elbashir, N. O. M. (2004). *Utilization of supercritical fluids in the Fischer-Tropsch synthesis over cobalt-based catalyst systems.* (Doctor of Philosophy), Auburn University.

EPA. (2007). *Biomass Conversion: Emerging Technologies, Feedstocks, and Products* (EPA/600/R-07/144).

Evans, R. J., Knight, R. A., Onischak, M., & Babu, S. P. (1988). *Development of biomass gasification to produce substitute fuels* (PNL-6518).

Fan, L., & Fujimoto, K. (1999). Fischer-Tropsch synthesis in supercritical fluid: characteristics and application. *Applied Catalysis A: General, 186*, 343-354.

Fischer, F., & Tropsch, H. (1923). *Brennst. Chem., 4*, 276.

Fox, J. M. (1993). The different catalytic routes for methane valorization: An assessment of processes for liquid fuels. *Catalysis Reviews-Science and Engineering, 35*, 169-212.

Fujimoto, K., & Kajioka, M. (1987). Hydrogenation of carbon monoxide over solid catalysis dispersed in the liquid medium. 1. Slurry-phase Fischer-Tropsch synthesis with supported ruthenium catalysts. *Bull. Chem. Soc. Jpn., 60*, 2237-2243.

Goyal, H. B., Seal, D., & Saxena, R. C. (2008). Bio-fuels from thermochemical conversion of renewable resources: A review. *Renewable and Sustainable Energy Reviews, 12*(2), 504-517.

Gregor, J. H. (1990). Fischer-Tropsch products as liquid fuels or chemicals. *Catalysis Letters, 7*, 317-331.

Huang, X., Elbashir, N. O., & Roberts, C. B. (2004). Supercritical solvent effects on hydrocarbon product distributions from Fischer–Tropsch synthesis over an alumina-supported cobalt catalyst. *Ind. Eng. Chem. Res., 43*, 6369-6381.

Huang, X., & Roberts, C. B. (2003). Selective Fischer–Tropsch synthesis over an Al_2O_3 supported cobalt catalyst in supercritical hexane. *Fuel Processing Technology, 83*, 81-99.

Jahangiri, H., Bennett, J., Mahjoubi, P., Wilson, K., & Gu, S. (2014). A review of advanced catalyst development for Fischer–Tropsch synthesis of hydrocarbons from biomass derived syn-gas. *Catal. Sci. Technol., 4*(8), 2210-2229.

Jana, K., & De, S. (2014). Biomass integrated combined power plant with post combustion CO_2 capture – performance study by ASPEN Plus®. *Energy Procedia, 54*, 166-176.

Keim, W. (1983). *Catalysis in C_1 Chemistry*. ISBN 978-9-027-71527-2.

Khodakov, Y., Chu, W., & Fongarland, P. (2007). Advances in the development of novel cobalt Fischer-Tropsch catalysts for synthesis of long-chain hydrocarbons and clear fuels. *Chemical Reviews, 107*, 1692-1744.

Kölbel, H., & Ralek, M. (1980). The Fischer-Tropsch synthesis in the liquid phase. *Catalysis Reviews-Science and Engineering, 21*, 225-274.

Kumar, A., Jones, D. D., & Hanna, M. A. (2009). Thermochemical Biomass Gasification: A Review of the Current Status of the Technology. *Energies, 2*(3), 556-581.

Lalou, C. (2014). Distributed power with advanced clean coal gasification technology. Webpage.

Lang, X., Akgerman, A., & Bukur, D. B. (1995). Steady state Fischer-Tropsch synthesis in supercritical propane. *Ind. Eng. Chem. Res., 34*, 72-77.

Li, M.-L., Lee, H.-Y., Lee, M.-W., & Chien, I.-L. (2014). Simulation and formula regression of an air separation unit in China Steel corporation. *ADCONP*, 213-218.

Linghu, W., Li, X., Asami, K., & Fujimoto, K. (2006). Process design and solvent recycle for the supercritical Fischer–Tropsch synthesis. *Energy & Fuels, 20*, 7-10.

Løver, K. A. (2007). *Biomass gasification integration in recuperative gas turbine cycles and recuperative fuel cell integrated gas turbine cycles.* (Master), Norwegian University of Science and Technology.

Magnusson, H. (2005). *Process simulation in Aspen Plus of an integrated ethanol and CHP plant.* (Master), Umeå University.

Malek Abbaslou, R. M., Soltan Mohammadzadeh, J. S., & Dalai, A. K. (2009). Review on Fischer–Tropsch synthesis in supercritical media. *Fuel Processing Technology, 90*(7-8), 849-856.

McKendry, P. (2002). Energy Production from Biomass (Part 1): Overview of Biomass. *Bioresource Technology, 83*, 37-46.

Morrin, S., Lettieri, P., Chapman, C., & Mazzei, L. (2012). Two stage fluid bed-plasma gasification process for solid waste valorisation: technical review and preliminary thermodynamic modelling of sulphur emissions. *Waste Manag, 32*(4), 676-684.

Ong'iro, A. O., Ugursal, V. I., & Taweel, A. M. A. (1995). Simulation of combined cycle power plants using the Aspen Plus shell. *Heat Recovery Systems & CHP, 15*, 105-113.

Oukaci, R. (2002). *Fischer-Tropsch synthesis.* Paper presented at the 2nd Annual Global GTL Summit Executive Briefing, London.

Pegego, C. (2007). Development of a Fischer-Tropsch catalyst: From laboratory to commercial scale demonstration. *Rend. Fis. Acc. Lincei, 18*, 305-317.

Perego, C., Bortolo, R., & Zennaro, R. (2009). Gas to liquids technologies for natural gas reserves valorization: The Eni experience. *Catalysis Today, 142*(1-2), 9-16.

Phillips, S. D., Tarud, J. K., Biddy, M. J., & Dutta, A. (2011). *Gasoline from wood via integrated gasification, synthesis, and methanol-to-gasoline technologies* (NREL/TP-5100-47594).

Raibhole, V. N., & Sapali, S. N. (2012). Simulation and Parametric Analysis of Cryogenic Oxygen Plant for Biomass Gasification. *Mechanical Engineering Research, 2*(2), 97-107.

Ruiz, J. A., Juárez, M. C., Morales, M. P., Muñoz, P., & Mendívil, M. A. (2013). Biomass Gasification for Electricity Generation: Review of Current Technology Barriers. *Renewable and Sustainable Energy Reviews, 18*, 174-183.

Satyendra. (2013). Non Cryogenic processes of Air Separation. Retrieved from webpage.

Saxena, R. C., Adhikari, D. K., & Goyal, H. B. (2009). Biomass-based energy fuel through biochemical routes: A review. *Renewable and Sustainable Energy Reviews, 13*(1), 167-178.

Schulz, H. (1999). Short history and present trends of Fischer-Tropsch synthesis. *Applied Catalysis A: General, 186*, 3-12.

Shafer, L., Striebich, R., Gomach, J., & Edwards, T. (2006). *Chemical class composition of commercial jet fuels and other specialty kerosene fuels*. Paper presented at the 14th AIAA/AHI Space Planes and Hypersonic Systems and Technologies Conference, Canberra, Australia.

Smith, A. R., & Klosek, J. (2001). A review of air separation technologies and their integration with energy conversion processes. *Fuel Processing Technology, 70*, 115-134.

Song, H.-S., Ramkrishna, D., Trinh, S., & Wright, H. (2004). Operationg strategies for Fischer-Tropsch reactors: A model-directed study. *Korean J. Chem. Eng., 21(2)*, 308-317.

Soudham, V. P. (2015). *Biochemical Conversion of Biomass to Biofuels Pretreatment-Detoxification-Hydrolysis-Fermentation.* (Doctor of Philosophy), Umeå University.

Swanson, R. M., Platon, A., Satrio, J. A., & Brown, R. C. (2010). Techno-economic analysis of biomass-to-liquids production based on gasification. *Fuel, 89, Supplement 1*, S11-S19.

Thomas, S. G., Kleiman, J. P., & Brandt, V. O. *Analysis of commercial diesel fuels by preparative high performance liquid chromatography and gas chromatography - mass spectrometry*. Ethyl Corporation, Baton Rouge, LA 70898

Tian, C., Li, B., Liu, Z., Zhang, Y., & Lu, H. (2014). Hydrothermal liquefaction for algal biorefinery: A critical review. *Renewable and Sustainable Energy Reviews, 38*, 933-950.

Tijmensen, M., Faaij, A., Hamelinck, C., & Hardeveld, M. (2002). Exploration of the possibilities for production of Fischer-Tropsch liquids and power via biomass gasification. *Biomass and Bioenergy, 23*, 129-152.

Van Der Laan, G. P., & Beenackers, A. A. C. M. (1999). Kinetics and Selectivity of the Fischer–Tropsch Synthesis: A Literature Review. *Catalysis Reviews, 41*(3-4), 255-318.

Wang, B., Gebreslassie, B. H., & You, F. (2013). Sustainable design and synthesis of hydrocarbon biorefinery via gasification pathway: Integrated life cycle assessment

and technoeconomic analysis with multiobjective superstructure optimization. *Computers & Chemical Engineering, 52*, 55-76.

Yokota, K., & Fujimoto, K. (1991). Supercritical-phase Fischer–Tropsch synthesis reaction. 2. The effective diffusion of reactant and products in the supercritical-phase reaction. *Ind. Eng. Chem. Res., 30*, 95-100.

Yokota, K., Hanakata, Y., & Fujimoto, K. (1990). Supercritical phase Fischer-Tropsch synthesis. *Chemical Engineering Science, 45*, 2743-2750.

Yuan, W. (2011). *Modeling and optimization of novel fuel production strategies.* (Doctor of Philosophy), Auburn University.

Zwart, R. W. R., & Boerrigter, H. (2005). High efficiency co-production of synthetic natural gas (SNG) and Fischer-Tropsch (FT) transportation fuels from biomass. *Energy & Fuels, 19*, 591-597.

Appendix A

Process Flow Diagrams

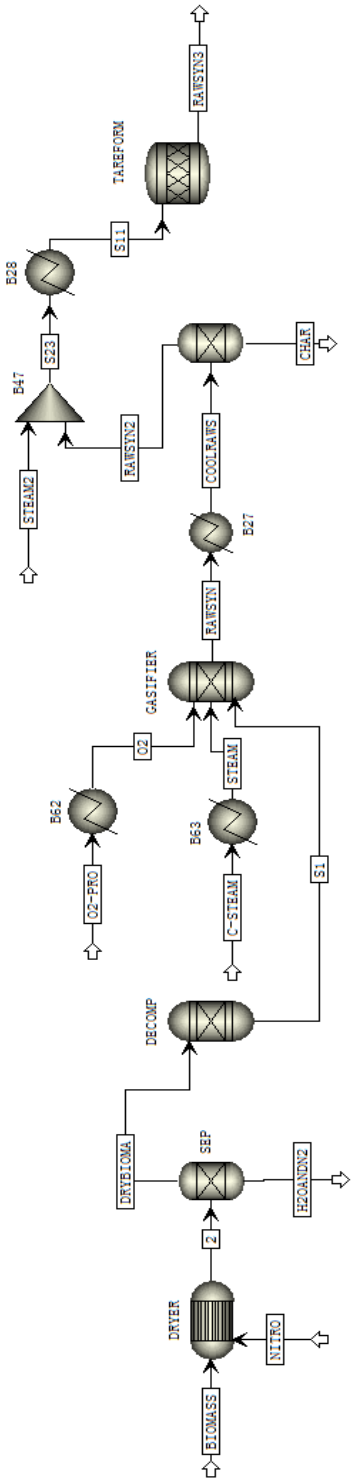

Figure A1: Biomass drying and gasification Aspen Plus model for all three biomass conversion processes

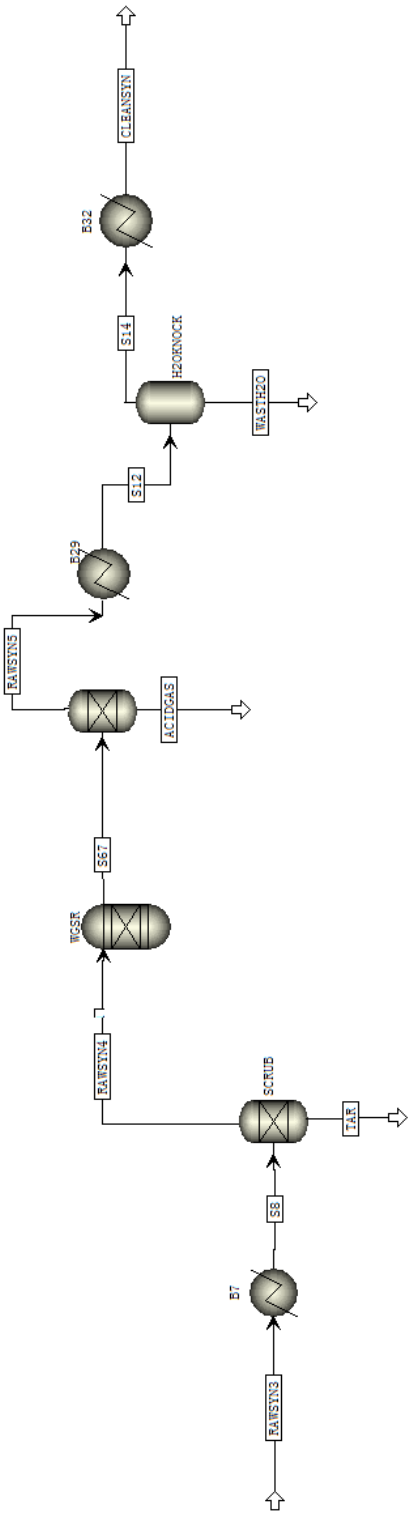

Figure A2: Syngas cleanup unit Aspen Plus model for supercritical FTS biomass conversion process

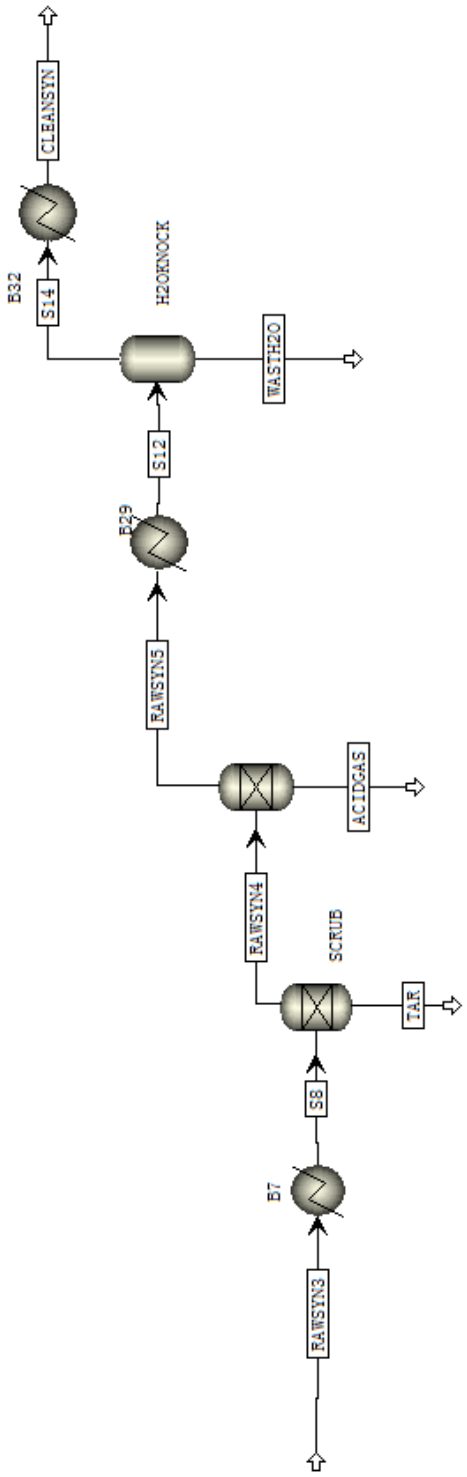

Figure A3: Syngas cleanup unit Aspen Plus model for once-through FTS and conventional FTS biomass conversion process

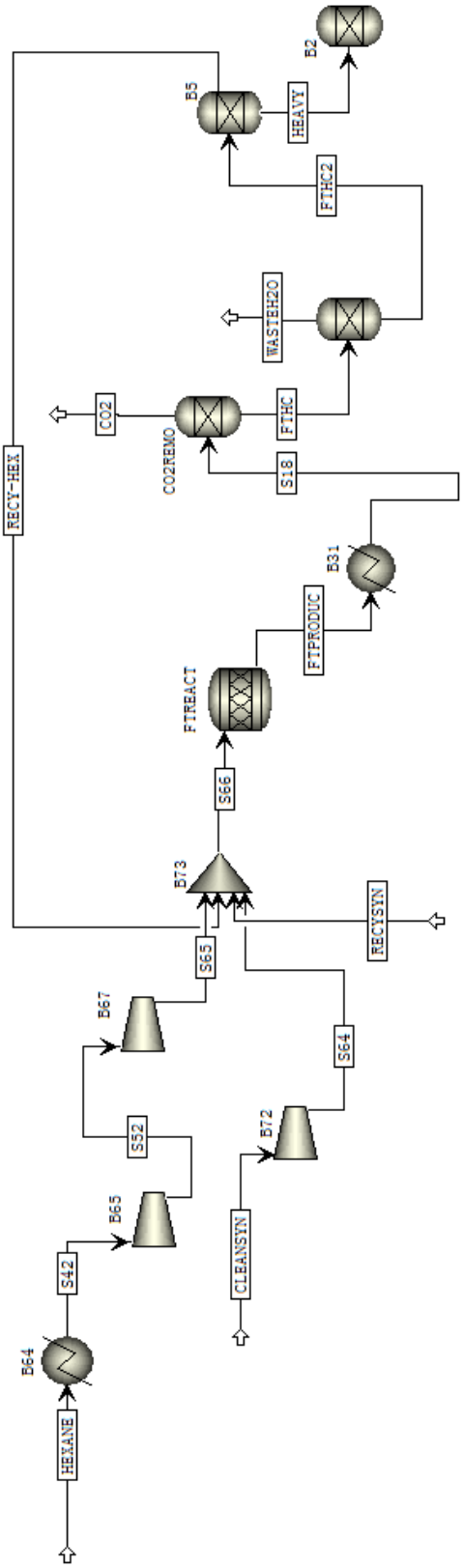

Figure A4: Supercritical FTS unit Aspen Plus model

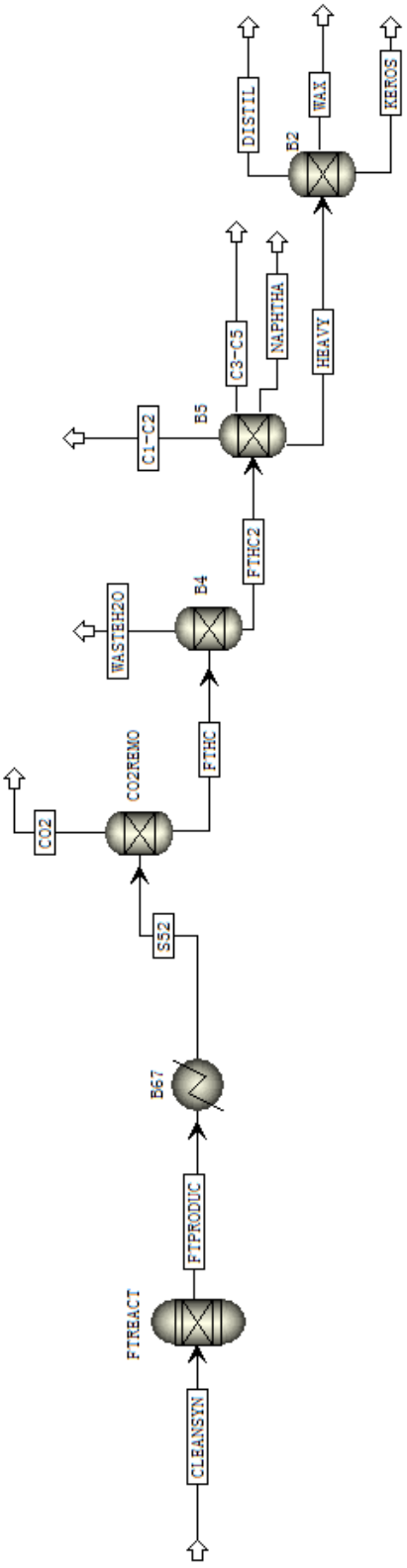

Figure A5: Once-through FTS unit Aspen Plus model

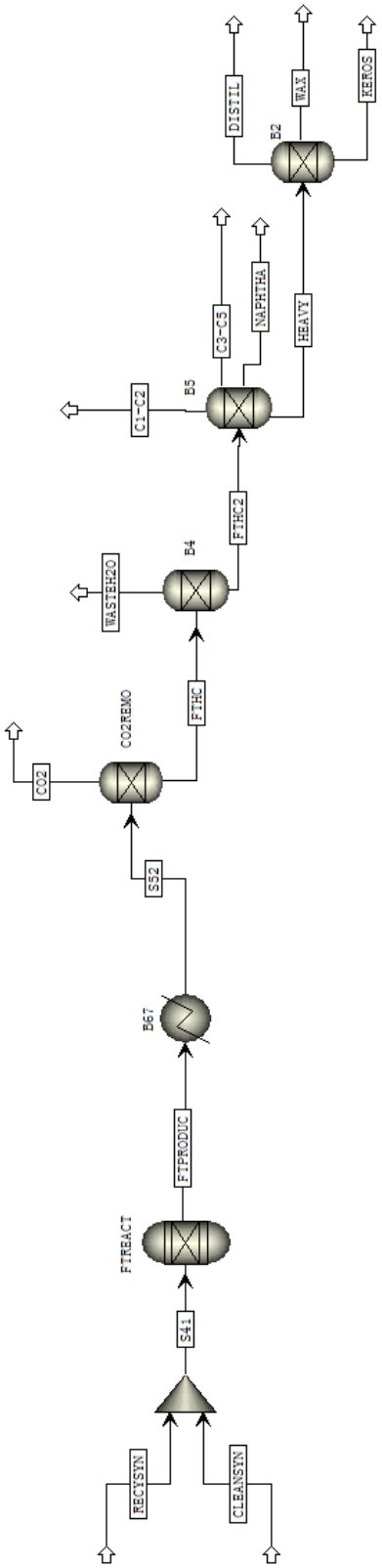

Figure A6: Conventional FTS unit Aspen Plus model

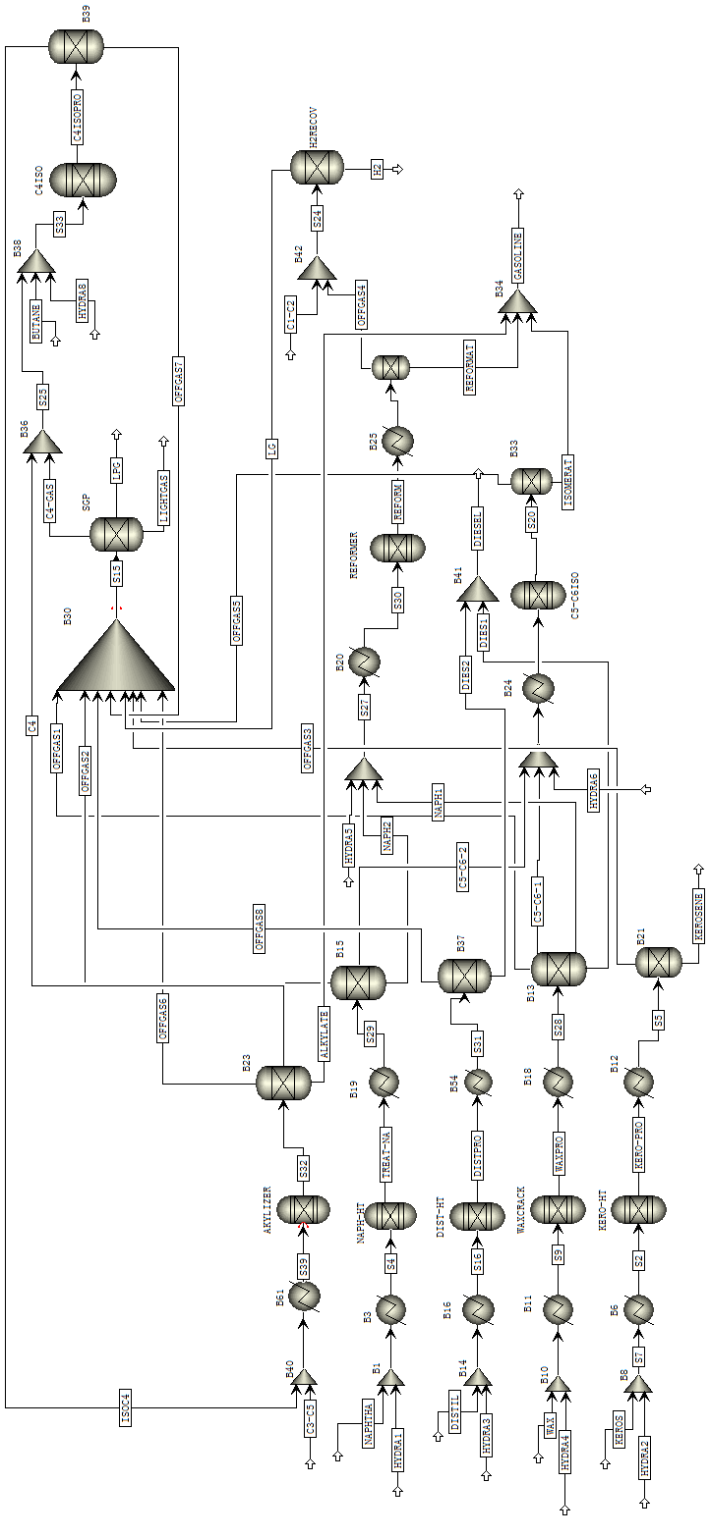

Figure A7: Hydrocarbon upgrading unit Aspen Plus model for all three biomass conversion processes

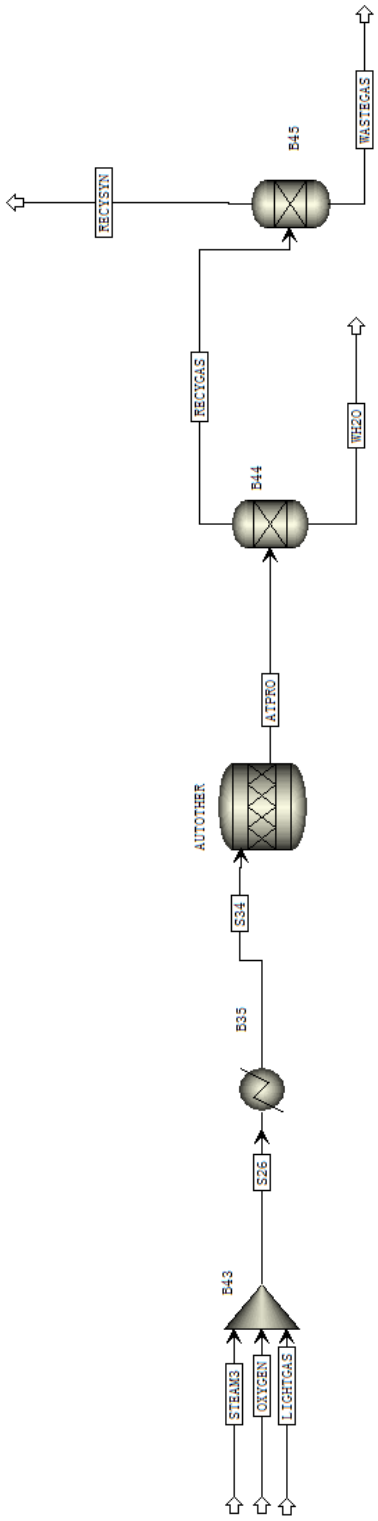

Figure A8: Auto-thermal reforming unit Aspen Plus model for supercritical FTS biomass conversion process

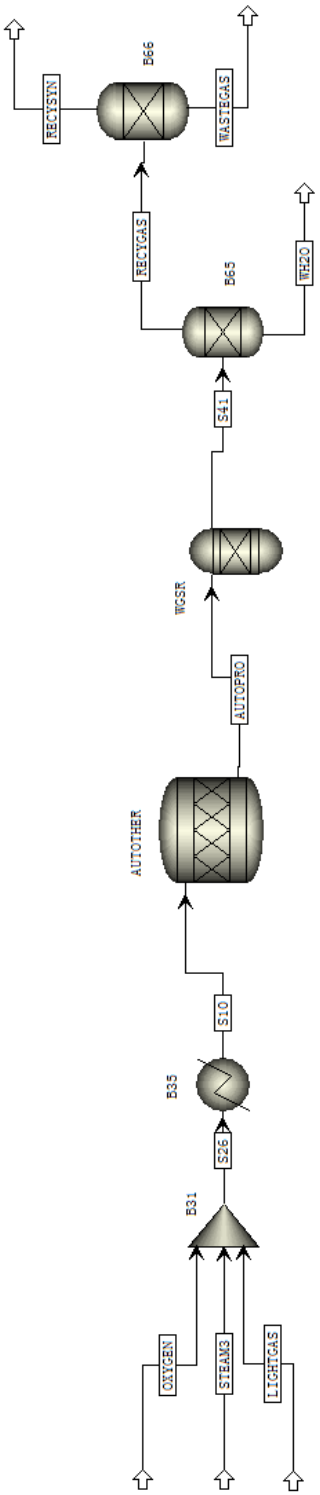

Figure A9: Auto-thermal reforming unit Aspen Plus model for conventional FTS biomass conversion process

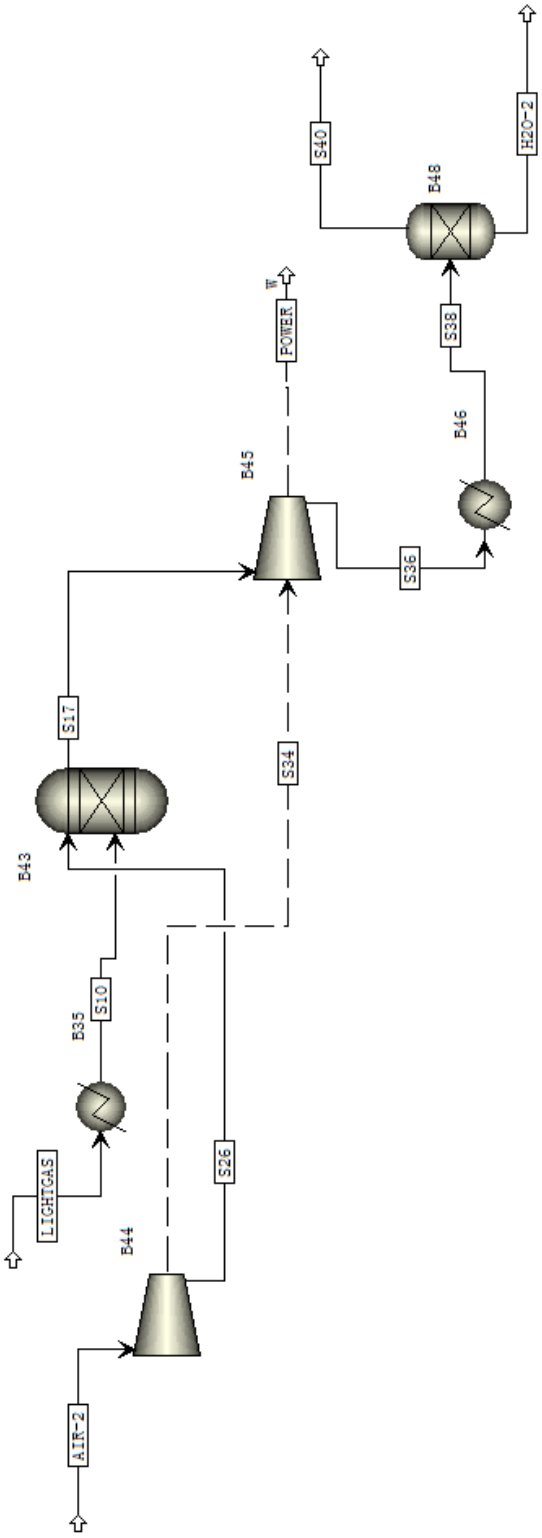

Figure A10: Power plant Aspen Plus model for once-through FTS biomass conversion process

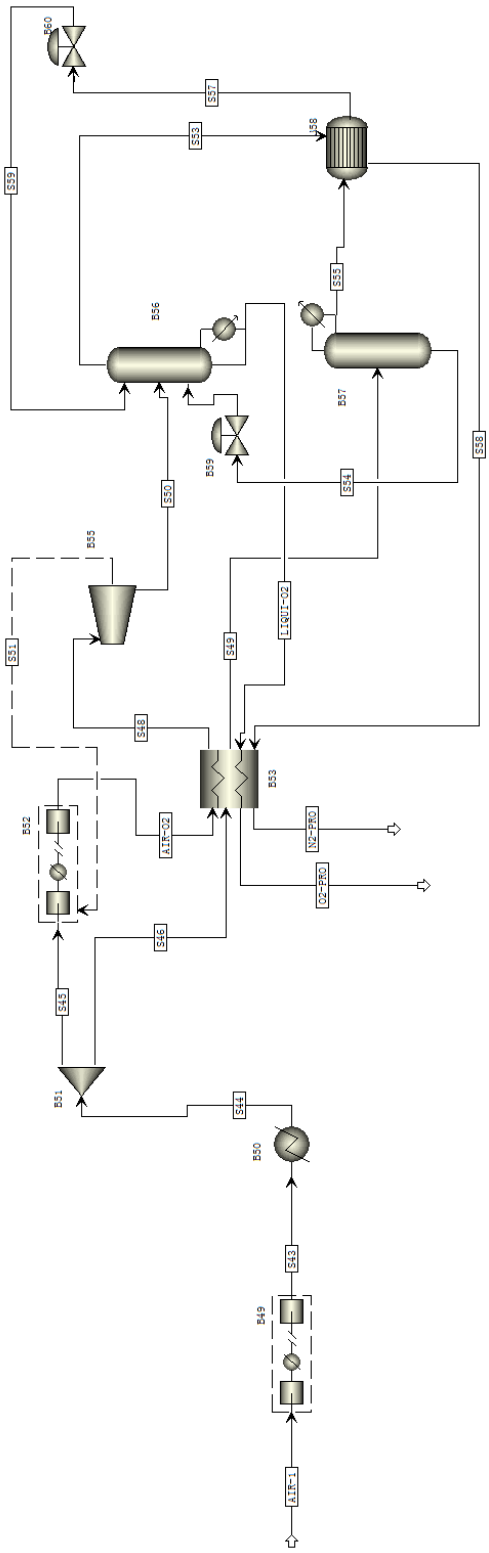

Figure A11: Air separation unit Aspen Plus model for all three biomass conversion processes

Appendix B

Syngas Correlations of Biomass Gasification

Table B1: GTI Gasifier Correlation

Eq.	Form	A	B	C	D	E	R^2
1	$H_2/Feed\ H = A + B*P + C*T + D*(\frac{O_2}{Feed\ C}) + E*(\frac{H_2O}{Feed\ C})$	-3.830761E-01	1.894350E-04	2.666675E-04	1.060088E-01	7.880955E-02	0.7828
2	$CO/Feed\ \ C = A + B*P + C*T + D*(\frac{O_2}{Feed\ C}) + E*(\frac{H_2O}{Feed\ C})$	-8.130017E-02	-3.340050E-04	2.614482E-04	1.495730E-01	-5.268367E-02	0.7984
3	$CO_2/Feed\ \ C = A + B*P + C*T + D*(\frac{O_2}{Feed\ C}) + E*(\frac{H_2O}{Feed\ C})$	7.157172E-02	3.843454E-04	1.286060E-05	6.124545E-01	9.980868E-02	0.9080
4	$CH_4/Feed\ \ C = A + B*P + C*T + D*(\frac{O_2}{Feed\ C}) + E*(\frac{H_2O}{Feed\ C})$	1.093589E-02	1.388446E-04	8.812765E-05	-2.274854E-01	3.427825E-02	0.6243
5	$C_2H_4/Feed\ \ C = A + B*P + C*T + D*(\frac{O_2}{Feed\ C}) + E*(\frac{H_2O}{Feed\ C})$	5.301812E-02	-6.740399E-05	-1.372749E-05	-9.076286E-03	-4.854082E-03	0.8910
6	$C_2H_6/Feed\ C = A + B*P + C*T + D*(\frac{O_2}{Feed\ C}) + E*(\frac{H_2O}{Feed\ C})$	1.029750E-01	-5.440777E-06	-5.350103E-05	-3.377091E-02	-1.915339E-03	0.7451
7	$C_6H_6/Feed\ C = A + B*P + C*T + D*(\frac{O_2}{Feed\ C}) + E*(\frac{H_2O}{Feed\ C})$	4.676833E-02	-1.937444E-05	-1.270868E-05	-1.046762E-02	-8.459647E-03	0.3242
8	$C_{10}H_8/Feed\ C = A + B*P + C*T + D*(\frac{O_2}{Feed\ C}) + E*(\frac{H_2O}{Feed\ C})$	1.827359E-02	-2.328921E-06	-5.951746E-06	-1.936385E-02	-7.678310E-04	0.4726
9	$\%\ Feed\ N\ in\ Char = A$	3.360000E+00					
10	$\%\ Feed\ S\ in\ Char = A$	8.450000E+00					
11	$\%\ Feed\ O\ in\ Char = A + B*P + C*T + D*(\frac{O_2}{Feed\ C}) + E*(\frac{H_2O}{Feed\ C})$	1.512040E+00	1.582010E-04	-6.972612E-04	1.573581E-01	-1.420915E-01	0.3332

[a]All ratios are on a molar basis, pressure in psia, temperature in °F

The following assumptions are used for the gasifier production:

(1) The amount of carbon in the syngas and tar is determined from the gasifier correlations. Residual carbon is parsed in the char.

(2) The amount of oxygen in the syngas is determined from the gasifier correlations. A minimum fraction of the biomass oxygen is required to the parsed to the char based on equation 11 in gasifier correlations. If there is a deficit of oxygen, then the associated water is decomposed to make sure that this amount of oxygen is parsed to the char; if there is excess oxygen, then that is parsed to the char without decomposing hydrogen.

(3) A set amount of sulfur is parsed to the char (8.4%). All remaining sulfur is set as H_2S in the syngas.

(4) A set amount of nitrogen is parsed to the char (3.4%). All remaining nitrogen is set as NH_3 in the syngas.

(5) The amount of hydrogen in the syngas (including tar, H_2S, NH_3, and decomposed water) is determined from the gasifier correlations. All remaining hydrogen is parsed to the char.

(6) All ash is parsed to the char

Appendix C

Pinch Analysis

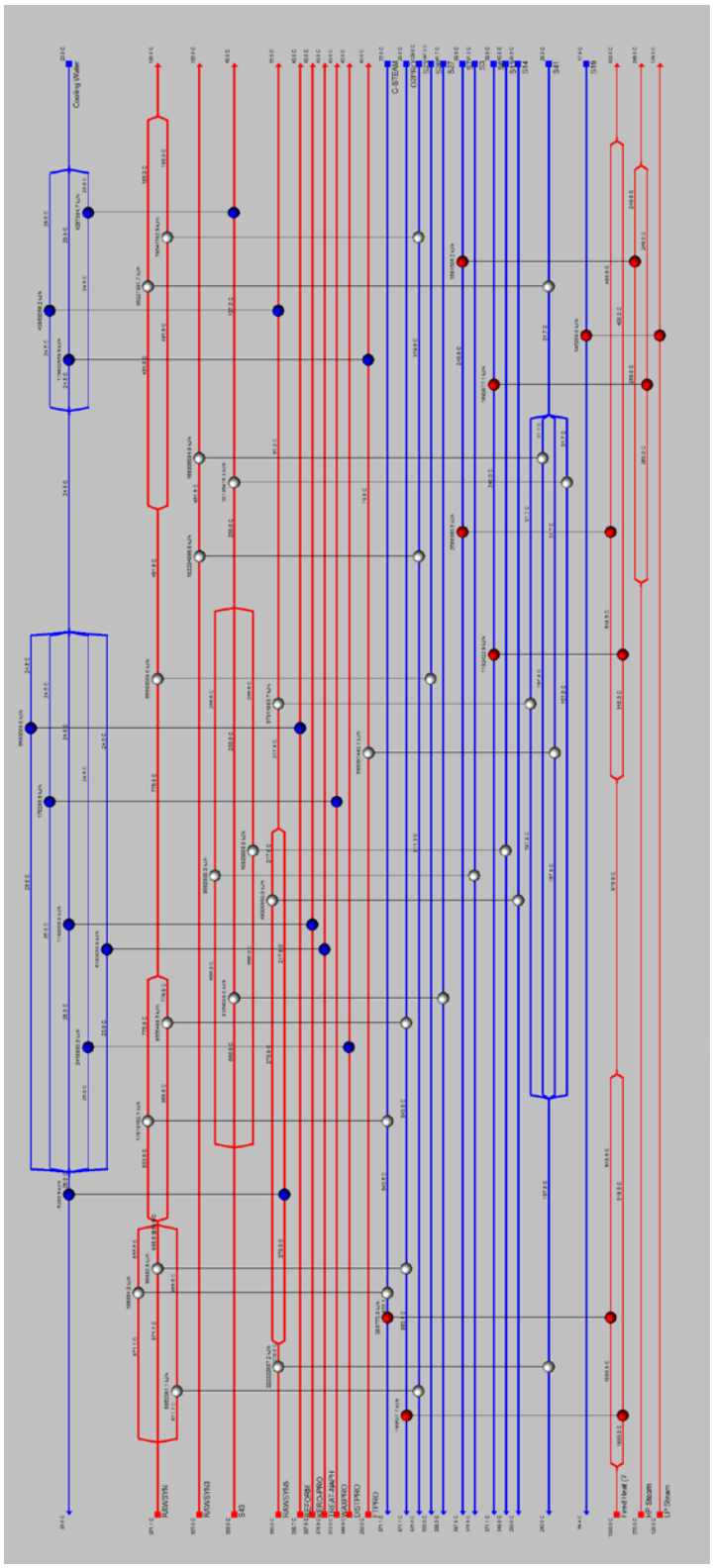

Figure C1: Supercritical FTS biomass conversion process pinch analysis

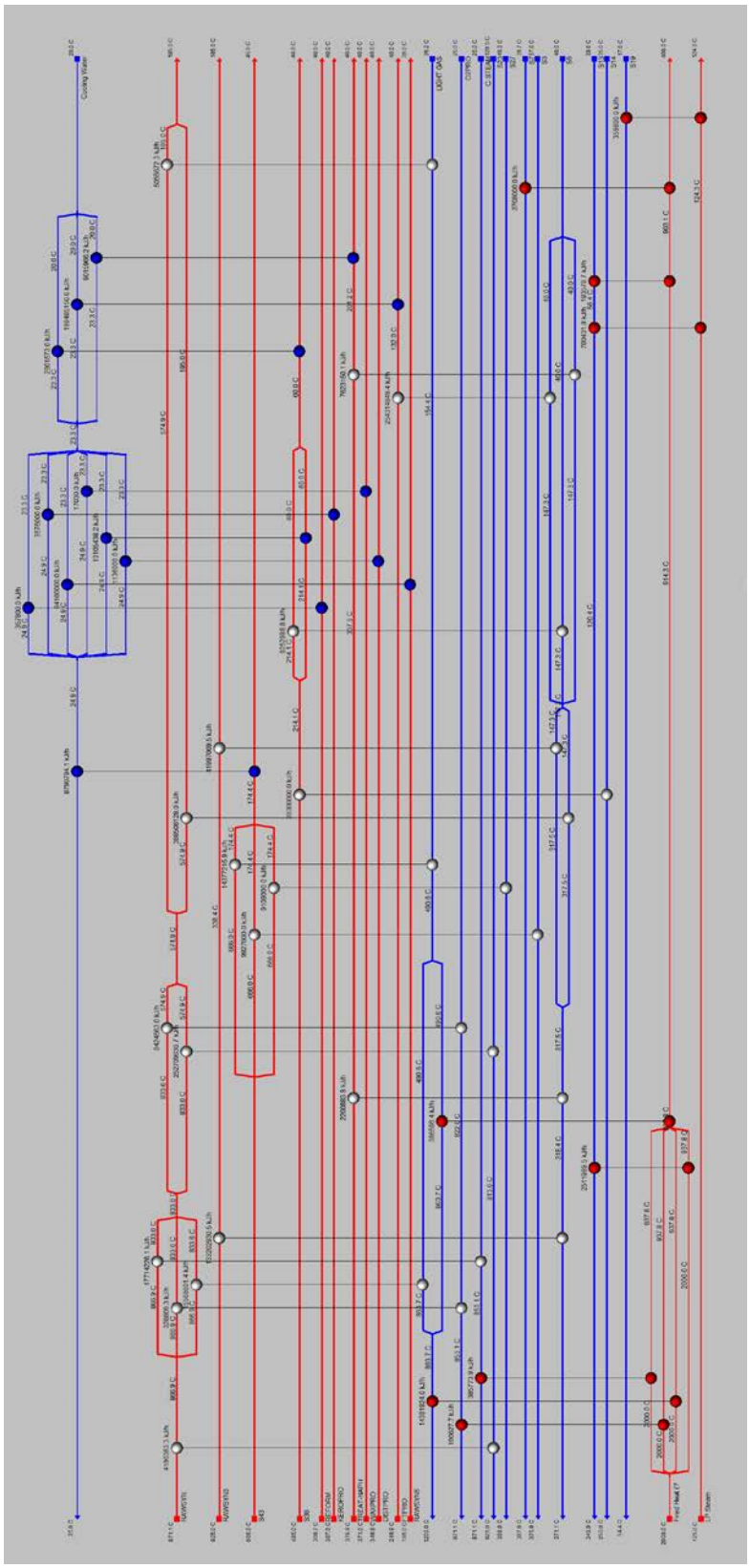

Figure C2: Once-through FTS biomass conversion process pinch analysis

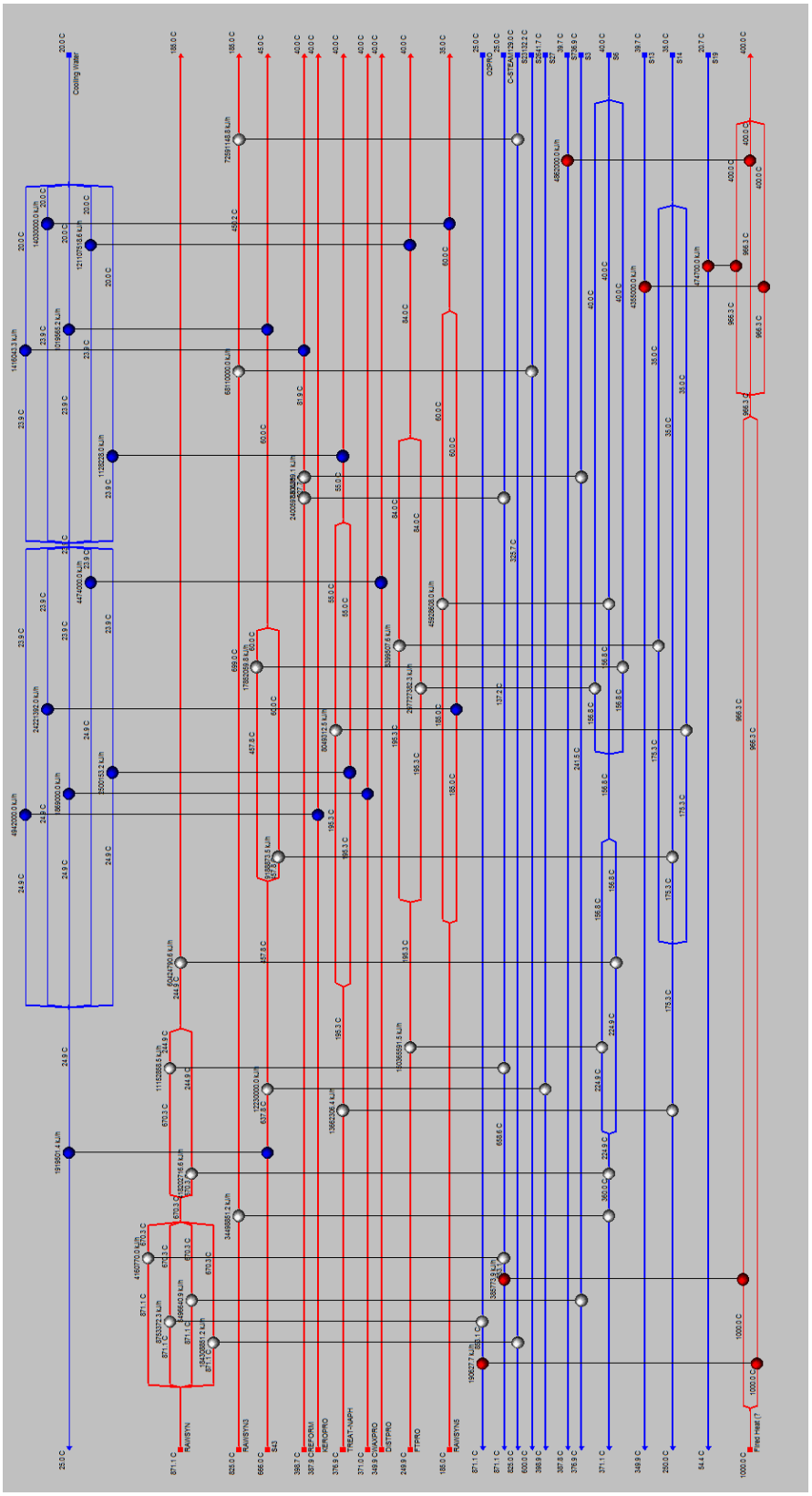

Figure C3: Conventional FTS biomass conversion process pinch analysis

Appendix D

Individual Equipment Cost Summary

Table D1: Supercritical FTS Biomass Conversion Process Individual Equipment Cost Summary

Component	Equipment name	Equipment Cost (USD)	Base Year	Equipment Cost in 2016 (USD)	Installed Cost in 2016 (USD)
DRYER	Biomass Handling and Drying	3813728.00	2002	6174653.14	15251393.27
SEP	Separator	167100.00	2013	188661.29	465993.39
Gasifier	Biomass Gasifier	5805883.00	2002	9400070.93	23218175.21
CYCLONE	Ash Cyclone	6200.00	2013	7000.00	17290.00
TAREFORM	Tar Reformer	284900.00	2013	321661.29	794503.39
SCRUB	Syngas Scrubber	52000.00	2013	58709.68	145012.90
WGSR	Water Gas Shift Reactor	397200.00	2013	448451.61	1107675.48
B9	Separator	495900.00	2013	559887.10	1382921.13
H2OKNOCK	Water Knockout Vessel	30400.00	2013	34322.58	84776.77
B72	Compressor	3114500.00	2013	3516370.97	8685436.29
B67	Compressor	5135300.00	2013	5797919.35	14320860.81
FTREACT	Fischer-Tropsch Reactor	4280100.00	2013	4832370.97	11935956.29
CO2REMO	Separator	287300.00	2013	324370.97	801196.29
B4	Separator	271500.00	2013	306532.26	757134.68
B5	Separator	219700.00	2013	248048.39	612679.52
B2	Separator	18300.00	2013	20661.29	51033.39
WAXCRACK	Wax Hydrocracker	84000.00	2013	94838.71	234251.61
DIST-HT	Distillate Hydrotreater	91000.00	2013	102741.94	253772.58
KERO-HT	Kerosene Hydrotreater	108200.00	2013	122161.29	301738.39
NAPH-HT	Naphtha Hydrotreater	249200.00	2013	281354.84	694946.45
REFORMER	Catalytic Reformer	2794100.00	2013	3154629.03	7791933.71
C5-C6ISO	C_5/C_6 Isomerizer	27500.00	2013	31048.39	76689.52
C4ISO	C_4 Isomerizer	43300.00	2013	48887.10	120751.13
AKYLIZER	$C_3/C_4/C_5$ Alkylation Unit	31600.00	2013	35677.42	88123.23

Table D1 (*Cont.*): Supercritical FTS Biomass Conversion Process Individual Equipment Cost Summary

Component	Equipment name	Equipment Cost (USD)	Base Year	Equipment Cost in 2016 (USD)	Installed Cost in 2016 (USD)
SGP	Saturated Gas Plant	41400.00	2013	46741.94	115452.58
H2RECOV	Hydrogen Recovery Unit	41400.00	2013	46741.94	115452.58
B45	Separator	99500.00	2013	112338.71	277476.61
B44	Separator	239000.00	2013	269838.71	666501.61
B39	Separator	14500.00	2013	16370.97	40436.29
B37	Separator	30200.00	2013	34096.77	84219.03
B33	Separator	14300.00	2013	16145.16	39878.55
B26	Separator	18100.00	2013	20435.48	50475.65
B23	Separator	14300.00	2013	16145.16	39878.55
B21	Separator	24000.00	2013	27096.77	66929.03
B15	Separator	19400.00	2013	21903.23	54100.97
B13	Separator	26200.00	2013	29580.65	73064.19
AUTOTHER	Auto-thermal Reformer	250300.00	2013	282596.77	698014.03
ASU	Air Separation Unit	15756915.42	1999	25837952.70	63819743.18
E-142	Cooler	25730.15	2013	29050.17	71753.91
E-144	Heater	13222.20	2013	14928.29	36872.87
E-148	Cooler	452057.76	2013	510387.79	1260657.85
E-146	Heat Exchanger	95981.30	2013	108365.99	267663.99
E-150	Heater	39692.83	2013	44814.48	110691.78
E-127	Heat Exchanger	2354555.26	2013	2658368.84	6566171.04
E-129	Heat Exchanger	62996.92	2013	71125.55	175680.12
E-133	Heat Exchanger	52772.47	2013	59581.82	147167.10
E-125	Heater	26775.45	2013	30230.35	74668.96
E-123	Heat Exchanger	19138.47	2013	21607.95	53371.63
E-121	Heater	14280.64	2013	16123.30	39824.56

Table D1 (*Cont.*): Supercritical FTS Biomass Conversion Process Individual Equipment Cost Summary

Component	Equipment name	Equipment Cost (USD)	Base Year	Equipment Cost in 2016 (USD)	Installed Cost in 2016 (USD)
E-143	Cooler	41828.96	2013	47226.24	116648.81
E-141	Cooler	18377.23	2013	20748.49	51248.77
E-145	Heat Exchanger	160265.55	2013	180944.98	446934.10
E-147	Heat Exchanger	579988.54	2013	654825.77	1617419.66
E-128	Heat Exchanger	103146.82	2013	116456.09	287646.54
E-130	Heat Exchanger	420284.42	2013	474514.67	1172051.24
E-132	Heat Exchanger	51793.59	2013	58476.64	144437.29
E-136	Heat Exchanger	637169.09	2013	719384.45	1776879.59
E-134	Heat Exchanger	58681.00	2013	66252.74	163644.27
E-124	Heat Exchanger	90148.06	2013	101780.07	251396.76
E-152	Cooler	49677.04	2013	56086.98	138534.83
E-140	Cooler	11879.88	2013	13412.76	33129.52
E-137	Heat Exchanger	10258946.57	2013	11582681.61	28609223.58
E-139	Cooler	53989.42	2013	60955.79	150560.81
E-131	Cooler	10054.65	2013	11352.03	28039.51
E-135	Heat Exchanger	2190433.76	2013	2473070.38	6108483.84
E-119	Heat Exchanger	987726.92	2013	1115175.55	2754483.61
E-151	Heater	26547.01	2013	29972.43	74031.90
E-149	Cooler	1272599.75	2013	1436806.17	3548911.25
E-138	Heat Exchanger	348042.77	2013	392951.52	970590.25
E-126	Heater	18281.51	2013	20640.41	50981.82
E-120	Heater	17523.61	2013	19784.72	48868.25
E-122	Heat Exchanger	26061.67	2013	29424.47	72678.44

Table D2: Once-through FTS Biomass Conversion Process Individual Equipment Cost Summary

Component	Equipment name	Equipment Cost (USD)	Base Year	Equipment Cost in 2016 (USD)	Installed Cost in 2016 (USD)
DRYER	Biomass Handling and Drying	3813728.00	2002	6174653.14	15251393.27
SEP	Separator	167100.00	2013	2272.74	5613.67
Gasifier	Biomass Gasifier	5805883.00	2002	9400070.93	23218175.21
CYCLONE	Ash Cyclone	6200.00	2013	7000.00	17290.00
TAREFORM	Tar Reformer	471200.00	2013	532000.00	1314040.00
SCRUB	Syngas Scrubber	52000.00	2013	58709.68	145012.90
B9	Separator	52000.00	2013	58709.68	145012.90
H2OKNOCK	Water Knockout Vessel	30900.00	2013	34887.10	86171.13
FTREACT	Fischer-Tropsch Reactor	340100.00	2013	383983.87	948440.16
CO2REMO	Separator	31300.00	2013	35338.71	87286.61
B4	Separator	31000.00	2013	35000.00	86450.00
B5	Separator	28200.00	2013	31838.71	78641.61
B2	Separator	22300.00	2013	25177.42	62188.23
WAXCRACK	Wax Hydrocracker	1860100.00	2013	2100112.90	5187278.87
DIST-HT	Distillate Hydrotreater	91000.00	2013	102741.94	253772.58
KERO-HT	Kerosene Hydrotreater	90300.00	2013	101951.61	251820.48
NAPH-HT	Naphtha Hydrotreater	337900.00	2013	381500.00	942305.00
REFORMER	Catalytic Reformer	2653300.00	2013	2995661.29	7399283.39
C5-C6ISO	C_5/C_6 Isomerizer	27500.00	2013	31048.39	76689.52
C4ISO	C_4 Isomerizer	43300.00	2013	48887.10	120751.13
AKYLIZER	$C_3/C_4/C_5$ Alkylation Unit	27500.00	2013	31048.39	76689.52
SGP	Saturated Gas Plant	20900.00	2013	23596.77	58284.03
H2RECOV	Hydrogen Recovery Unit	18100.00	2013	20435.48	50475.65
B48	Separator	112100.00	2013	126564.52	312614.35

Table D2 (*Cont.*): Once-through FTS Biomass Conversion Process Individual Equipment Cost Summary

Component	Equipment name	Equipment Cost (USD)	Base Year	Equipment Cost in 2016 (USD)	Installed Cost in 2016 (USD)
B23	Separator	16600.00	2013	18741.94	46292.58
B37	Separator	28000.00	2013	31612.90	78083.87
B43	Separator	468000.00	2013	528387.10	1305116.13
B15	Separator	14400.00	2013	16258.06	40157.42
B13	Separator	26200.00	2013	29580.65	73064.19
B21	Separator	24000.00	2013	27096.77	66929.03
B33	Separator	14300.00	2013	16145.16	39878.55
B26	Separator	17900.00	2013	20209.68	49917.90
B39	Separator	14500.00	2013	16370.97	40436.29
B44	Air Compressor	6042800.00	2013	6822516.13	16851614.84
B45	Gas Turbine	2786700.00	2013	3146274.19	7771297.26
ASU	Air Separation Unit	15756915.42	1999	25837952.70	63819743.18
E-151	Cooler	18468.67	2013	20851.72	51503.76
E-143	Heat Exchanger	2157965.31	2013	2436412.45	6017938.74
E-145	Heat Exchanger	49769.78	2013	56191.69	138793.47
E-130	Heat Exchanger	176578.19	2013	199362.47	492425.30
E-124	Heater	14434.19	2013	16296.66	40252.76
E-150	Cooler	67047.58	2013	75698.88	186976.24
E-152	Heater	20905.31	2013	23602.77	58298.84
E-129	Heater	14775.21	2013	16681.68	41203.76
E-131	Heat Exchanger	58980.68	2013	66591.09	164480.00
E-133	Heat Exchanger	70332.74	2013	79407.93	196137.59
E-119	Heat Exchanger	676580.64	2013	763881.37	1886786.98
E-153	Cooler	55586.27	2013	62758.69	155013.97
E-139	Heat Exchanger	31714.69	2013	35806.91	88443.07

Table D2 (*Cont.*): Once-through FTS Biomass Conversion Process Individual Equipment Cost Summary

Component	Equipment name	Equipment Cost (USD)	Base Year	Equipment Cost in 2016 (USD)	Installed Cost in 2016 (USD)
E-141	Cooler	73613.69	2013	83112.23	205287.20
E-147	Cooler	29879.75	2013	33735.20	83325.93
E-149	Cooler	10283.59	2013	11610.50	28677.94
E-138	Heat Exchanger	1236128.44	2013	1395628.88	3447203.33
E-128	Heater	28620.39	2013	32313.34	79813.96
E-126	Heat Exchanger	46505.99	2013	52506.76	129691.69
E-134	Heat Exchanger	68886.09	2013	77774.62	192103.30
E-132	Heat Exchanger	225010.31	2013	254043.90	627488.44
E-136	Heat Exchanger	1494973.14	2013	1687872.90	4169046.06
E-120	Heat Exchanger	73166.16	2013	82606.95	204039.18
E-122	Heater	11512.08	2013	12997.51	32103.85
E-154	Cooler	1332273.68	2013	1504179.97	3715324.52
E-140	Heat Exchanger	2664725.54	2013	3008561.10	7431145.91
E-142	Heater	13329.29	2013	15049.20	37171.52
E-144	Heat Exchanger	237470.14	2013	268111.45	662235.28
E-146	Cooler	13098.79	2013	14788.96	36528.73
E-148	Cooler	547759.33	2013	618437.95	1527541.73
E-137	Heater	10689.22	2013	12068.47	29809.12
E-127	Heat Exchanger	183019.25	2013	206634.63	510387.54
E-135	Heat Exchanger	82164.83	2013	92766.75	229133.87
E-123	Heater	83146.27	2013	93874.82	231870.81
E-125	Heat Exchanger	95000.30	2013	107258.40	264928.26
E-121	Heater	12657.61	2013	14290.86	35298.41
E-155	Cooler	69936.80	2013	78960.90	195033.43

Table D3: Conventional FTS Biomass Conversion Process Individual Equipment Cost Summary

Component	Equipment name	Equipment Cost (USD)	Base Year	Equipment Cost in 2016 (USD)	Installed Cost in 2016 (USD)
DRYER	Biomass Handling and Drying	3813728.00	2002	6174653.14	15251393.27
SEP	Separator	167100.00	2013	188661.29	465993.39
Gasifier	Biomass Gasifier	5805883.00	2002	9400070.93	23218175.21
CYCLONE	Ash Cyclone	6200.00	2013	7000.00	17290.00
TAREFORM	Tar Reformer	320200.00	2013	361516.13	892944.84
SCRUB	Syngas Scrubber	52000.00	2013	58709.68	145012.90
B9	Separator	52000.00	2013	58709.68	145012.90
H2OKNOCK	Water Knockout Vessel	30900.00	2013	34887.10	86171.13
FTREACT	Fischer-Tropsch Reactor	473100.00	2013	534145.16	1319338.55
CO2REMO	Separator	33900.00	2013	38274.19	94537.26
B4	Separator	34000.00	2013	38387.10	94816.13
B5	Separator	24800.00	2013	28000.00	69160.00
B2	Separator	21800.00	2013	24612.90	60793.87
WAXCRACK	Wax Hydrocracker	57300.00	2013	64693.55	159793.06
DIST-HT	Distillate Hydrotreater	140900.00	2013	159080.65	392929.19
KERO-HT	Kerosene Hydrotreater	107500.00	2013	121370.97	299786.29
NAPH-HT	Naphtha Hydrotreater	453700.00	2013	512241.94	1265237.58
REFORMER	Catalytic Reformer	3414900.00	2013	3855532.26	9523164.68
C5-C6ISO	C_5/C_6 Isomerizer	27600.00	2013	31161.29	76968.39
C4ISO	C_4 Isomerizer	43500.00	2013	49112.90	121308.87
AKYLIZER	$C_3/C_4/C_5$ Alkylation Unit	21300.00	2013	24048.39	59399.52
B39	Separator	14500.00	2013	16370.97	40436.29
B37	Separator	26200.00	2013	29580.65	73064.19
B33	Separator	14300.00	2013	16145.16	39878.55
B26	Separator	19400.00	2013	21903.23	54100.97

Table D3 (*Cont.*): Conventional FTS Biomass Conversion Process Individual Equipment Cost Summary

Component	Equipment name	Equipment Cost (USD)	Base Year	Equipment Cost in 2016 (USD)	Installed Cost in 2016 (USD)
B23	Separator	16600.00	2013	18741.94	46292.58
B21	Separator	24000.00	2013	27096.77	66929.03
B15	Separator	19400.00	2013	21903.23	54100.97
B13	Separator	26200.00	2013	29580.65	73064.19
SGP	Saturated Gas Plant	25300.00	2013	28564.52	70554.35
H2RECOV	Hydrogen Recovery Unit	23900.00	2013	26983.87	66650.16
AUTOTHER	Auto-thermal Reformer	251200.00	2013	283612.90	700523.87
WGSR	Water Gas Shift Reactor	335700.00	2013	379016.13	936169.84
B65	Separator	356900.00	2013	402951.61	995290.48
B66	Separator	134000.00	2013	151290.32	373687.10
ASU	Air Separation Unit	15756915.42	1999	25837952.70	63819743.18
E-144	Cooler	35943.47	2013	40581.34	100235.91
E-146	Cooler	22252.66	2013	25123.97	62056.22
E-148	Cooler	26771.87	2013	30226.30	74658.97
E-133	Heat Exchanger	20200.01	2013	22806.46	56331.95
E-135	Heat Exchanger	151704.72	2013	171279.52	423060.41
E-123	Heater	13433.92	2013	15167.33	37463.31
E-157	Cooler	33027.75	2013	37289.39	92104.79
E-143	Heat Exchanger	399741.47	2013	451321.02	1114762.91
E-145	Cooler	111760.05	2013	126180.70	311666.34
E-138	Heat Exchanger	5853873.02	2013	6609211.47	16324752.34
E-136	Heat Exchanger	216696.23	2013	244657.03	604302.86
E-134	Heat Exchanger	2057424.00	2013	2322898.06	5737558.21
E-150	Heater	28374.30	2013	32035.50	79127.69
E-152	Heat Exchanger	691642.96	2013	780887.21	1928791.41

Table D3 (*Cont.*): Conventional FTS Biomass Conversion Process Individual Equipment Cost Summary

Component	Equipment name	Equipment Cost (USD)	Base Year	Equipment Cost in 2016 (USD)	Installed Cost in 2016 (USD)
E-140	Heat Exchanger	166602.89	2013	188100.03	464607.08
E-142	Heat Exchanger	324151.76	2013	365977.80	903965.16
E-137	Heat Exchanger	254551.02	2013	287396.32	709868.90
E-127	Heat Exchanger	980122.37	2013	1106589.77	2733276.73
E-125	Heat Exchanger	67339.96	2013	76028.99	187791.61
E-129	Heat Exchanger	46997.58	2013	53061.78	131062.60
E-131	Heat Exchanger	3006268.62	2013	3394174.25	8383610.39
E-121	Heat Exchanger	74970.05	2013	84643.61	209069.72
E-153	Cooler	30992.95	2013	34992.04	86430.35
E-155	Cooler	28262.44	2013	31909.21	78815.75
E-151	Heater	25825.24	2013	29157.53	72019.10
E-139	Heat Exchanger	1596230.05	2013	1802195.21	4451422.17
E-141	Heat Exchanger	101524.43	2013	114624.35	283122.16
E-147	Cooler	35545.74	2013	40132.29	99126.76
E-149	Heater	11962.53	2013	13506.09	33360.04
E-128	Cooler	12655.36	2013	14288.31	35292.13
E-126	Heat Exchanger	23397.46	2013	26416.49	65248.73
E-130	Heat Exchanger	308265.67	2013	348041.89	859663.47
E-132	Heat Exchanger	3887920.36	2013	4389587.50	10842281.14
E-122	Heater	16035.42	2013	18104.51	44718.14
E-124	Heat Exchanger	349075.08	2013	394117.02	973469.04
E-156	Cooler	1159650.70	2013	1309283.05	3233929.14
E-154	Cooler	218461.34	2013	246649.90	609225.26

Appendix E

Discounted Cash Flow Rate of Return and Operating Costs Summary

Table E1: Cash flow of supercritical FTS biomass conversion process

Year	1	2	3	4	5	6	7	8	9	10
Working Capital			14786627							
Salvage Value										
Capital Costs	74672464	150838378	90960007							
Operating Costs										
Biomass				52030205	52550507	53076012	53606772	54142840	54684268	55231111
Hydrogen				1266030	1278691	1291478	1304392	1317436	1330611	1343917
Butane				949954	959454	969049	978739	988526	998412	1008396
Hexane				12293290	12416223	12540385	12665789	12792447	12920371	13049575
labor				2081208	2102020	2123040	2144271	2165713	2187371	2209244
Maintenance				4448776	4493264	4538197	4583579	4629415	4675709	4722466
Insurance				4448776	4493264	4538197	4583579	4629415	4675709	4722466
Utility										
Cooling Water				330263	333565	336901	340270	343673	347109	350581
LP Steam				5475	5530	5585	5641	5698	5755	5812
HP Steam				108130	109211	110303	111406	112520	113645	114782
Fired Heat				150866	152375	153898	155437	156992	158562	160147
Electricity				25755552	26013108	26273239	26535971	26801331	27069344	27340038
SOC				103868526	104907212	105956284	107015847	108086005	109166865	110258534
Operating Expense				8309482	8392577	8476503	8561268	8646880	8733349	8820683
Plant Overhead				3264992	3297642	3330619	3363925	3397564	3431540	3465855
Tax Rate				0.4						
Annual Depreciation				29573253	29573253	29573253	29573253	29573253	29573253	29573253
Product sales										
Break-Even Oil Price				2.6297262						
Gasoline				82268235	83090917	83921826	84761045	85608655	86464742	87329389
Kerosene				40533445	40938780	41348167	41761649	42179266	42601058	43027069
Diesel				89154975	90046525	90946990	91856460	92775025	93702775	94639803
Propane				4808303	4856386	4904950	4954000	5003540	5053575	5104111
Total product sales				216764959	218932608	221121934	223333154	225566485	227822150	230100371
Cash Flow	-74672464	-150838378	-90960007	48963873	49571805	50185816	50805967	51432320	52064936	52703879
	-64932578	-114055484	-59807681	27995254	24645948	21696713	19099845	16813317	14800104	13027593
Net Present Value	0									

Table E1 (*Cont.*): Cash flow of supercritical FTS biomass conversion process

Year	11	12	13	14	15	16	17	18	19	20
Working Capital										
Salvage Value										
Capital Costs										
Operating Costs										
Biomass	55783422	56341256	56904669	57473715	58048452	58628937	59215226	59807379	60405452	61009507
Hydrogen	1357356	1370930	1384639	1398485	1412470	1426595	1440861	1455269	1469822	1484520
Butane	1018480	1028665	1038951	1049341	1059834	1070432	1081137	1091948	1102868	1113896
Hexane	13180071	13311871	13444990	13579440	13715234	13852387	13990911	14130820	14272128	14414849
labor	2231337	2253650	2276187	2298948	2321938	2345157	2368609	2392295	2416218	2440380
Maintenance	4769690	4817387	4865561	4914217	4963359	5012993	5063123	5113754	5164891	5216540
Insurance	4769690	4817387	4865561	4914217	4963359	5012993	5063123	5113754	5164891	5216540
Utility										
Cooling Water	354086	357627	361203	364816	368464	372148	375870	379629	383425	387259
LP Steam	5870	5929	5988	6048	6109	6170	6232	6294	6357	6420
HP Steam	115930	117089	118260	119442	120637	121843	123062	124292	125535	126790
Fired Heat	161749	163366	165000	166650	168316	170000	171700	173417	175151	176902
Electricity	27613438	27889572	28168468	28450153	28734654	29022001	29312221	29605343	29901397	30200411
SOC	111361119	112474730	113599478	114735472	115882827	117041655	118212072	119394193	120588135	121794016
Operating Expense	8908890	8997978	9087958	9178838	9270626	9363332	9456966	9551535	9647051	9743521
Plant Overhead	3500514	3535519	3570874	3606583	3642648	3679075	3715866	3753024	3790555	3828460
Tax Rate										
Annual Depreciation	29573253.1	29573253.1	29573253.1							
Product sales										
Break-Even Oil Price										
Gasoline	88202683	89084710	89975557	90875313	91784066	92701906	93628925	94565215	95510867	96465975
Kerosene	43457340	43891913	44330832	44774140	45221882	45674101	46130842	46592150	47058071	47528652
Diesel	95586201	96542063	97507483	98482558	99467384	100462057	101466678	102481345	103506158	104541220
Propane	5155152	5206704	5258771	5311358	5364472	5418117	5472298	5527021	5582291	5638114
Total product sales	232401375	234725389	237072643	239443369	241837803	244256181	246698743	249165730	251657388	254173961
Cash Flow	53349211	54000996	54659299	67153486	67825021	68503271	69188304	69880187	70578989	71284778
	11467051	10093172	8883664	9490712	8335321	7320586	6429384	5646677	4959255	4355520
Net Present Value										

Table E1 (*Cont.*): Cash flow of supercritical FTS biomass conversion process

Year	21	22	23	24	25	26	27	28	29	30
Working Capital										
Salvage Value										59146506
Capital Costs										-59146506
Operating Costs										
Biomass	61619602	62235798	62858156	63486738	64121605	64762821	65410449	66064554	66725199	67392451
Hydrogen	1499365	1514359	1529503	1544798	1560246	1575848	1591607	1607523	1623598	1639834
Butane	1125035	1136286	1147648	1159125	1170716	1182423	1194248	1206190	1218252	1230435
Hexane	14558998	14704588	14851634	15000150	15150151	15301653	15454669	15609216	15765308	15922961
labor	2464784	2489432	2514326	2539469	2564864	2590513	2616418	2642582	2669008	2695698
Maintenance	5268706	5321393	5374607	5428353	5482636	5537463	5592837	5648766	5705253	5762306
Insurance	5268706	5321393	5374607	5428353	5482636	5537463	5592837	5648766	5705253	5762306
Utility										
Cooling Water	391132	395043	398993	402983	407013	411083	415194	419346	423540	427775
LP Steam	6485	6549	6615	6681	6748	6815	6883	6952	7022	7092
HP Steam	128058	129339	130632	131939	133258	134591	135937	137296	138669	140056
Fired Heat	178671	180458	182262	184085	185926	187785	189663	191560	193475	195410
Electricity	30502415	30807439	31115513	31426668	31740935	32058344	32378928	32702717	33029744	33360042
SOC	123011956	124242076	125484496	126739341	128006735	129286802	130579670	131885467	133204321	134536365
Operating Expense	9840956	9939366	10038760	10139147	10240539	10342944	10446374	10550837	10656346	10762909
Plant Overhead	3866745	3905412	3944466	3983911	4023750	4063988	4104627	4145674	4187131	4229002
Tax Rate										
Annual Depreciation										
Product sales										
Break-Even Oil Price										
Gasoline	97430635	98404942	99388991	100382881	101386710	102400577	103424583	104458828	105503417	106558451
Kerosene	48003939	48483978	48968818	49458506	49953091	50452622	50957148	51466720	51981387	52501201
Diesel	105586632	106642498	107708923	108786013	109873873	110972611	112082338	113203161	114335192	115478544
Propane	5694495	5751440	5808954	5867044	5925714	5984971	6044821	6105269	6166322	6227985
Total product sales	256715701	259282858	261875687	264494443	267139388	269810782	272508890	275233978	277986318	280766181
Cash Flow	71997626	72717603	73444779	74179226	74921019	75670229	76426931	77191200	77963112	137889250
	3825283	3359596	2950602	2591398	2275924	1998855	1755516	1541801	1354103	2082549
Net Present Value										

Table E2: Cash flow of once-through FTS biomass conversion process

Year	1	2	3	4	5	6	7	8	9	10
Working Capital			12508725							
Salvage Value										
Capital Costs	63169062	127601505	76947485	0	0	0	0	0	0	0
Operating Costs										
Biomass				52030205	52550507	53076012	53606772	54142840	54684268	55231111
Hydrogen				2015783	2035941	2056300	2076863	2097632	2118608	2139794
Butane				949954	959454	969049	978739	988526	998412	1008396
Labor				2081208	2102020	2123040	2144271	2165713	2187371	2209244
Maintenance				3692402	3729326	3766620	3804286	3842329	3880752	3919559
Insurance				3692402	3729326	3766620	3804286	3842329	3880752	3919559
Utility										
Cooling Water				568819	574507	580252	586055	591915	597835	603813
Fired Heat				1389381	1403275	1417308	1431481	1445796	1460254	1474856
LP Steam				16771	16939	17108	17279	17452	17626	17803
Electricity				20689024	20895914	21104873	21315922	21529081	21744372	21961816
SOC				87125950	87997210	88877182	89765953	90663613	91570249	92485952
Operating Expense				6970076	7039777	7110175	7181276	7253089	7325620	7398876
Plant Overhead				2886805	2915673	2944830	2974278	3004021	3034061	3064402
Tax Rate				0.4						
Annual Depreciation				25017450	25017450	25017450	25017450	25017450	25017450	25017450
Product Sales										
Break-Even Oil Price				2.673862951						
Gasoline				102525999	103551259	104586771	105632639	106688965	107755855	108833414
Kerosene				28480547	28765353	29053006	29343536	29636972	29933341	30232675
Diesel				37641312	38017725	38397903	38781882	39169700	39561397	39957011
Propane				5199367	5251361	5303875	5356913	5410483	5464587	5519233
Electricity				8848768	8937255	9026628	9116894	9208063	9300144	9393145
Total product sales				182695993	184522953	186368183	188231864	190114183	192015325	193935478
Cash Flow	-63169062	-127601505	-76947485	41420917	41935196	42454618	42979234	43509096	44044257	44584769
	-54929619	-96485070	-50594220	23682544	20849204	18354303	16157486	14223201	12520127	11020673
Net Present Value	0.0									

Table E2 (*Cont.*): Cash flow of once-through FTS biomass conversion process

Year	11	12	13	14	15	16	17	18	19	20
Working Capital										
Salvage Value										
Capital Costs	0	0	0	0	0	0	0	0	0	0
Operating Costs										
Biomass	55783422	56341256	56904669	57473715	58048452	58628937	59215226	59807379	60405452	61009507
Hydrogen	2161192	2182804	2204632	2226679	2248945	2271435	2294149	2317091	2340262	2363664
Butane	1018480	1028665	1038951	1049341	1059834	1070432	1081137	1091948	1102868	1113896
Labor	2231337	2253650	2276187	2298948	2321938	2345157	2368609	2392295	2416218	2440380
Maintenance	3958755	3998343	4038326	4078709	4119496	4160691	4202298	4244321	4286764	4329632
Insurance	3958755	3998343	4038326	4078709	4119496	4160691	4202298	4244321	4286764	4329632
Utility										
Cooling Water	609851	615950	622109	628330	634613	640960	647369	653843	660381	666985
Fired Heat	1489605	1504501	1519546	1534741	1550089	1565589	1581245	1597058	1613028	1629159
LP Steam	17981	18160	18342	18525	18711	18898	19087	19278	19470	19665
Electricity	22181434	22403248	22627281	22853554	23082089	23312910	23546039	23781500	24019315	24259508
SOC	93410811	94344919	95288368	96241252	97203665	98175701	99157458	100149033	101150523	102162028
Operating Expense	7472865	7547594	7623069	7699300	7776293	7854056	7932597	8011923	8092042	8172962
Plant Overhead	3095046	3125996	3157256	3188829	3220717	3252924	3285454	3318308	3351491	3385006
Tax Rate										
Annual Depreciation	25017450	25017450	25017450							
Product Sales										
Break-Even Oil Price										
Gasoline	109921748	111020965	112131175	113252487	114385012	115528862	116684150	117850992	119029502	120219797
Kerosene	30535001	30840351	31148755	31460242	31774845	32092593	32413519	32737654	33065031	33395681
Diesel	40356581	40760147	41167749	41579426	41995221	42415173	42839324	43267718	43700395	44137399
Propane	5574426	5630170	5686471	5743336	5800770	5858777	5917365	5976539	6036304	6096667
Electricity	9487077	9581947	9677767	9774545	9872290	9971013	10070723	10171430	10273145	10375876
Total product sales	195874833	197833581	199811917	201810036	203828137	205866418	207925082	210004333	212104376	214225420
Cash Flow	45130687	45682063	46238954	56808393	57376477	57950242	58529744	59115042	59706192	60303254
	9700535	8538304	7515123	8028654	7051253	6192839	5438928	4776798	4195275	3684546
Net Present Value										

Table E2 (*Cont.*): Cash flow of once-through FTS biomass conversion process

Year	21	22	23	24	25	26	27	28	29	30
Working Capital										
Salvage Value										50034900
Capital Costs	0	0	0	0	0	0	0	0	0	-50034900
Operating Costs										
Biomass	61619602	62235798	62858156	63486738	64121605	64762821	65410449	66064554	66725199	67392451
Hydrogen	2387301	2411174	2435286	2459639	2484235	2509077	2534168	2559510	2585105	2610956
Butane	1125035	1136286	1147648	1159125	1170716	1182423	1194248	1206190	1218252	1230435
Labor	2464784	2489432	2514326	2539469	2564864	2590513	2616418	2642582	2669008	2695698
Maintenance	4372928	4416658	4460824	4505432	4550487	4595992	4641952	4688371	4735255	4782607
Insurance	4372928	4416658	4460824	4505432	4550487	4595992	4641952	4688371	4735255	4782607
Utility										
Cooling Water	673655	680392	687195	694067	701008	708018	715098	722249	729472	736767
Fired Heat	1645450	1661905	1678524	1695309	1712262	1729385	1746679	1764145	1781787	1799605
LP Steam	19862	20060	20261	20464	20668	20875	21084	21295	21508	21723
Electricity	24502103	24747124	24994595	25244541	25496987	25751956	26009476	26269571	26532266	26797589
SOC	103183649	104215485	105257640	106310216	107373319	108447052	109531522	110626838	111733106	112850437
Operating Expense	8254692	8337239	8420611	8504817	8589865	8675764	8762522	8850147	8938648	9028035
Plant Overhead	3418856	3453045	3487575	3522451	3557675	3593252	3629185	3665476	3702131	3739153
Tax Rate										
Annual Depreciation										
Product Sales										
Break-Even Oil Price										
Gasoline	121421995	122636215	123862577	125101203	126352215	127615737	128891894	130180813	131482621	132797447
Kerosene	33729638	34066935	34407604	34751680	35099197	35450189	35804691	36162737	36524365	36889608
Diesel	44578773	45024561	45474806	45929554	46388850	46852738	47321266	47794478	48272423	48755147
Propane	6157634	6219210	6281402	6344216	6407658	6471735	6536452	6601817	6667835	6734513
Electricity	10479635	10584431	10690275	10797178	10905150	11014202	11124344	11235587	11347943	11461422
Total product sales	216367674	218531351	220716664	222923831	225153069	227404600	229678646	231975433	234295187	236638139
Cash Flow	60906287	61515349	62130503	62751808	63379326	64013119	64653250	65299783	65952781	116647209
	3235992	2842045	2496057	2192189	1925314	1690928	1485076	1304284	1145502	1761729
Net Present Value										

Table E3: Cash flow of conventional FTS biomass conversion process

Year	1	2	3	4	5	6	7	8	9	10
Working Capital			12760753							
Salvage Value			0							
Capital Costs	64441804	130172445	78497838	0	0	0	0	0	0	0
Operating Costs										
Biomass				52030205	52550507	53076012	53606772	54142840	54684268	55231111
Hydrogen				2984714	3014561	3044706	3075154	3105905	3136964	3168334
Butane				949954	959454	969049	978739	988526	998412	1008396
Labor				2081208	2102020	2123040	2144271	2165713	2187371	2209244
Maintenance				3900914	3939924	3979323	4019116	4059307	4099900	4140899
Insurance				3900914	3939924	3979323	4019116	4059307	4099900	4140899
Utility										
Fired Heat				363229	366861	370530	374235	377978	381757	385575
Cooling Water				315877	319036	322227	325449	328703	331990	335310
Electricity				19433395	19627729	19824006	20022246	20222468	20424693	20628940
SOC				85960411	86820015	87688215	88565097	89450748	90345256	91248708
Operating Expense				6876833	6945601	7015057	7085208	7156060	7227620	7299897
Plant Overhead				2991061	3020972	3051182	3081693	3112510	3143635	3175072
Tax Rate				0.4						
Annual Depreciation				25521507	25521507	25521507	25521507	25521507	25521507	25521507
Product Sales										
Break-Even Oil Price				2.046943516						
Gasoline				109058395	110148979	111250469	112362974	113486603	114621469	115767684
Kerosene				29452248	29746771	30044238	30344681	30648128	30954609	31264155
Diesel				37799663	38177660	38559436	38945030	39334481	39727826	40125104
Propane				6958126	7027707	7097984	7168964	7240654	7313060	7386191
Total Product Sales				183268432	185101117	186952128	188821649	190709866	192616964	194543134
Cash Flow	-64441804	-130172445	-78497838	42255474	42780115	43310002	43845188	44385726	44931669	45483072
	-56036352	-98429070	-51613603	24159704	21269278	18724109	16483030	14509772	12772385	11242720
Net Present Value	0.0									

Table E3 (*Cont.*): Cash flow of conventional FTS biomass conversion process

Year	11	12	13	14	15	16	17	18	19	20
Working Capital										
Salvage Value										
Capital Costs	0	0	0	0	0	0	0	0	0	0
Operating Costs										
Biomass	55783422	56341256	56904669	57473715	58048452	58628937	59215226	59807379	60405452	61009507
Hydrogen	3200017	3232017	3264337	3296981	3329951	3363250	3396883	3430851	3465160	3499812
Butane	1018480	1028665	1038951	1049341	1059834	1070432	1081137	1091948	1102868	1113896
Labor	2231337	2253650	2276187	2298948	2321938	2345157	2368609	2392295	2416218	2440380
Maintenance	4182308	4224131	4266373	4309036	4352127	4395648	4439604	4484001	4528841	4574129
Insurance	4182308	4224131	4266373	4309036	4352127	4395648	4439604	4484001	4528841	4574129
Utility										
Fired Heat	389431	393325	397258	401231	405243	409296	413389	417522	421698	425915
Cooling Water	338663	342050	345470	348925	352414	355939	359498	363093	366724	370391
Electricity	20835229	21043582	21254018	21466558	21681223	21898036	22117016	22338186	22561568	22787184
SOC	92161195	93082807	94013635	94953772	95903309	96862343	97830966	98809276	99797368	100795342
Operating Expense	7372896	7446625	7521091	7596302	7672265	7748987	7826477	7904742	7983789	8063627
Plant Overhead	3206822	3238891	3271280	3303992	3337032	3370403	3404107	3438148	3472529	3507255
Tax Rate										
Annual Depreciation	25521507	25521507	25521507							
Product Sales										
Break-Even Oil Price										
Gasoline	116925361	118094614	119275561	120468316	121672999	122889729	124118627	125359813	126613411	127879545
Kerosene	31576797	31892565	32211490	32533605	32858941	33187531	33519406	33854600	34193146	34535077
Diesel	40526355	40931618	41340935	41754344	42171887	42593606	43019542	43449738	43884235	44323077
Propane	7460053	7534654	7610000	7686100	7762961	7840591	7918997	7998187	8078168	8158950
Total Product Sales	196488565	198453451	200437985	202442365	204466789	206511457	208576571	210662337	212768961	214896650
Cash Flow	46039988	46602474	47170585	57952980	58532510	59117835	59709013	60306103	60909164	61518256
	9895983	8710336	7666539	8190417	7193323	6317614	5548513	4873042	4279802	3758783
Net Present Value										

Table E3 (*Cont.*): Cash flow of conventional FTS biomass conversion process

Year	21	22	23	24	25	26	27	28	29	30
Working Capital										
Salvage Value										51043013
Capital Costs	0	0	0	0	0	0	0	0	0	-51043013
Operating Costs										
Biomass	61619602	62235798	62858156	63486738	64121605	64762821	65410449	66064554	66725199	67392451
Hydrogen	3534810	3570158	3605859	3641918	3678337	3715120	3752272	3789794	3827692	3865969
Butane	1125035	1136286	1147648	1159125	1170716	1182423	1194248	1206190	1218252	1230435
Labor	2464784	2489432	2514326	2539469	2564864	2590513	2616418	2642582	2669008	2695698
Maintenance	4619870	4666069	4712730	4759857	4807455	4855530	4904085	4953126	5002657	5052684
Insurance	4619870	4666069	4712730	4759857	4807455	4855530	4904085	4953126	5002657	5052684
Utility										
Fired Heat	430174	434476	438820	443208	447641	452117	456638	461205	465817	470475
Cooling Water	374095	377836	381614	385430	389285	393178	397109	401081	405091	409142
Electricity	23015055	23245206	23477658	23712435	23949559	24189055	24430945	24675255	24922007	25171227
SOC	101803295	102821328	103849542	104888037	105936917	106996287	108066250	109146912	110238381	111340765
Operating Expense	8144264	8225706	8307963	8391043	8474953	8559703	8645300	8731753	8819070	8907261
Plant Overhead	3542327	3577750	3613528	3649663	3686160	3723021	3760252	3797854	3835833	3874191
Tax Rate										
Annual Depreciation										
Product Sales										
Break-Even Oil Price										
Gasoline	129158341	130449924	131754423	133071968	134402687	135746714	137104181	138475223	139859975	141258575
Kerosene	34880428	35229232	35581525	35937340	36296713	36659681	37026277	37396540	37770505	38148211
Diesel	44766308	45213971	45666111	46122772	46584000	47049840	47520338	47995542	48475497	48960252
Propane	8240540	8322945	8406174	8490236	8575139	8660890	8747499	8834974	8923324	9012557
Total Product Sales	217045617	219216073	221408234	223622316	225858539	228117124	230398296	232702279	235029301	237379594
Cash Flow	62133438	62754773	63382320	64016144	64656305	65302868	65955897	66615456	67281610	118997440
	3301192	2899307	2546348	2236358	1964106	1724997	1514998	1330563	1168582	1797225
Net Present Value										